The Development of a Medical Biomarker Test to Aid in Rapid Screening for the Presence of Infectious Diseases

by

Dean John Bradford

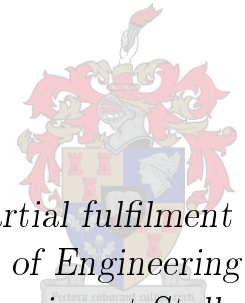

Thesis presented in partial fulfilment of the requirements for the degree of Master of Engineering (Mechatronic) in the Faculty of Engineering at Stellenbosch University

Supervisor: Prof. PR Fourie
Co-supervisor: Prof. WJ Perold

April 2019

Declaration

By submitting this thesis electronically, I declare that the entirety of the work contained therein is my own, original work, that I am the sole author thereof (save to the extent explicitly otherwise stated), that the reproduction and publication thereof by Stellenbosch University will not infringe any third party rights and that I have not previously in its entirety or in part submitted it for obtaining any qualification.

Date: April 2019 .....

Plagiarism Declaration

1. Plagiarism is the use of ideas, material and other intellectual property of another's work and to present it as my own.
2. I agree that plagiarism is a punishable offence because it constitutes theft.
3. I also understand that direct translations are plagiarism.
4. Accordingly all quotations and contributions from any source whatsoever (including the internet) have been cited fully. I understand that the reproduction of text without quotation marks (even when the source is cited) is plagiarism.
5. I declare that the work contained in this assignment, except where otherwise stated, is my original work and that I have not previously (in its entirety or in part) submitted it for grading in this module/assignment or another module/assignment.

17624363 Student number	 Signature
DJ Bradford Initials and surname	3 April 2019 Date

Abstract

The Development of a Medical Biomarker Test to Aid in Rapid Screening for the Presence of Infectious Diseases

DJ Bradford

Department of Mechanical and Mechatronic Engineering,
University of Stellenbosch,
Private bag X1, Matieland 7602.

Research assignment: Masters Thesis

April 2019

The widespread threat of antimicrobial resistance poses a major problem worldwide. A low-cost rapid biomarker test to aid in the screening of infectious diseases could potentially play a major role in promoting antimicrobial stewardship, thus combating antimicrobial resistance. Here, the prototype development of such a test is reported. C-reactive protein (CRP) and procalcitonin (PCT) were the chosen biomarkers for the test, based on recommendations from literature. Organic electrochemical transistors (OECTs) were chosen for the sensing platform, and were subsequently designed and fabricated using a desktop inkjet printer. The OECT was made sensitive to the target biomarkers by immobilising antibodies, as biorecognition elements, onto the sensor surface. The sensor was then characterised and tested using a National Instruments data acquisition device (DAQ) controlled by a series of LabVIEW programs. The CRP sensors displayed sensitivity to CRP concentrations between 0.3125 μg/mL and 10 μg/mL, whilst the PCT sensors showed no discernible response to the PCT protein. Further work is recommended to enable exact quantification of CRP concentrations, as well as enable the correct detection of PCT proteins.

Uittreksel

The Development of a Medical Biomarker Test to Aid in Rapid Screening for the Presence of Infectious Diseases

DJ Bradford

Department of Mechanical and Mechatronic Engineering,
University of Stellenbosch,
Private bag X1, Matieland 7602.

Navorsingswerkstuk: Masters Thesis

April 2019

Wydverspreide antimikrobiese weerstand is 'n wêreldwye probleem. 'n Goedkoop, vinnige biomerker toets, om te help met die sifting van aansteeklike siektes, kan dus 'n groot rol in die bevordering van antimikrobiese weerstand speel. In hierdie studie word die ontwikkeling van so 'n prototiepe aangemeld. C-reactive protein (CRP) en procalcitonin (PCT) is gekies as biomerkers na aanleiding van aanbevelings vanuit die literatuur studie. Organiese elekrochemiese transistors (OECTs) is gekies vir die sensor platform, en is ontwerp om deur 'n goedkoop huishoudelike drukker vervaardig te word. Die OECT is sensitief tot die teiken biomerkers by geïmmobiliseerde teenligaampies as bio-erkenning elemente, op die sensor oppervlak te gebruik. Die sensor is gekarakteriseer en getoets met 'n National Instruments (NI) data verkrygings toestel (DAQ) en is gekontroleer deur LabVIEW sagteware. Die CRP sensors het sensitiwiteit vir CRP konsentrasies tussen 0.3125 μg/mL en 10 μg/mL gewys, terwyl die PCT sensors geen waarneembare reaksie tot PCT protein gewys het nie. Verdere navorsing om die presiese kwantifisering van CRP konsentrasies aan te dui en die effektiewe opsporing van PCT proteïne vergemaklik word aanbeveel.

Acknowledgements

The author thanks Carel Chris van Dyk and Daniel Retief for laboratory assistance, advice and input into the project.

The author thanks Prof Patrick Bouic, Matti Kimberg and Bertus Moolman, from Synexa Life Sciences, for their invaluable advice, input into the project and access to the Synexa laboratory facilities, and guidance in the antibody pairing tests.

The author thanks Keith Ryan from Biocom Biotech for his efficient handling of all biocomponent orders and constant advice.

Finally, the author would like to thank the CSIR for their financial support and encouragement throughout the project.

Contents

List of Figures

List of Tables

Abbreviations

ADC	Analogue to digital converter
AuNP	Gold nanoparticles
BSA	Bovine serum albumin
CP	Conductive polymer
CRP	C-reactive protein
DAC	Digital to analogue converter
DAQ	Data acquisition system
ECL	Electrochemiluminescence
ECP	Extrinsically conductive polymer
ELISA	Enzyme-linked immunosorbent assay
HRP	Horseradish peroxidase
ICP	Intrinsically conductive polymer
MSD	Meso scale discovery
NI	National Instruments
NMOS	N-channel MOSFET
OECT	Organic electrochemical transistor
OFET	Organic field-effect transistor
OTFT	Organic thin-film transistor
PBS	Phosphate buffered saline
PCT	Procalcitonin
PEDOT:PSS	poly(3,4-ethylenedioxythiophene):poly(styrene sulphate)
PMOS	P-channel MOSFET
POC	Point-of-care
RTI	Respiratory Tract Infection
VI	Virtual Interface

Chapter 1

Introduction

1.1 Background

Infectious diseases, such as viral and bacterial infections, present a major health concern around the world due to their associated high morbidity (condition of being diseased) and mortality (death) rates [1]. One of the main causes of concern is the increasing threat of antimicrobial resistance, in which antimicrobial-resistant bacteria cause various common infections to become increasingly challenging to treat and take longer to resolve [2; 3; 4; 1]. According to Sambursky et al. [1], antibiotic-resistant infections contribute almost USD20 billion in excess healthcare costs, and account for productivity losses of up to USD35 billion every year in the United States alone.

Antimicrobial-resistant bacteria result from the common overuse, misappropriation and mishandling of antibiotics in the healthcare sector. Reasons for this misuse include: patients' expectations about the benefits of antibiotic therapy, the lack of clinically differentiable features between viral and bacterial infections, the time pressures associated with diagnosis and treatment [2], and the high costs of more complex decision systems, such as blood tests [5].

Complex clinical analysis techniques allow physicians access to a broad array of quantifiable markers, known as biomarkers, that can assist in the diagnosis, prognosis and monitoring of infections. Biomarker analyses are generally carried out by specialised staff in a laboratory setting. Furthermore, they are often removed from the point-of-care, require expensive equipment, are highly costly and are time-consuming. In most cases, however, the clinical outcome is dependent on the specificity and speed of diagnosis, thus limiting the effectiveness and accessibility of current test methods.

Therefore, there is great need for a fast, low cost and accessible biomarker test to aid in the screening of infectious diseases, thus supporting the worldwide effort of antimicrobial stewardship and combating the imminent threat of antimicrobial resistance.

1.2 Motivation

According to Sambursky et al. [1], an affordable rapid medical-biomarker testing device, able to assist in the differential diagnosis of viral and bacterial infections, aid in the determination of prognosis, and aid in monitoring of an infection, could have a profound impact on worldwide healthcare. Use of such a test could impact the foundational causes of antibiotic misuse, and promote the worldwide stewardship of antimicrobials. A rapid medical-biomarker test would allow the physician to know the value of a specific biomarker at a given time. Knowing the specific value of a medical-biomarker for infectious diseases could:

1. assist physicians in screening for infectious diseases and in the differentiation between viral and bacterial infections.
2. enable the early detection of bacterial infections within the critical window of diagnosis, decreasing the rate of morbidity and mortality associated with these infections.
3. lead to an improvement in the immune-response of a patient by guiding the prescription, initiation and termination of antibiotic therapy [2], thus limiting the overuse of antibiotics.
4. impact physician-patient relationships, allowing physicians, in the case of viral infection, to reassure patients that antibiotics are not necessary.
5. allow tests to be carried out in any setting, whether it be a rural clinic, doctor's office, or even surgical theater, where the decision whether to use antibiotics may be crucial.
6. be made at low cost, and on a commercial scale, due to the affordability of newly developed biosensing technologies.

Over the past decade, an array of new biosensors have demonstrated high sensitivity to a large number of microbiological substances, such as protein biomarkers, DNA, cells, and ions. Additionally, many of these biosensors have demonstrated high volume and low cost fabrication methods. The development of a rapid biomarker test based on new biosensor technology could, therefore, present an affordable and effective solution.

1.3 Objectives

The primary objective of the reported project is to develop a rapid biosensor test to aid in the diagnosis, prognosis and monitoring of infectious disease. The sub-objectives of the project are:

1. to identify applicable biomarkers that could be used for the screening of infectious diseases;
2. to identify a rapid and cost effective sensing method for the quantification of these biomarkers;
3. to develop a prototype/proof-of-concept sensor based on the identified sensing method;
4. to develop a measurement system on which to validate and test the prototype sensor;
5. to validate and characterise the prototype sensor and its main components;
6. to carry out tests to determine the performance of the sensors in detecting the relevant biomarkers.

The following report details the development of a rapid biomarker test to aid in the screening of infectious diseases. The report begins by detailing the comprehensive literature study conducted to establish the background of the project, assess the relevant biosensor technologies, and assist in the design, fabrication and testing of the prototype. Following the literature review, the conceptualisation phase of the project is described, in which the main subsystems were identified, relevent biomarkers chosen, and requirements for each subsystem defined. The design of the main subsystems and their integration, as well as the verification of each respective subsystem is then outlined. The final testing of the proof-of-concept biosensor, developed as a rapid biomarker test, is described followed by the conclusions and recommendations in the final two chapters.

Chapter 2

Literature Study

The following chapter describes all important literature reviewed during the execution of the reported project.

2.1 Biomarkers of Infectious Disease

The purpose of the following chapter is to define and highlight the fundamental theory behind biomarkers and their use as diagnostic tools, thereafter focusing on biomarkers specifically used as tools for the diagnosis of infections.

2.1.1 What is a Biomarker?

In order to discuss the use of biomarkers as diagnostic tools, it is helpful to first adopt a generally accepted definition of a biomarker. The term "biomarker" is a portmanteau made up from the combination of the words "biological" and "marker" [6]. Historically, the term's definition was surrounded by ambiguity, stemming from its use in multiple different fields. However, in 1998, the Biomarkers Definition Working Group, was convened by the U.S. National Institutes of Health (NIH) and U.S. Food and Drug Administration (FDA), in order to improve communication and standardise terminology across all fields. One of the outputs developed by the working group is the BEST Resource (Biomarkers, EndpointS and other Tools), which is comprised of a glossary of terms that "clarifies important definitions and describes some of the hierarchical relationships, connections and dependencies among the terms it contains." Furthermore, the intention of the "BEST Resource" is for professionals and researchers in all fields to "use the definitions included in this glossary when communicating on topics related to its contents (e.g., biomarkers) to ensure a consistent use of the terms and therefore, a common understanding of the issues." [7] In the interest of clarity of communi-

cation and progress, therefore, all terminology relating to "biomarkers" and subsequent definitions thereof in this document will be aligned with those contained in the BEST Resource.

According to BEST, a biomarker is described as: "A defined characteristic that is measured as an indicator of normal biological processes, pathogenic processes, or responses to an exposure or intervention, including therapeutic interventions. Molecular, histologic, radiographic, or physiologic characteristics are types of biomarkers. A biomarker is not an assessment of how an individual feels, functions, or survives." [7] In other words, a biomarker is an objectively, accurately and reproducibly measurable characteristic of the human body, which may be molecular, histologic, radiographic or physiologic in nature, that is directly proportional to some normal biological process, pathogenic process, or pharmacologic response to an exposure or intervention (e.g. drugs, surgery, vaccines [8]). Importantly, a biomarker is a subcategory of medical signs, in contrast to medical symptoms, which are patient's perceived indications of health or illness [6]. Thus, as stated in the definition, biomarkers are not an "assessment of how an individual feels, functions, or survives", but are rather objective measures of some biological characteristic which may, but do not always, correlate to a patient's sense of wellbeing.

The definition of a "clinical endpoint" is "a characteristic or variable that reflects how a subject feels, functions or survives" in a study or clinical trial. In other words, it is a measurement of some disease characteristic that reflects the effect of an intervention [8]. Clinical endpoints have, for a long time, been considered the primary, and in many cases the only suitable, endpoints of all clinical research. This is because they are directly concerned with the end goal of clinical research: to decrease morbidity and mortality [6]. After all, patients themselves are not concerned about a measurable biological characteristic, but are only concerned with treatment of the disease or illness that this characteristic may reflect, to increase their sense of wellbeing. Thus, the closer the relationship between a biomarker and a clinical endpoint, the more valuable the biomarker to clinical research.

The highest status that a biomarker can achieve, therefore, is the status of "surrogate endpoint". A surrogate endpoint is, as the name suggests, a biomarker that can serve as a substitute (but not replacement) for a clinical endpoint [6]. The formal definition of a surrogate endpoint, taken from BEST, is: "An endpoint that is used in clinical trials as a substitute for a direct measure of how a patient feels, functions, or survives. A surrogate endpoint does not measure the clinical benefit of primary interest in and of itself, but rather is expected to predict that clinical benefit or harm based on epidemiologic, therapeutic, pathophysiologic, or other

scientific evidence." [7] Surrogate endpoints are a subset of biomarkers, and the use of a biomarker as a surrogate endpoint requires demonstration of its accuracy (correlation of the biomarker with the endpoint) and precision (the reproducibility of the measure) [8].

In addition to the four types of biomarkers (molecular, histologic, radiographic and physiologic), there are seven categories of biomarkers, as shown in table G.1 of appendix G. Of the seven stated categories, four are associated with illness and disease, and four are associated with exposure to a medical product or an environmental agent, with the overlap being the monitoring biomarker, which is associated with the monitoring of either illness and disease or exposure to a medical product or environmental agent. The four biomarker categories associated with illness and disease have the most potential for clinical use - each fulfilling a different function: susceptibility/ risk biomarkers can be used to assess the potential of a patient developing an illness or disease, such as identification of immunocomprimised/ immunodeficient individuals; diagnostic biomarkers can be used as a tool for the diagnosis and differentiation of many different types of illness and disease; monitoring biomarkers can be used to assess the status of an illness or disease; and prognostic biomarkers can be used to identify the likelihood of the progression of an illness or disease.

Biomarkers of particular interest are diagnostic, prognostic and monitoring biomarkers, specifically of infection, that give clinicians measurable parameters for the appropriation of antibiotics, and can thus play a key role in reducing the worldwide problem of antibiotic resistance.

2.1.2 Diagnostic, Prognostic and Monitoring Biomarkers of Infectious Disease

As mentioned above, the biomarkers of particular interest are diagnostic, prognostic and monitoring biomarkers. Thus, the ideal biomarker of infectious disease should have diagnostic, prognostic and monitoring characteristics [1] [9]. Its uses should entail:

1. aiding in the differentiation between viral and bacterial infections,
2. aiding prognosis,
3. aiding in the monitoring of host response to an infection and antibiotic therapy,
4. guidance in antibiotic therapy [2].

There is an increasing amount of literature concerned with the pursuit of the do-it-all biomarker. Some of the most researched biomarkers of infectious diseases include: C-reactive protein (CRP), serum procalcitonin (PCT), myxovirus resistance protein A (MxA), CD64, erythrocyte sedimentation rate (ESR), interleukin 6 (IL-6), interleukin 8 (IL-8), interferon – gamma (IFN-γ), tumor nectrosis factor – alpha (TNF-α) and serum amyloid A (SAA) [10; 11; 12; 13; 1].

According to two studies concerned with literature relating to biomarkers as diagnostic tools for bacterial infection and sepsis, one conducted by Meem et al. [14] and the other by Hedegaard et al. [13], two of the most widely researched biomarkers for infectious disease are: CRP and PCT. This is due to, amongst others, their suitability to daily testing (for monitoring purposes), early response to infection (for early diagnostic purposes), and predictive accuracy of the level of infection (for prognostic purposes). The following section describes, more specifically, the usefulness of CRP and PCT as biomarkers for infectious disease.

2.2 C-Reactive Protein (CRP) and Procalcitonin (PCT) as Biomarkers of Infection

The following section focuses on the use of C-reactive protein (CRP) and procalcitonin (PCT) as biomarkers for infection. It begins with a physiological description of the two proteins, thereafter outlining how they are used as biomarkers in practice, and finally current measurement methods for CRP and PCT.

2.2.1 Description of C-Reactive Protein (CRP) and Procalcitonin (PCT)

This subsection provides a brief overview of the CRP and PCT proteins, their basic physiological function and how they are produced.

What is C-Reactive Protein (CRP)?

C-reactive protein (CRP) is a 24 kDa (kilodalton) acute phase protein, with a half-life of 19 hours, which is commonly used as a general inflammation and infection biomarker [15]. Acute phase proteins are plasma proteins, the production and serum concentrations of which are up-regulated in response to inflammation, infection, cardiovascular disease, cancer and tissue injury [16]. Normal serum concentrations of CRP are generally below 3 $\mu g/ml$ [1] in healthy patients without any form of infection, inflammation or injury. CRP levels, however, have been reported to rise as high as 500 $\mu g/ml$ in cases of severe systemic infection.

CRP levels respond differently to viral and bacterial infections. Bacterial infection is a strong stimulus for the elevation of CRP levels, with CRP levels rising corresponding to the level of infection, as early as 4 to 6 hours after infection. Peak CRP levels occur about 36 hours after infection and drop rapidly after antibiotic therapy [1]. Viral infections do not generally increase the serum concentration of CRP above 10 $\mu g/ml$, with the exceptions of influenza and invasive adenovirus, which can yield CRP levels between 10 and 80 $\mu g/ml$ [17].

The main advantages of CRP as a biomarker for infection are: that it has been extensively researched and has well defined cut-off values, it can be used as a screening method for a wide range of infectious diseases and inflammation, and the difference in CRP response between viral and bacterial infections (in some cases) can give an initial indication about the type (viral or bacterial) of the infection.

What is Procalcitonin (PCT)?

Procalcitonin is a 13 kDa, 113-amino acid, polypeptide (proteins are made up of one or more polypeptide chain) precursor to the calcitonin hormone, and is often referred to as a "hormokine" [9]. Hormokines, as their names suggest, can either exhibit hormonal characteristics or, upon inflammatory response, can show cytokine-like behaviour [10]. From the hormonal standpoint, PCT is produced exclusively by endocrine cells, such as C cells in the thyroid and K cells in the lungs [11]. The inflammatory release of PCT can be induced in two different ways: either directly - through microbial toxins such as endotoxin, or indirectly - through cell-mediated host response such as tumor nectrosis factor – alpha (TNF-α) and interleukin 6 (IL-6), amongst others [10]. The physiology behind the production of PCT after inflammation and its function are still reportedly unknown [18].

It has been shown that normal serum concentrations of PCT in a healthy patient is 0.033 ng/ml, which can elevate up to 5000 times within 2 to 4 hours of infection, in cases of severe bacterial infection, and these levels persist until recovery [10]. Importantly, PCT levels do not elevate in cases of viral infection, but are only elevated during bacterial infection.

One of the main advantages of PCT as a biomarker for infectious disease is its quick response to bacterial infection (early induction time), allowing early diagnosis. A second important advantage is its long half-life of 22 to 26 hours, thus allowing daily measurement, which is essential for monitoring purposes (showing a patient's response to antibiotic therapy), and its aid in prognosis (the course

of PCT predicting the risk of mortality in critically ill patients) [9]. Finally, the ability of PCT to assist in the differentiation between viral and bacterial infections is highly advantageous and can play a key role in the appropriation of antibiotics.

2.2.2 Current and Historical uses of CRP and PCT

CRP is one of the most widely used diagnostic and prognostic biomarkers [12], especially in the emergency room [19], and is often used as a first screening method for suspected bacterial infection [1]. One of the most useful diagnostic traits of CRP as a biomarker is its ability to assist in the differentiation between pneumonia and acute bronchitis. Studies have shown that CRP levels associated with pneumonia seldom rise above 10 $\mu g/ml$, in comparison to levels above 100 $\mu g/ml$ associated with acute bronchitis [12]. Despite, over recent years, receiving much scrutiny for its lack of specificity and late appearance, along with other more sensitive and specific biomarkers for infection being discovered, CRP remains a popular biomarker and is often used in conjunction with other biomarkers for diagnostic purposes.

PCT, on the other hand, has received much attention over recent years for its fast response time, high specificity (especially to bacterial infections), and long half-life, thus displaying ideal traits for a diagnostic, monitoring and prognostic biomarker. Its uses include, amongst others: aiding in the discrimination between viral and bacterial infections, identification of bacterial infection, early diagosis of sepsis, guidance in antibiotic therapy and the termination thereof, determination of the effectiveness of antibiotic therapy, and information regarding the extent and severity of an infection - aiding in prognosis and determining the risk of mortality [10; 12; 9; 19; 11; 18]. Apart from its well known diagnostic capability, many studies have shown that PCT is also a highly informative biomarker for monitoring host response to the infection and treatment thereof. It has been shown that if PCT levels decrease by 30% of the initial value after 24 hours of antibiotic treatment, the treatment is effective and the infection is under control [18]. Conversely, an increase in PCT levels indicates that the current antibiotic treatment is not effective and should be changed.

The cut-off value for a diagnostic test, in short, is a statistical term that refers to a threshold value, either a maximum or minimum, which separates a negative reading from a positive reading. In the case of a biomarker, for example, cut-off values are often maximum values, above which, the presence of the biomarker indicates the corresponding presence of a particular condition or disease. There are many different publications on the ideal cut-off values for CRP and PCT relating to the diagnosis of infection. Sambursky et al. prescribes CRP diagnostic cut-off

Table 2.1: Recommended CRP diagnostic cut-off values for suspected upper respiratory tract infections by Sambursky et al. [1]

Concentration range (μg/mL)	Diagnostic Indication	Antibiotics?
CRP $>$ 60	Highly likely bacterial infection	Yes
20 $<$ CRP $<$ 60	Likely bacterial infection	Yes
10 $<$ CRP $<$ 20	Likely viral infection	No
CRP $<$ 10	Neither viral nor bacterial infection	No

Table 2.2: Recommended PCT diagnostic cut-off values for suspected respiratory tract infections by Lee et al. [10]

Concentration range (ng/mL)	Diagnostic Indication	Antibiotics?
PCT $>$ 0.5	Highly likely bacterial infection	Yes
0.25 $<$ PCT $<$ 0.5	Likely bacterial infection	Yes
0.10 $<$ PCT $<$ 0.25	Bacterial infection unlikely	No
PCT $<$ 0.10	Bacterial infection highly unlikely	No

values for suspected respiratory tract infections as shown in table 2.1. Here, the recommended cut-off value for bacterial infection being 20 μg/mL and the cut-off value for viral infection being 10 μg/mL. Qu et al. [11] recommend the optimised CRP cut-off value for bacterial infection in febrile patients to be 73.8 μg/mL.

Similarly, a study by Lee et al. prescribed PCT cut-off values for the diagnosis of respiratory tract infections as shown in table2.2. Here, with the recommended cut-off value for bacterial infection being 0.25 ng/mL. Comparatively, both Qu et al. [11] and Mohan et al. [9] recommend the optimised PCT cut-off value for bacterial infection in febrile patients to be 0.26 ng/mL.

2.2.3 The Combination of CRP and PCT in a Point-Of-Care Rapid Diagnostic Test

Although both CRP and PCT are ubiquitously used to diagnose, monitor and aid in the prognosis of infections [1], literature suggests that PCT is better than CRP as a biomarker for infection [11; 12; 9]. Despite this, there is evidence that these biomarkers on their own lack the specificity for accurate diagnosis [19]. Furthermore, there is an increasing amount of literature concerned with the multiplexing of different biomarkers to yield better decision making criteria for infections.

Therefore, the combination of CRP and PCT has been recommended, in literature, due to increased specificity and sensitivity in the the diagnosis of infection [19; 2; 20; 1]. This is especially helpful for the differentiation between viral and bacterial infections, which is one of the largest problems facing clinical practitioners today, and plays a major role in the prevention of antimicrobial resistance [11; 1].

2.2.4 Current Measurement of CRP and PCT

Today, CRP and PCT detection and quantification are generally carried out on immunoassay, in highly regulated lab environments [12]. The most common of which being Enzyne-Linked Immunosorbent Assay (ELISA) and the Meso Scale Discovery (MSD) - Electrochemiluminescence (ECL) proprietary technology. ELISA, or more specifically sandwich-type ELISA, makes use of an antibody-protein-antibody-enzyme sandwich, whereby the detection of a particular protein and the subsequent binding of the enzyme-linked secondary antibody to an enzymatic marker, produces a measurable signal. The signal is generally colorimetric in nature, and is often read by complex lab equipment. MSD is similar to ELISA, for the most part, but the signal reading in this case makes use of electrochemiluminescence.

In developing countries, which often lack access to proper lab facilities, latex agglutination has been used for the qualitative and semi-quantitative detection of CRP. Immunoassays, which are the method of choice, however, are seldom available in these settings. Current measurement methods of CRP and PCT, therefore, pose large barriers to their use as biomarkers. The main disadvantages of these methods are that they rely on complex and expensive equipment, require highly trained lab personnel, are time-consuming, and are highly expensive [9]. In South Africa, the cost of a standard CRP test is about R171.40 and the cost of a PCT test is as high as R726.50 [21]. Along with the high cost of these respective tests, results may only return from the lab between 6 and 48 hours after the request, by which time the patient's condition may have dramatically worsened. For these reasons doctors, especially in primary care, often forgo these tests and diagnose patients according to clinical symptoms alone.

The development of a rapid and cost effective test, for CRP, PCT or the combination thereof, has the potential to have a large impact on developing countries and the reduction of antibiotic resistance worldwide [1].

2.3 Biosensors and Biosensing Technology

2.3.1 What is a Biosensor?

A biosensor, as defined by the International Union of Pure and Applied Chemistry (IUPAC) is "a device which uses specific biochemical reactions mediated by isolated enzymes, immunosystems, tissues, organelles or whole cells to detect chemical or biological compounds, usually by use of electrical, thermo or optical signals" [22]. Put simply, a biosensor is an analytical device that converts the molecular or biological recognition of a target analyte, into a readable signal via some form of transducer [23]. Biosensors have been applied in a wide range of industries, including healthcare, food science and environmental screening [24].

2.3.2 Biosensing Mechanisms and Types of Biosensors

The primary detection strategies used in biosensors for healthcare applications are optical, mechanical and electrical-based biosensors. This section describes the basic advantages and disadvantages of each approach.

Optical Biosensors

The main type of optical biosensor is called surface plasmon resonance (SPR), which relies on the intensity of reflected light for detection. SPR allows for real-time measurement and high throughput [23], but requires costly equipment and test preparation can be tedious.

Mechanical Biosensors

There are two main types of mechanical-based biosensors, namely microcantilever (MCL) and quartz crystal microbalance (QCM) [25]. MCLs rely on changes in mass upon target binding causing deflection of the cantilever, whilst QCMs rely on modification of the resonant frequency of an oscillating quartz crystal upon binding of the target to the surface. Both methods enable real-time detection, but are highly sensitive to changes in environmental conditions, such as temperature [23]. They also require complex micro-fabrication techniques.

Electrical Biosensors

Electrical biosensors are by far the most widely researched biosensors due to their high sensitivity and straightforward integration with electronics. Electrical sensing methods most commonly employed for healthcare applications are generally based

on impedance, potentiometric, amperometric , voltammetric, or transistor readings. Among these, transistor-based biosensors have recently become the subject of much attention, due to multiple demonstrations of the low cost and easily manufacturable subclass of transistors called organic thin-film transistors (OTFTs).

OTFT-based biosensors can be easily fabricated and are suitable for mass production [26], have simple architectures, are highly biocompatible and have exhibited high sensitivities in a plethora of biosensing applications. OTFTs, therefore, are the ideal platform for biosensing applications.

2.4 Organic Thin-Film Transistors (OTFTs) as Biosensors

A transistor or "transfer resistor", defined by the 1956 Nobel Prize Winners in Physics, is "a resistor or semiconductor device able to amplify an electrical signal as it is transferred from the input to the output of the device" [24]. They are typically three terminal devices made functional by the use of a semiconductor as the functional active material. The basic function of a transistor is to modulate or amplify the current between two terminals of the device by controlling the current or voltage through the third terminal of the device. This is typically done by modulating the width of a region in the active material, known as the channel. The properties of the active material, or semiconductor, are the main variables that determine the performance characteristics of a particular transistor.

With the advances in material manufacture and processing, a relatively new class of transistors has emerged, known as organic thin film transistors (OTFTs). These are also three terminal devices, consisting of a drain, source and a gate electrode. The primary difference that distinguishes OTFTs from traditional devices is the semiconductor material and device geometry of OTFTs. Where traditional devices are mainly composed of inorganic semiconductors and have three-dimensional structures, OTFTs, as their name suggests, are composed of organic semiconductors and have thin film, near two-dimensional, architectures.

Transistors have been implemented in a plethora of different sensing applications, demonstrating high-sensitivity detection of chemicals and biological matter, including proteins [27]. One of the main pitfalls of traditional silicon-based transistors is the combination of their high material and manufacture costs, which dramatically increases upon miniaturisation. OTFTs have shown many advantages over traditional inorganic transistors, leading to the unprecedented rise of

disposable OTFT-based chemical and biological sensors [28]. The advantages of OTFTs and their primary attraction to researchers over recent years are: their low detection limits, high sensitivity, high selectivity, easy miniaturization and scalability, good bio-compatibility, low power requirements and simple and low cost manufacture [29; 30; 26]. Indeed, OTFTs posses incredibly high potential as disposable biosensors. Other applications of OTFTs include implementation as memory devices, such as RFID tags [31], incorporation into flexible active matrix displays [32] for the use in portable electronics.

OTFTs are generally divided into two main subcategories: organic field-effect transistors (OFETs) and organic electrochemical transistors (OECTs), according to their different device architectures and working principles [26].

The following section begins with a description of the organic semiconductors vital to the operation of OTFTs, followed by a description of each of the four main categories of OTFTs: Organic Field Effect Transistors (OFETs), Electrolyte-Gated Organic Electrochemical Transistors (EGOFETS), Ion-Sensitive Organic Field-Effect Transistors (ISOFETs), and Organic Electrochemical Transistors (OECTs). This section concludes by describing the primary fabrication techniques of OFETs found in literature.

2.4.1 Conductive Polymers as Organic Semiconductors

In order to understand OTFTs, it is first important to understand the organic semiconductors which make OTFT technology possible. The discovery of the conductive properties of the iodine-doped polymer, polyacetylene, by Shirakawa et al. [33] paved the way forward for organic electronics research. Before this discovery, organic π-conjugated polymers were considered insulators. Aptly, the discovery subsequently earned the authors the 2000 Nobel prize in Chemistry for "the discovery and development of conductive polymers". Since then, organic semiconductors, or more specifically polymer semiconductors (also known as conductive polymers or CPs), have become attractive alternatives to commercialised inorganic semiconductors, such as silicon and germanium [26]. An organic semiconductor generally refers to a material consisting of carbon and hydrogen atoms, with interspersions of heteroatomic functional groups containg oxygen, sulphur or nitrogen, that displays typical semiconductor properties. In other words, they refer to an organic material that exhibits conductive properties sufficient for the operation of conventional semiconductor devices such as light emitting diodes (LEDs), solar cells and transistors [34].

One of the main attractions of organic semiconductors is their customisability,

both physically and chemically, allowing them to be tailored to meet specific design, performance and manufacture requirements [35]. This can be done, for example, by the manipulation of physical conditions or the addition of specific functional groups to the π-conjugated backbone. This high customisability makes them more versatile than inorganic semiconductors, allowing for new and novel devices to be realised using a wide range of manufacturing techniques. Another advantage of organic semiconductors is their relatively simple processing requirements in comparison to inorganic semiconductors, which often require state of the art machinery contained in a clean environment [26]. The widespread commercialisation of organic semiconductors has already been established, from OLED (organic light emitting diode) television and smartphone displays to the xerographic process common to any typical photocopy machine [34].

Polymer semiconductors or conductive polymers (CPs) consist of a π-conjugated backbone and side chains that can increase their solubility in solvents, a key characteristic that allows them to be processed by many different solution-processing techniques, such as screen printing, inkjet printing and spin-coating [26]. Many other advantages of CPs have been reported, including their light weight, corrosion resistance, low cost, and mechanical, electrical, chemical, optical and conducting properties [36; 37]. Polymer semiconductors can be separated into two different categories: intrinsically conductive polymers and extrinsically conductive polymers. The term 'conductive polymer' generally refers to intrinsically conductive polymers (ICPs); however, in applications where high metal-like conductivity is required, extrinsically conductive polymers (ECPs), also known as conductive composites, can be used [38]. ECPs are comprised of conductive metals embedded into CPs or other polymer matrices, making them conductive. Intrinsically conductive polymers (ICPs) are conductive due to conjugation in the backbone of the polymer allowing the flow of electronic charge [39].

ICPs are generally of far more interest to researchers due to their suitability to many different applications. ICPs perform particularly well where wet processability, high transparency, high flexibility, high bio-compatibility and good conductivity are required [38; 36]. Conduction due to conjugation in the backbone happens as a result of π-conjugation, and can be increased by the addition of dopant species [40]. Conduction due to π-conjugation is inherent to the polymer itself, specifically to polymers containing double bonds and lone pairs of electrons.

The conductivity of a CP can be increased by doping. Doping refers to either the reduction or oxidation of a π-conjugated CP [37]. The oxidation of a π-conjugated system results in a p-doped semiconductor; this occurs by exposing a CP to P-

type dopants, or electron-deficient species. Conversely, reduction of a π-conjugated system forms an n-doped semiconductor, which occurs by exposing the polymer to n-type dopants, or electron-rich species. CPs in which only π-conjugation is present, generally have fairly low conductivities, therefore, it is often necessary to increase their conductivities through doping, especially for transistor-based applications. This doping is mostly achieved electrochemically, and enhances electron transfer, ion mobility within the polymer and the ion-exchange properties of the polymer [36].

High performance organic thin film transistors, which fundamentally rely on these organic semiconductors (or more specifically conductive polymers), have been made realisable with the increase in customisable, high performance conductive polymers. This has led to an increase in the amount of OTFT-related research over recent years, especially OTFT-based biosensors.

OTFT-based biosensors require organic semiconductors with high conductivity, resistance to operation in aqueous mediums, good bio-compatibility and that are solution processable. Different doped ICPs tailored by the addition of side chains and functional groups have been developed for use in OTFT applications. The most common ICPs that have been implemented in OTFT-based biosensor applications are Poly(3-hexylthiophene) (P3HT), poly(3-alkylthiophene) (P3AT), poly(3,4-ethylenedioxythiophene):poly(styrene sulphate) (PEDOT:PSS), poly(3,4-ethylenedioxythiophene):p-toluenesulphonate (PEDOT:TOS), and pentacene [26; 28]. These ICPs generally fit the requirements of OTFT-based biosensors as mentioned above.

The most common conductive polymers of the ones mentioned above are PEDOT:PSS and P3HT. P3HT has mostly been implemented in OFET-based chemical and biological sensors, such as pH, ion, DNA and cell sensors, due to its high carrier mobility [26]. PEDOT:PSS has been implemented mostly in OECT-based sensors due to its ion-permeability and good performance in aqueous solutions. PEDOT:PSS is also one of the only conductive polymers available commercially tailored for the use as an ink, ideal for printing applications.

2.4.2 Organic Field-Effect Transistors (OFETs)

OFETs are made up of similar components to their inorganic counterparts, such as MOSFETs. That is, they are comprised of three electrodes: the source, drain and gate, a gate insulator or dielectric layer, and a semiconductor. The distinct difference between OFETs and conventional FETs is the choice of semiconductor and device geometry. The conventional inorganic semiconductor is replaced by

an organic semiconductor, and the device takes on a two-dimensional, thin-film, geometry. Thus, each component of an OFET (being a subcategory of OTFTs) is comprised of a thin film deposited onto a substrate, by one of a variety of deposition techniques. Figure 2.1 shows the typical layered structure of an OFET. The gate of an OFET is separated from the semiconductor by a gate insulator or dielectric layer. This layer may be made of different materials including a vacuum, polymers and oxides, as used in MOSFETs [28]. The organic semiconductor layer is connected to the insulating layer, this is known as the semiconductor-insulator interface. The grain boundaries of the semiconductor-insulator interface are of particular importance since the active channel is located in this region. Finally, the source and drain electrodes are in contact with the organic semiconductor layer and they form connection points between the transistor and external circuitry.

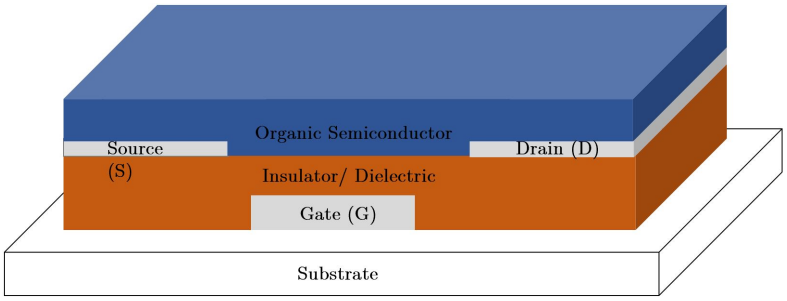

Figure 2.1: Schematic illustration of a typical thin-film OFET. Adapted from own understanding and Kergoat et al. [28].

OFET Working Principle

The working principle of an OFET is based on controlling the density of electronic carriers in the semiconductor, at the semiconductor-insulator boundary, by an electric field [26]. The electric field is caused by the application of a voltage at the gate electrode. An increase in the density of the majority charge carrier in the semiconductor causes a channel to open between the source and drain electrodes, allowing charge to flow. The current through this channel is highly controllable and can be controlled over a broad range of values via the gate voltage. This behaviour is indicative of that of an amplifier. The device also shows characteristics of a sensor, where changes in gate voltage can cause a change in the channel current.

The operation of a p-channel OFET is shown in figure 2.2. A p-channel transistor refers to a device with a p-doped semiconductor. That is, a semiconductor with

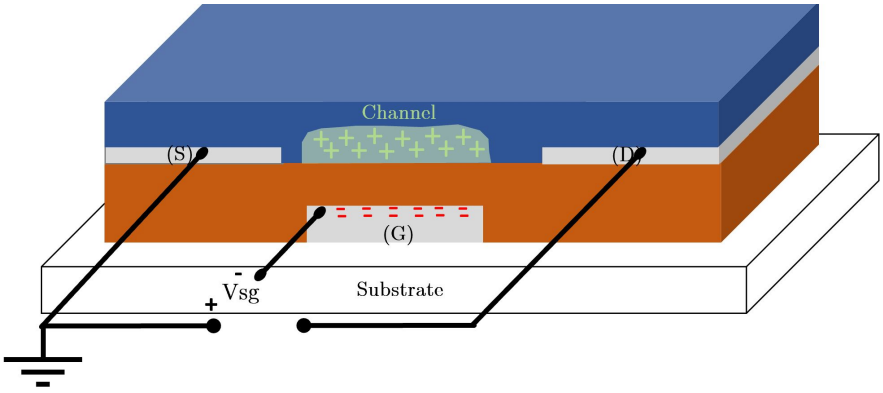

(a) Upon application of a negative gate voltage, the accumulation of negative charge at the gate-insulator interface causes the accumulation of positive charge carriers at the semiconductor-insulator interface, via an electric field.

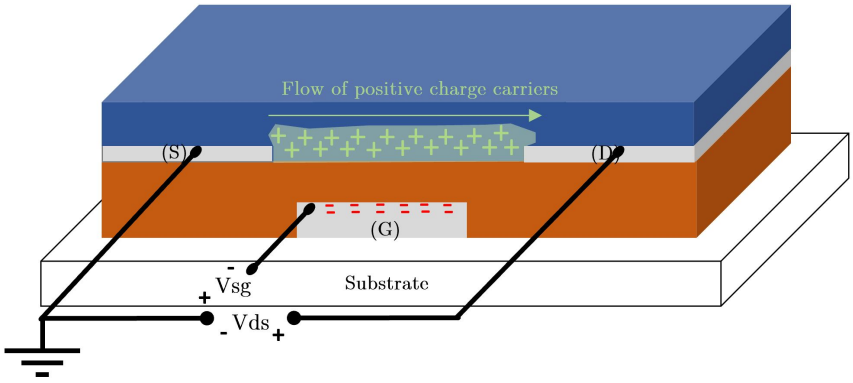

(b) With the channel in place, applying a voltage between the source and drain electrodes causes charge to flow in the channel.

Figure 2.2: Schematic illustration of the working principle of an OFET. Adapted from own understanding and Costelloe et al. [4].

excess positive charge carriers, or holes. In a p-channel OFET, upon the application of a negative voltage at the gate, free holes in the semiconductor gather at the semiconductor-insulator interface. This happens in compensation for the negative charge at the gate-insulator interface. The collection of positive charge carriers at the semiconductor-insulator interface forms a conductive channel, which is usually referred to as the active channel. With the conducting channel in place due to the gate voltage, application of a negative voltage between the source and drain causes holes to be "injected" into the channel at the source electrode. These holes flow through the channel and exit at the drain electrode, thus creating an electronic

current between the source and drain electrodes. The drain current, controlled in this process of field-effect doping, can be described by the well-documented equations given in equations 2.1 and 2.2 citepLiao2013.

$$I_D = \frac{W}{L}\mu C_i(V_g - V_t - \frac{V_{DS}}{2}) \quad \text{for} \quad V_{DS} \ll V_g - V_t, \tag{2.1}$$

$$I_D = \frac{W}{2L}\mu C_i(V_g - V_t)^2 \quad \text{for} \quad V_{DS} > V_g - V_t \tag{2.2}$$

where I_D is the current flowing in the active channel between the source and drain electrodes; W and L are the width and length of the channel respectively; μ is the mobility of the majority carrier; C_i is the capacitance of the gate insulator; V_g is the gate voltage; V_t is the threshold voltage, and V_{DS} is the applied voltage across the drain and source electrodes.

OFET-based Biosensors

OFETs have been implemented in a vast array of sensing applications, typically operating in aqueous media. Their applications include chemical sensors, able to detect pH levels, ion concentrations and other chemicals in aqueous media; as well as biosensors, able to detect different bio-species such as proteins and DNA in aqueous media. The configuration of an OFET sensor is identical to that shown in figure 2.1, with the exception of the semiconductor layer being exposed to the target analyte. OFET sensors are able to detect the properties of target analytes due to physical and chemical changes of the active layer upon exposure to the analyte. The performance of an OFET is highly dependent on the grain boundaries at the semiconductor-analyte interface. This change in the physical and chemical properties at the grain boundaries can often be measured, which is the primary sensing mechanism of OFET sensors. More specifically, from equations 2.1 and 2.2, the channel current, I_D, can be controlled by the carrier mobility (μ), and the threshold voltage (V_t), both of which important in sensing applications [26]. The carrier mobility is typically influenced by the change of surface topography at the semiconductor-analyte interface when the OFET is exposed to an analyte. Upon exposure, molecules from the analyte diffuse into the semiconductor at the grain boundaries, thus altering the surface interface [41]. The threshold voltage is changed due to the doping effect when the OFET is exposed to a target analyte, as a result of a change in the density of majority carriers in the semiconductor [42]. This is one of the properties that makes OFETs well suited to sensing applications [28].

The classic OFET, as described above, has been further optimised into two, more convenient and sensitive, configurations specifically for sensing applications. These are known as the Electrolyte-Gated OFET (EGOFET) and the Ion-Sensitive OFET (ISOFET).

The configuration of EGOFETs is substantially different from classic OFETs. An EGOFET has a similar layout to an OECT, shown in 2.3, in which the gate electrode is separated from the semiconductor layer by an electrolyte, instead of a dielectric layer [24]. Although EGOFETs are classified as a type of OFET, there have been reports that they operate in a similar manner to OECTs (addressed in section 2.4.3), due to the electrochemical doping of the semiconductor [26]. Wang et al. [24] and Kergoat et al [28] have suggested that capacitive processes, rather than electrochemical processes, govern the operation of an EGOFET. According to [26], further work is needed to classify their working principle. In any case, the figure of merit that distinguishes EGOFETs from classic OFETs, is their low operating voltage in comparison to conventional OFETs ($<$1 V vs $<$10 V) [24]. This low voltage operation enables them to work below the electrolysis point of water and within a safe potential for biological matter, making them suitable for the detection of biomolecules in aqueous media [28].

ISOFETs are, too, different in configuration to the typical OFET. They consist of an insulator deposited onto the semiconductor layer, with an electrolyte being in contact with the insulator surface and the gate electrode being immersed in the electrolyte. This is the most popular configurations of OFET-based biosensors. Here, the detection interface is at the insulator-electrolyte boundary. Thus, by making the insulator sensitive to specific biomolecules, the detection of a vast array of biomolecules is possible [28]. Many ISOFETs make use of poly(3-hexlythiophene) (P3HT) as the semiconductor layer. This, however, results in the operating voltage of the ISOFET dramatically increasing, above the point at which many bio-species, such as proteins, denature. This characteristic thus makes them unsuitable for most biosensing applications.

2.4.3 Organic Electrochemical Transistors (OECTs)

Organic electrochemical transistors (OECTs) were first reported by White et al. [43] in 1984 and have been researched extensively, especially in recent years, for their potential application as chemical and biological sensors [29; 44; 45]. OECTs are three terminal devices, consisting of a source, drain, and gate electrode. However, as is the case with EGOFETs, the solid-state insulating layer is replaced by an electrolytic medium (liquid or solid), separating the gate electrode from the organic semiconductor. The organic semiconductor, to which the source and drain

electrodes are connected, is generally in the form of a doped conducting polymer, the most common of which being poly(3,4-ethylenedioxythiophene):poly(styrene sulphonate) (PEDOT:PSS). The typical layered structure of an OECT, with an immersed gate electrode, is shown in figure 2.3a. An alternative, and in many cases more convenient, layout with the gate in the form of a thin film, is given in figure 2.3b

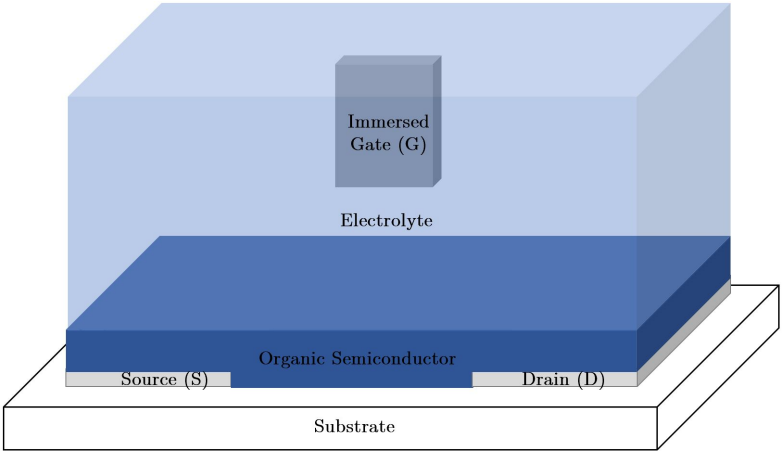

(a) The layered structure of a typical OECT with an immersed gate electrode

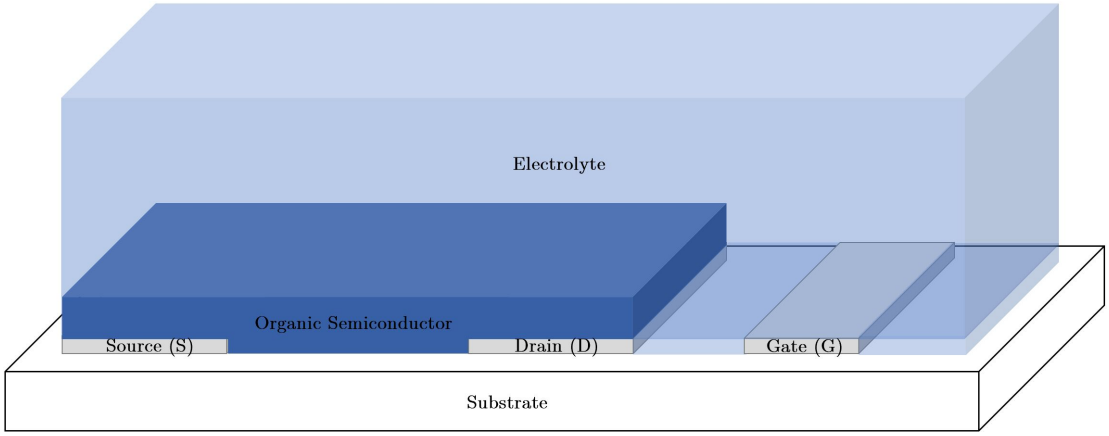

(b) A convenient configuration of an OECT with a thin film gate electrode

Figure 2.3: Schematic of the two most common layouts of an OECT. Adapted from own understanding and Kergoat et al. [28].

OECT Working Principle

The working principle of an OECT, similarly to other transistors, is based on the modulation of the majority carrier density in the active channel of the semiconductor or conductive polymer [35]. In an OECT, however, this is done by controlling the level of ion doping in the conductive polymer. Conductive polymers based on poly(3,4-ethylenedioxythiophene) (PEDOT) with degenerately doped polyanions such as poly(styrene sulphonate) (PSS) or p-toluenesulphonate (TOS) contain large anions that compensate for the holes in the p-type polymer. These anions are fixed (that is, they are not mobile); however, the holes in the p-type material are mobile and are considered the majority carrier in the active material. The conductivity of the active channel can be modulated by controlling the electrochemical migration of mobile ions between the electrolyte and the polymer [26] via reversible electrochemical reactions. These reversible electrochemical reactions are mediated by the voltage at the gate electrode.

OECTs based on PEDOT:PSS or PEDOT:TOS are normally-on devices [28], able to conduct at zero gate voltage, due to the excess of majority charge carriers caused by the presence of the large anions PSS or TOS. Thus, there exists a current path within the organic semiconductor, dominated by the excess majority carriers, that allows current flow in any direction between the source and drain electrode, depending on the direction of potential between the two electrodes. Upon the application of a positive gate voltage, mobile cations in the electrolyte are injected into the polymer bulk, compensating for the fixed dopant anions. This is generally referred to as the "de-doping" of the polymer [29]. The presence of these cations thus decreases the hole density in the active channel, in turn reducing the conductivity of the polymer, since ions are less mobile than holes [35; 28; 26]. This, therefore, results in an overall reduced current between the source and drain electrodes. Thus, the current between two electrodes of the OECT (drain and source) can be modulated by the voltage at the third electrode (gate), consistent with the definition of a transistor. The working principle of an OECT is illustrated in figure 2.4, and the output and transfer characteristics of an OECT are given by figures 2.5 and 2.6 respectively. Note that current flows between the source and drain electrodes according to the direction of potential difference across these two electrodes.

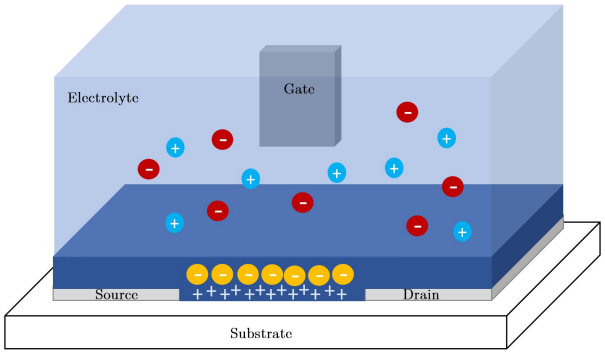

(a) Diagram of an OECT showing the excess of majority carriers (holes) along with the fixed dopant anions, in the absence of a gate voltage. This results in the "normally-on" nature of many OECTs.

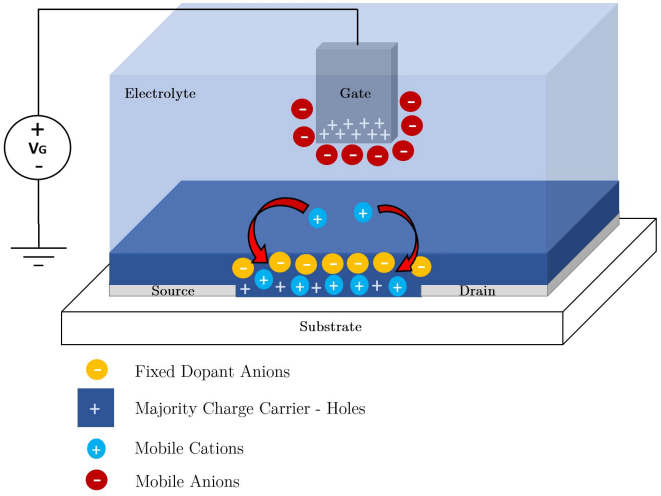

(b) The application of a positive voltage at the gate electrode of an OECT, causing the effective "de-doping" of the polymer as a result of the injection of positive ions from the electrolyte into the polymer.

Figure 2.4: Simple illustration of the working principle of a typical OECT. Adapted from own understanding and Costelloe et al. [4].

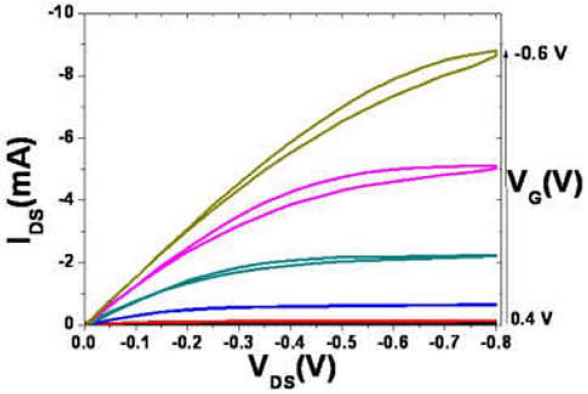

Figure 2.5: Example of the output characteristics of an OECT for forward and backward drain voltage sweeps. Reproduced from Macchia et al. [46].

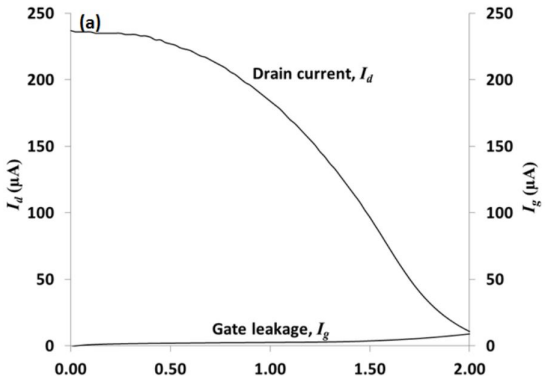

Figure 2.6: Example transfer characteristics of an OECT. Reproduced from Faddoul et al. [47].

At a low source-drain voltage, upon the application of an effective gate voltage, the current in the active channel of an OECT is directly proportional to the density of majority carrier in the channel. An estimate of the channel current can then be given by equation 2.3 [48; 49].

$$I_{DS} = \frac{q\mu p_0 tW}{LV_P}(V_P - V_g^{eff} + \frac{V_{DS}}{2})V_{DS} \quad \text{for} \quad |\, V_{DS} \,| \ll |\, V_P - V_g^{eff} \,| \tag{2.3}$$

$$V_P = \frac{qp_0 t}{C_i} \tag{2.4}$$

$$V_g^{eff} = V_G + V_{offset} \tag{2.5}$$

where V_P is the pinch-off voltage; V_G^{eff} is the effective gate voltage; q is the electric charge; μ is the hole mobility; p_0 is the initial hole density in the active layer in the absence of an applied gate voltage; t is the thickness of the active layer (conductive polymer or semiconductor); W and L are the channel width and length respectively; C_i is the effective gate capacitance of the transistor; and V_{offset} is the offset voltage which is determined by the drop in potential at the gate-electrolyte interface and the electrolyte-channel interface [45; 26].

The OECT can be described by two circuits, an electronic circuit and an ionic circuit. The flow of holes in the active material between the source and drain electrodes being the electronic circuit, and the flow of ions between the electrolyte and active material across the electrolyte-semiconductor interface being the ionic circuit. Since hole transport is far more rapid than ion transport, the response is limited and highly dominated by the diffusion of ions in the ionic circuit under an applied gate voltage [44; 26].

The above-mentioned properties of OECTs make them ideal candidates for biosensing applications - wherein their real potential lies.

OECT-based Biosensors

Over recent years, as researchers have begun to unlock their potential, OECTs have fast become the new 'darling' of the biosensing world. To begin with, their inherent operation in aqueous electrolytes, converting an ionic current into an electronic one, provides a simple way to interface biological systems with electronics [45; 35; 50; 51; 44]. This property is essential to real-time biosensing applications [26], since the analyte such as serum or whole blood, can serve the additional function of the acting electrolyte. This stands in contrast to OFET-based sensors, which are not necessarily tailored for operation in electrolytes, with the exception of EGOFETs and ISOFETs. Additionally, OECTs operate under very low voltages, generally below 1 V, which is a requirement in most biosensing applications to prevent water hydrolysis and unwanted redox reactions in biomolecules [27; 28; 26]. This, along with the simple signal readout inherent to OECTs [45], broadens the variety of peripheral electronics required for sensing applications, allowing simple, low-voltage electronics to be incorporated for voltage supply and measurement. The use of simple and low cost electronics is particularly ideal for developing hand-held point-of-care biosensing devices.

Another advantage of OECTs for biosensing applications is their inherent signal amplification [45], leading to higher sensitivity than other electrochemical sensing approaches[50]. This is a desirable characteristic in any sensor, where small changes in the input signal cause large relative changes in the output signal. It also eliminates the need for output signal amplification using electronic circuitry, further decreasing the requirement for complex peripherals.

Along with the above-mentioned simple and minimal peripheral circuitry requirement, the device architecture of an OECT is also straightforward [45]. In the absence of an insulating layer, OECTs are comprised of a conducting polymer, such as PEDOT:PSS, and electrodes made of conductive metal-based materials, such as silver or gold; thus simplifying their fabrication process, which can be achieved by low-cost solution-processable deposition methods, such as printing.

Finally, many OECT sensors based on conductive polymers have shown good biocompatibility [51], showing little to no toxicity to bio-molecules such as proteins, antibodies, DNA and living cells. This stands in contrast to traditional inorganic semiconductor-based transistors, which present high toxicity to bio-molecules.

The above-mentioned characteristic advantages of OECTs makes them ideally suited to biosensing applications.

2.4.4 OTFT Fabrication

One of the hallmarks of OTFTs is their low cost and easy manufacturability, owing to their simple structures and the wet solution processibility of their active materials - organic semiconductors in the form of conductive polymers. The manufacture of OFET devices consists of the deposition of thin layers of material onto a particular substrate, and in some cases the curing of these materials.

There are several well-established low cost deposition techniques that have been applied to OTFT fabrication, including vacuum thermal evaporation, spin coating, and inkjet printing, amongst others. These techniques differ tremendously and their use is dependent on application.

Vacuum Thermal Evaporation

In this process, both the semiconductor material as well as the substrate are placed in a vacuum. The organic semiconductor is then thermally heated until the point of sublimation, upon which it is then condensed to form a thin layer on the surface of the substrate, which is kept at a low temperature [24]. The main disadvantage of this process is that the deposition is not easily patterned, and is thus only suitable for the deposition of the organic semiconductor, with an additional process being required for the deposition of the patterned electrodes of the OTFT.

Spin Coating

Spin coating is a well known coating process used in many laboratories to achieve an evenly deposited layer of material onto a substrate. It consists of spinning a substrate and dripping the coating material in the center of the spinning substrate. The coating material is evenly spread over the substrate under centrifugal force. The main variables controlling the layer thickness of the deposited layer are the centrifugal force (controlled by the rotational speed) and the viscosity of the coating solution [24]. The coating solution is required to be diluted with a solvent which, during the coating process is evaporated, leaving the coated substrate. Just as it is the case with thermal evaporation, this process does not allow for pattern coating, but rather the coating of the entire substrate with a thin layer of the coating solution. This limits spin coating to the deposition of the organic semiconductor layer only, and the patterned electrodes of OTFT devices need to be

deposited using another technique. Additionally, an extra annealing step is often required to ensure the crystallisation of the organic semiconductor molecules and increase its conductivity [52; 53].

An advantage of this method over thermal deposition is that the organic semiconductor does not need to be heated, preventing its thermal degradation [24]. Another advantage of the spin coating process is that it is highly accessible, due to its simplicity. One drawback of this process is that not all organic semiconductors are able to dissolve in solvents.

Inkjet Printing

Inkjet printing is a well known and widespread solution process used for the deposition of inks in specific patterns onto a substrate. In some cases, patterning with a lateral resolution of up to 5 μm has been achieved using this technique [54]. Inkjet printing provides a cost effective and efficient alternative to lithographic patterning, and allows materials to be deposited on flexible, lightweight substrates, such as paper. It has the additional advantage of being an additive process as opposed to a subtractive process, such as lithography, which ensures less wastage of materials [24].

This has become a popular method for the fabrication of OTFTs due to the fact that both the patterned electrodes and the organic semiconductor can be deposited with high accuracy and repeatability, in the same process. Indeed, by filling separate ink cartridges with the relevant material (one with the electrode material, and the other with the organic semiconductor), it is possible to print the patterned electrodes followed by the organic semiconductor layer in the same print cycle. Furthermore, there are commercially available conductive inks, based both on conductive polymers (specifically PEDOT:PSS), and metals (such as silver nano-particle-based ink). These inks have been specifically tailored for inkjet printed electronic applications, and make this technique highly convenient.

2.5 Antibodies and Immunosensors

Many biosensors operate in aqueous analytes, such as whole blood, serum or saliva, containing millions of different biological components. In order to enable the detection of specific bio-molecules, it is often necessary to capture the molecule of interest out of the analyte and onto the surface of the sensor. Antibodies can be used effectively for this purpose and are often referred to as bio-recognition elements in sensing applications. Sensors employing antibodies as bio-recognition

elements are referred to as immunosensors.

The following section begins by describing some basic theory necessary to the understanding of the structure of antibodies and their behaviour. It then outlines the function of antibodies in immunosensing, specifically in OTFT-based immunosensors. The section concludes by outlining different antibody immobilisation strategies and the labelling or conjugation of antibodies with various materials for signal amplification.

2.5.1 Antibodies

What is an Antibody?

An antibody, also known as an immunoglobulin, is a protein, produced by B cells in the immune system, that is capable of binding with high specificity to an antigen [55]. Antigens are typically defined as any substance foreign to the body that induces an immune response [56], and are often proteins, although they may also be other bio-molecules. Antibodies are Y-shaped proteins, with two different regions known as the constant region and the variable region. The structure of an antibody is shown in figure 2.7a.

The constant region of an antibody is the same for each antibody (as its name suggests), but the variable region of the antibody changes according to the epitope to which that antibody targets.

Epitopes

An epitope, also known as an antigenic determinant, refers to a specific target region on the surface of an antigen to which an antibody binds. An illustration of an antibody binding to a specific epitope on an antigen is given in figure 2.7b. Thus, a protein, for example, may have several different epitopes, allowing multiple different antibodies to bind to the same protein, due to the unique antibody-epitope specificity.

Antibody Specificity and Affinity

Antibody specificity and affinity are important characteristics which describe the ability of an antibody to bind to a target antigen. As it will be shown in section 2.5.2, these are key characteristics when selecting antibodies for immunosensing applications. Specificity refers to the ability of the antibody to bind only with the target antigen, whilst avoiding the detection of unrelated antigens. Antibody affinity refers to the strength of the bond between an antibody binding site and the

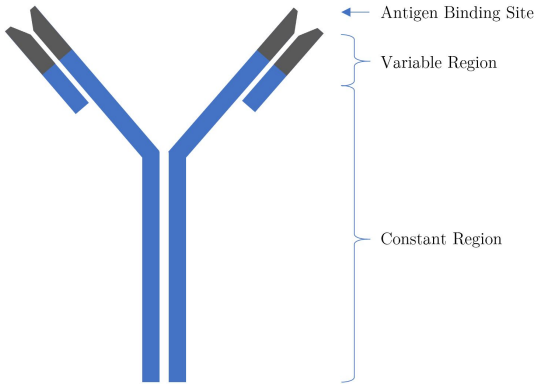

(a) Schematic illustration of the structure of an antibody or immunoglobulin.

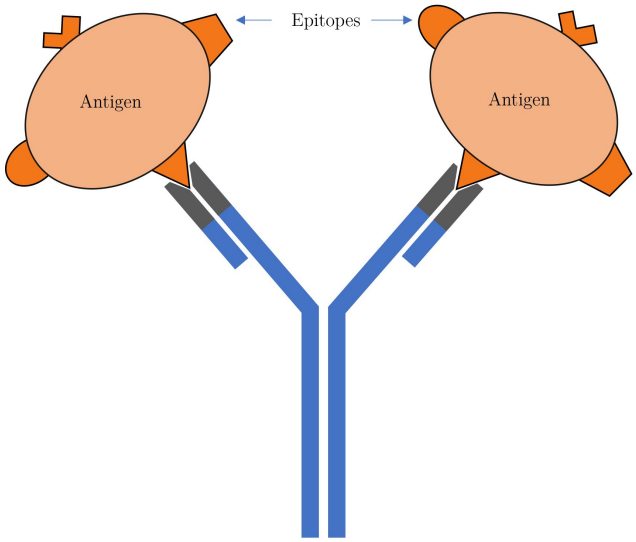

(b) Schematic illustration of the binding of an antibody to an antigen at a specific epitope.

Figure 2.7: Basic Schematic of the structure of an antibody and its binding to an antigen. Adapted from own understanding and Jung et al. [57].

target antigen. High affinity antibodies bind quickly, with high-strength bonds, and maintain a stable bond under harsh conditions. High specificity is crucial in immunosensing applications in order to ensure that the correct target antigen is being sensed, whilst high affinity is also crucial to immunosensing since it directly influences the sensitivity of an immunosensor.

Monoclonal vs Polyclonal Antibodies

Polyclonal antibodies represent a collection of antibodies produced by many different B cells that recognise many different epitopes on the same target antigen. By contrast, monoclonal antibodies are a collection of antibodies from the same B cell, and thus target the same epitope on the same target antigen [55]. The advantages and disadvantages of monoclonal and polyclonal antibodies are given in table 2.3.

2.5.2 Immunosensors

An immunosensor describes a subtype of biosensors, namely those that utilise antibodies as their biorecognition elements. The following section is a brief overview of literature concerned with the basic structure of an immunosensor, organic eletrochemical transistor (OECT) based immunosensors, methods of immobilizing antibodies onto sensor substrates and finally the labelling of antibodies with biocompatable materials.

What is an Immunosensor?

As described above, an immunosensor is a subclass of biosensors specifically concerned with the detection of antigens using antibodies as bio-recognition elements. The main mechanism of immunosensors, in general, is to take advantage of the change in signal (e.g. electronic, optical, piezoelectric) due to the formation of the antibody-antigen complex on the sensor surface [58]. Immunosensors are particularly useful when quantifying the immune response of a patient to a particular disease, by measuring well known biomarkers associated with an immune response [59].

Immunosensors have been demonstrated making use use of two different detection approaches, namely labelled and label-free detection. The label-free approach relies solely on the antibody-antigen complex causing a readable change in output signal of the immunosensor. By contrast, the labelled approach, also known as sandwich type immunosensors, consist of a second antibody, conjugated to a nanoparticle, that binds to a different epitope on the antigen. This is illustrated in figure 2.8.

In this case, the antibody immobilised on the substrate is referred to as the capture antibody, and the labelled antibody is known as the detection antibody. In this configuration, the detection antibody binds with the antigen part of the capture antibody-antigen complex, thus providing a detectable signal via the conjugated

Table 2.3: The advantages and disadvantages of monoclonal and polyclonal antibodies (adapted from Pacific Immunology [55])

Monoclonal Antibodies	Polyclonal Antibodies
Advantages	
Production of large quantities of the same antibody is possible, with high homogeneity between batches.	Inexpensive.
High specificity to epitopes. Far less chance of cross reactivity.	Stable and relatively unaffected by pH changes.
Can provide better results in assays requiring the exact quantification of a particular protein level.	High affinity due to binding of multiple epitopes.
	More robust detection due to the binding of multiple epitopes.
	High sensitivity for detecting proteins and other antigens in low concentrations, due to the binding of multiple antibodies to the same antigen.
	Easy storage.
Disadvantages	
Significantly more expensive than polyclonal antibodies.	High variability between batches.
More demanding storage conditions.	Less specific due to the detection of multiple different epitopes, resulting in a higher chance of cross reactivity (binding to unrelated antigens).
More sensitive to changes in pH levels.	
Less robust for detecting proteins that may be in a denatured state and small changes in epitope structure.	

nanoparticles [29]. Nanoparticles have been reported to assist in signal amplification [50], catalyse electrochemical reactions, and enhance electron transfer [29]. Common nanoparticles used in biosensing applications include gold nanoparticles (AuNPs) and horseradish peroxidase (HRP) due to their good biocompatibility. Gold nanoparticles have the added advantage of having a large surface area.

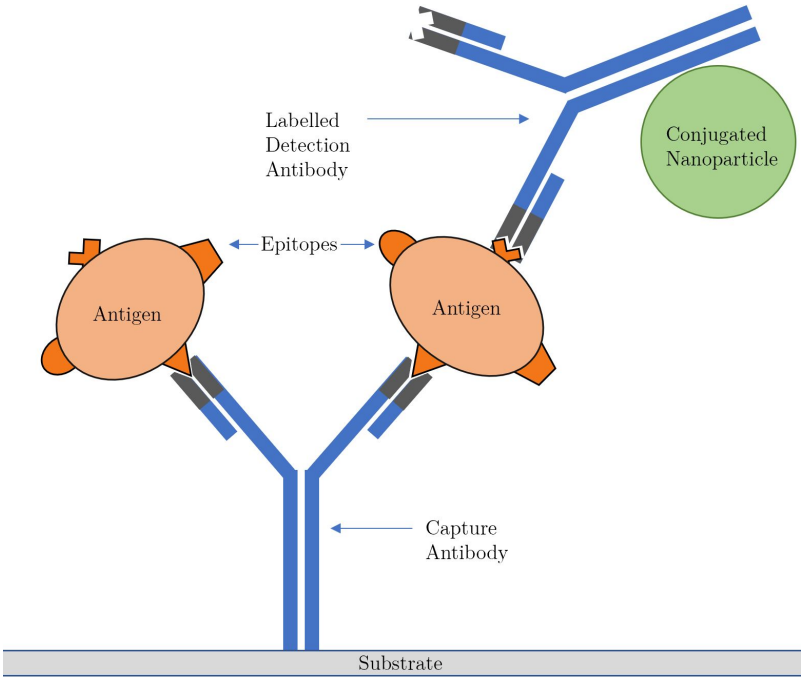

Figure 2.8: Schematic illustration of a sandwich type immunosensor at molecular level. Adapted from own understanding.

OECT-based Immunosensors

In OECT sensing applications requiring the quantification of a particular protein concentration in an analyte, the use of antibodies is necessary for the capture and detection of the target protein. Antibodies have been used in many OECT-based immunosensor applications. The use of antibodies in OECT sensing applications has been made possible by the excellent biocompatibility of conductive polymers, allowing the effective immobilisation of antibodies on the sensor surface [26].

OECTs have been applied as immunosensors for the detection of many different protein biomarkers. Kim et al. [29] demonstrated a sandwich type OECT-based immunosensor for prostate specific antigen (PSA), using gold nanoparticles for signal amplification. Here, the performance of the device, shown by the drain

current, was affected by the binding of PSA to the capture antibodies. The signal was greatly amplified by the addition of the detection antibodies labelled with gold nanoparticles. The calibration curves resulting from sweeping the gate voltage at a constant drain voltage, for different concentrations of PSA, both with and without gold nanoparticles, is shown in figure 2.9.

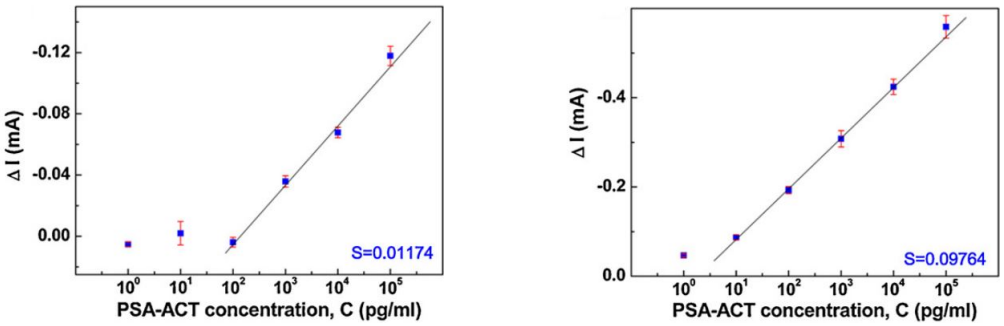

(a) Calibration curve without AuNPs (b) Calibration curve with AuNPs.

Figure 2.9: Calibration curves showing the increase of sensitivity of the OECT-based immunosensor after the addition of AuNP-labelled detection antibodies. Reproduced from Kim et al. [29].

From figure 2.9a, it can be seen that the OECT-based immunosensor detects PSA successfully down to a concentration of 100 pg/ml. It is further shown in figure 2.9b that the sensitivity of the immunosensor was dramatically increased by the addition of the AuNP-conjugated detection antibodies, and the device could then detect PSA down to a concentration of under 10 pg/ml.

2.5.3 Antibody Immobilization Strategies

In immunosensors, capture antibodies provide the interface between the sensor and the target protein contained in the analyte. There are several aspects of antibody immobilisation which affect the ability of the capture antibody to detect a specific antigen. These are: antibody denaturing, binding site modification, antibody orientation and the space between the bound antibody and the surface of the sensor [57]. Antibody denaturing refers to changes in the antibody's shape, making it lose its function. The denaturing of antibodies during or after the immobilisation step decreases the sensitivity of immunosensors. Antibody modification at antigen binding sites decreases the antibody's ability to bind to antigens. This often occurs due to random chemical tagging of an antibody. Antibody orientation is one of the

most important aspects affecting the performance of immunosensors. Correct antibody orientation, with the antigen binding sites exposed to the analyte, increases the antigen binding ability of the immobilised antibodies. It has been shown that randomly-coupled antibodies exhibit three-times less binding capacity compared to well-oriented antibodies [60; 57]. Finally, the space between the immobilised antibody and the surface to which it is immobilised has been shown to play a role in the effectiveness of antigen binding. Antibodies bound to a solid surface via a long linking molecule have shown greater binding capabilities [57].

Multiple studies have shown that optimised antibody immobilisation increases the sensing capability of immunosensors [57; 61; 62]. There are several different methods that have been used for antibody immobilisation onto sensor surfaces. Four of these are: adsorption, covalent immobilisation, biotin-streptavidin affinity and antibody-binding proteins.

Adsorption

Antibody adsorption refers to the interaction between an antibody itself and the surface, in the absence of any other molecules. It occurs by hydrophobic and hydrophilic interactions between the antibodies and the surface [57], and is achieved by incubation of the solid surface in an aqueous medium containing the antibodies. Adsorption is by far the simplest form of immobilisation since it is a single-step process and requires no additional antibody modification or additional substances. A disadvantage of this method is that it does not guarantee antibody orientation and in many cases the antibodies lose functionality of their binding sites due to denaturing. Furthermore, adsorbed antibodies form a relatively weak bond (and can be easily detached in harsh conditions, such as washing), and bond directly to the surface, decreasing the their antigen-binding capabilities.

Covalent Immobilisation

The covalent bonding of antibodies to a surface is also referred to as cross-linking, and is a common method of antibody immobilisation in immunosensor applications. This method is popular due to the strong and robust covalent bond formed between the antibody and a treated surface. In this method, amino groups on the antibody surface can be coupled with reactive substances coated on the solid surface to which the antibody is immobilised [57; 61]. The advantages of covalent immobilisation include: its simplicity, its short process, the well established chemistry for surface activation, no denaturing or binding-site modification, and the ability to use long linking molecules to space the antibody from the surface. The main disadvantage of this method is that a covalently-linked antibody, through its

amino groups, is randomly oriented.

Biotin-Streptavidin Affinity Immobilisation

Another common method for cross-linking makes use of the near-irreversible biotin-streptavidin reaction. By covalently labelling the antibody with biotin (also known as biotinylation), and activating the surface with streptavidin, the biotinylated antibodies can be immobilised on the streptavidin coated surface through the strongest non-covalent biological interaction known [60; 61]. This method is also often used in immunoassays, due to its binding efficiency, with one strepavidin molecule binding up to four biotin molecules. The advantages of this method include the binding efficiency, the affinity of the biotin-streptavidin bond, good orientation, no binding-site modification, no denaturing, and the large space between the antibody and the surface. A disadvantage of this method is that it can be time-consuming, due to the the antibody requiring modification and the surface requiring activation.

Antibody-binding Proteins

Antibody-binding proteins bind to specific regions of an antibody. This process is similar to the cross-linking process, whereby the surface to which the antibody is being immobilised requires activation, however in this case the surface is coated with antibody-binding proteins such as protein A and protein G [57]. An advantage of this method is that correct antibody orientation is guaranteed since the protein binds to the same region of the antibody repeatedly. Another advantage of this approach is that the antibody does not require modification, and thus maintains its antigen-binding functionality. The disadvantages of this approach include: the reduced stability of the immobilisation in comparison to cross-linking, the additional step of the immobilisation of antibody-binding protein and the unsuitability for sandwich type sensors.

Chapter 3

Functional Deconstruction and Design Specification

The following chapter begins by reviewing the project problem statement and developing requirements for the testing system, thereafter describing the basic overview of the system, describing relevant subsystems and finally describing broad design choices relating to those subsystems.

3.1 System Requirements

The title of the project, being the problem statement, is: "The development of a rapid biomarker test to aid in the diagnosis, prognosis and monitoring of infectious diseases." Drawing from this and the project objectives, described in section 1.3, the requirements for the development of the system are:

1. A functioning proof of concept (prototype) that can detect specific biomarker(s) of infectious disease, within a clinically relevant range.
2. The time per test should be significantly less than those currently used to test for biomarkers of infectious disease. This is to ensure the usefulness of the test for aiding in diagnosis, prognosis and monitoring.
3. The cost of each test to be suitable for the daily testing of a patient in resource-poor settings.
4. The sensor itself should be usable in any setting, without requiring a laboratory: including doctor's rooms, the ICU and rural clinics.

3.2 System Overview and Division of Subsystems

3.2.1 System Overview

The basic layout of a typical electronic sensor-measurement system is made up of six main components: the target of measurement, an input signal source (reference signal), a sensor/ transducer stage, an output signal conditioning stage, output signal measurement, and finally a signal interpretation stage. These components are shown in figure 3.1. The "target of measurement" refers to a physical

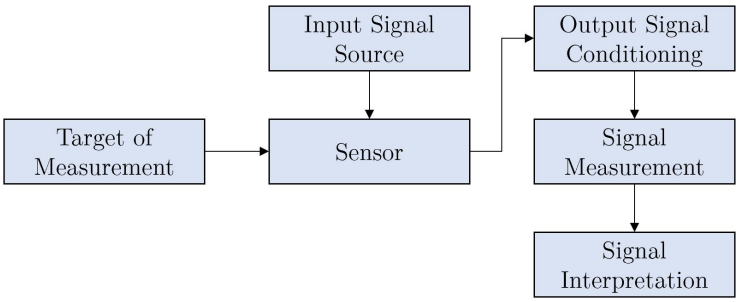

Figure 3.1: The components of a typical measurement setup. Adapted from Figliola and Beasley [63].

property or the presence of a particular substance, to be measured, either directly or indirectly, by the sensor. The input signal source generates the supply signal to the sensor. This is also referred to as the reference signal. The sensor/ transducer refers to the physical element that employs some natural phenomenon to sense a physical property or the presence of a particular substance, and consequently turns the sensed information into a detectable signal [63]. Output signal conditioning refers to the modification of a signal into desirable magnitude or gets rid of undesirable signal components. Examples of signal conditioning are filtration and amplification. Signal measurement refers to the storage of the sensed value in memory. Finally, signal interpretation refers to the processing and display of the information in a particular format (e.g. graphically).

Adapting the general layout to the case of a biosensor or, more specifically, an immunosensor, the layout can be shown by figure 3.2. Here, the target of measurement is an analyte containing the biomarkers of interest. Furthermore, the biosensor is functionalised with biorecognition elements that are sensitive to the biomarkers of interest. In most cases involving biomarkers, these biorecognition elements are antibodies. As noted in section 2.5.2, biosensors that make use of

antibodies as biorecognition elements are known as immunosensors. This subclass of biosensors exploits the antibody-antigen (immuno) reaction to separate the antigen, which in this case is the biomarker of interest, from the analyte.

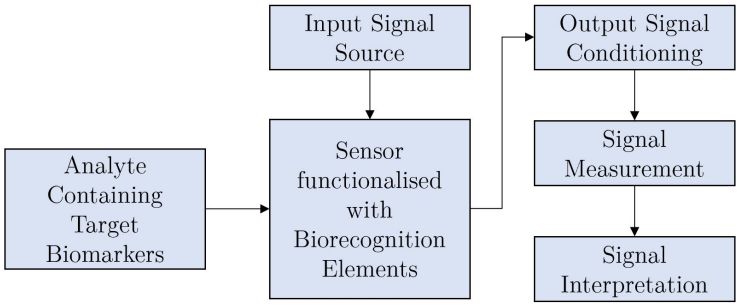

Figure 3.2: Immunosensor-specific components for the measurement setup. Adapted from own understanding and Figliola and Beasley [63].

3.2.2 Division into Subsystems

Immunosensors, being highly integrated compact devices, are at the intersection between biology and biotechnology, electronics, and chemical physics [58]. The biological species being sensed along with the biorecognition elements falls in the field of biology and biotechnology; the sensor falls in the field of chemical physics; and finally, the signal measurement and processing falls in the field of electronics. It is advantageous, therefore, to divide the system into separate subsystems according to their respective fields. This would allow the characterisation and optimisation of each subsystem according to criteria specific to each relevant field, before integrating them to form the complete system. The division of the system into three main subsystems is shown in figure 3.3.

The first subsystem is comprised of the biorecognition elements of the immunosensor - antibodies. This subsystem has two main functions: 1. to capture the biomarkers of interest (antigens) from the analyte; 2. to provide a detectable signal for the sensor (or strictly speaking, transducer) to detect. The second subsystem is the sensor itself. The function of this subsystem is to detect the signal, or change in signal, caused by the binding of the biomarkers (antigen). The third subsystem consists of the electronic components that send/receive signals to/from the sensor, store measurements and process the data. This subsystem will be referred to as the measurement system. The function of the measurement is to provide input signals, read output signals, store these output signals and process the stored information for display purposes.

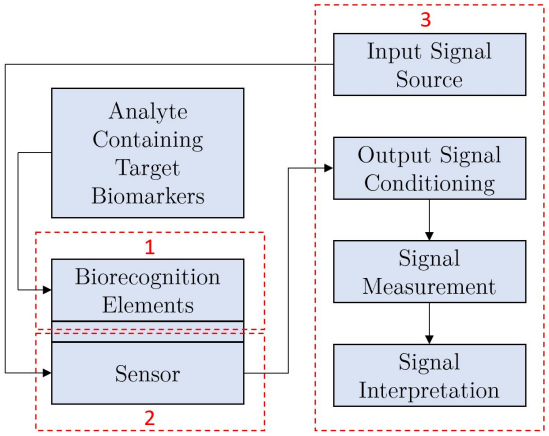

Figure 3.3: System overview showing the three main subsystems: 1. the biorecognition elements; 2. the sensor; 3. the measurement system.

3.2.3 Subsystem Requirements

Subsytsem 1: Biorecognition Elements

As mentioned above, the first subsystem involves the biorecognition elements, or more specifically the antibodies, for an immunosensor setup. The design of this subsystem requires knowledge of the physiology of the chosen biomarkers, and of the respective antibodies, to ensure that the antibody-antigen complex (referred to in section 2.5) has high binding affinity and that the binding of the antigens causes the largest possible detectable signal. The requirements of this subsystem are:

1. to capture as much of the required biomarker from the analyte as possible and bind it with high affinity.
2. to be specific to the biomarker and not bind to unrelated molecules.
3. to bind the biomarker in such a way that its presence has the greatest influence on the surface of the sensor, causing the largest possible detectable signal.

Subsytsem 2: Sensor

The second subsystem is the sensor, which is to detect a measurable signal upon binding of the target antigens to the antibodies immobilised to the sensor surface. The requirements of the sensor are:

1. to be sensitive to the binding of the target antigens.

2. to be cheap and disposable, suitable for daily use.
3. to be easily manufacturable.
4. to be stable in aqueous environments.
5. to be highly biocompatible - with regards to both materials and operating conditions.
6. to be suitable for antibody immobilisation.

Subsytsem 3: Measurement System

The measurement subsystem is concerned with the measurement and supply electronics of the system. The requirements for the design of the measurement subsystem are:

1. to convert AC and DC digital signals into analogue signals and supply the analogue signal to the sensor.
2. to control the input signal attributes to the sensor such as DC offset, amplitude, phase, etc.
3. to provide a stable interface with the sensor.
4. to measure and digitally record analogue signals received from the sensor in high resolution.
5. to display recorded signal data in real time.
6. to be capable of fully characterising the sensor.

3.3 Biomarker Selection

It was noted in section 2.1.2, that the ideal biomarker for infectious disease should: aid in the differentiation between viral and bacterial infections, aid in the determination of prognosis, aid in the monitoring of host response to an infection and antibiotic therapy, and finally guide antibiotic therapy. Furthermore, the studies by Meem et al. [12] and Hedegaard et al. [13] have shown that C-reactive protein (CRP) and procalcitonin (PCT) are two of the most widely used biomarkers for infectious disease, since they fulfil all of the requirements listed for the ideal biomarker. Based on the literature described in sections 2.1 and 2.2, C-reactive protein (CRP) and procalcitonin (PCT) were the chosen biomarkers for the rapid biomarker test.

Chapter 4

Design Finalisation and Manufacture

In the previous chapter, the system was divided into three subsystems: 1. the biorcognition elements; 2. the sensor; 3. the measurement system. The following chapter details the design, fabrication and finally integration of each subsystem, to form the complete system.

4.1 Biorecognition Element Design and Antibody Selection

The following section describes the design and selection of the main components of the biorecognition element subsystem.

4.1.1 Biorecognition Element Design

It was shown in section 2.5.2 that there are two main approaches to immunosensing, with regard to the antibody layout, namely the unlabelled and labelled approaches. Unlabelled immunosensors make sole use of the antibody-antigen bond to influence the sensor surface and produce a measurable change in signal. Labelled immunosensors, also known as sandwich type immunosensors, rely on an antibody-antigen-antibody-nanoparticle sandwich at the sensor surface to cause the change in signal.

It was shown that sandwich type immunosensors have yielded higher sensitivities and detection limits than unlabelled approaches due to signal amplification, mainly caused by the conjugated nanoparticles. It was therefore decided to use

this type of immunosensor design. A schematic of the antibody layout in a sandwich type immunosensor is shown in figure 2.8.

The chosen approach requires a pair of antibodies - one capture antibody and one detection antibody - that bind to different epitopes on the antigen. The capture antibody is required to be immobilised on the sensor surface and the detection antibody requires labelling with a nanoparticle.

Capture Antibody Immobilisation

It has been shown that optimised capture antibody immobilisation plays an essential role in increasing the performance of immunosensors, as described in section 2.5.3. Of the four methods described in section 2.5.3: adsorption, covalent immobilisation (cross-linking), biotin-streptavidin affinity immobilisation and antibody-binding proteins, the two methods showing the most promise for this application are cross-linking and biotin-streptavidin affinity immobilisation. Adsorption, although having the advantage of being simple and requiring no additional substances, does not guarantee a strong bond with the surface, does not guarantee antibody orientation, and poses the risk of antibody denaturing, thus negatively affecting the performance of the sensor. Antibody-binding protein immobilisation, although holding much potential, is ruled out due to the unsuitability to use in sandwich type immunosensors.

Both cross-linking and biotin-streptavidin affinity immobilisation have the advantages of no denaturing of the antibody, no binding site modification and linking molecules acting as spacers between the antibody and the sensor surface. Cross-linking has the added advantage of the formation of a strong, covalent, bond between the antibody and the surface. On the other hand, biotin-streptavidin affinity immobilisation has the advantages of good binding efficiency, with one streptavidin molecule binding up to four biotinylated antibodies; and importantly, good antibody orientation, increasing the antigen-binding effectiveness up to three times. Good antibody orientation and high binding efficiency are more valuable in immunosensor applications than the covalent bond presented by cross-linking, therefore, biotin-streptavidin affinity binding was the chosen immobilisation method.

An additional step is often included in the antibody immobilisation step, known as blocking. This is the process of blocking all binding sites after immobilisation, in order to ensure that no non-specific binding takes place when attempting to sense the target antigens, in this case CRP and PCT. Non-specific binding occurs when unrelated biomolecules bind to the surface of a sensor at binding sites, in this case the streptavidin binding sites and gaps in the streptavidin coating surface,

exposed after the immobilisation of antibodies. Blocking is usually accomplished by incubating an already immobilised surface with bovine-serum albumin (BSA) over a short time period. Therefore, the choice was made to include a blocking step after antibody immobilisation.

Detection Antibody - Nanoparticle Label Selection

The function of the nanoparticle label is to assist in signal amplification by enhancing the effect of the biomolecule complex, after binding of the antigen, on the surface of the sensor. Nanoparticles have also been reported to enhance electron transfer, and catalyse electrochemical reactions, as noted in section 2.5.2. Amongst the plethora of nanoparticles, gold nanoparticles (AuNPs) and horseradish peroxidase (HRP) nanoparticles have shown the most promise in immunosensing applications due to their biocompatibility. HRP is mainly used when the sensing mechanism requires an electrochemical catalyst upon binding of the target antigen and subsequent binding of the labelled detection antibody. AuNPs are more generally used due to their large surface area, which increases the "presence" of the detected antigen upon binding of the AuNP-labelled detection antibody. Many studies have demonstrated the large increase in sensitivity when using AuNPs for signal amplification, as shown in figure 2.9.

AuNPs were selected as the chosen detection antibody nanoparticle label due to the large array of evidence claiming an increase in sensitivity of an immunosensor when using AuNP-labelled detection antibodies.

Biorecognition Element Layout

According to the design choices made above, the layout of the biorecognition elements for the immunosensor are shown in figure 4.1.

4.1.2 Antibody Selection and Ordering

The sensitivity and specificity of a capture-detection antibody pair cannot be known before being tested together experimentally by immunoassay. Therefore, the goal of the antibody selection was to order several different antibodies for both CRP and PCT, thereafter testing experimentally, by immunoassay, the different antibody pairings, to find the optimal pairing.

Antibodies, however, are highly costly and can only be purchased in small quantities, limiting the number of different antibodies that could be ordered. The factors that were considered when choosing the antibodies were:

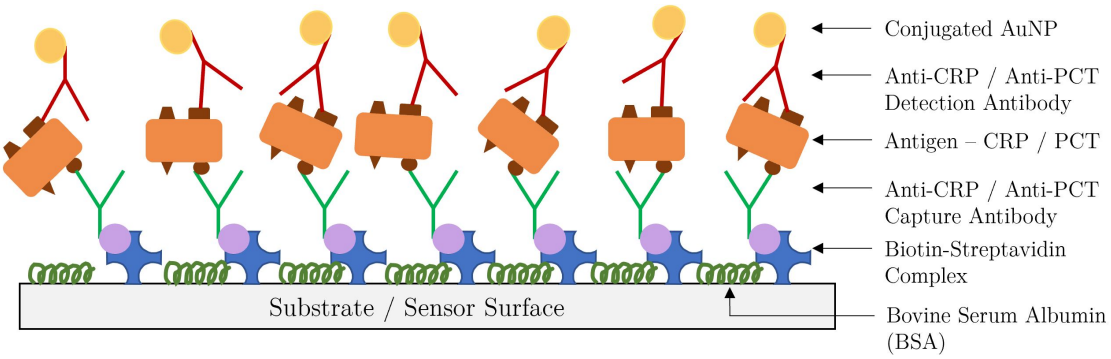

Figure 4.1: Illustration of the layout of the antibody-antigen-antibody-AuNP complex. Adapted from own understanding.

1. Cost - the combined cost of the antibodies were to stay within budget.
2. Clonality - The capture antibody was to be polyclonal, to ensure the highest amount of antigen was captured. The detection antibody was to be monoclonal to enhance specificity and ensure that a single detection antibody binds to each antigen, for quantification purposes (this was noted in section 2.5).
3. Host species - in order to test different antibody pairings using immunoassay, the requirement was that the capture and detection antibodies be from different host species.
4. Reactivity - all antibodies were to be reactive to human CRP or PCT.
5. Conjugation - all antibodies were to be unconjugated.
6. Application Suitability - all antibodies were to be made for application in ELISA or Western Blot.

All antibodies, along with CRP and PCT recombinant proteins, biotin, streptavidin and gold nanoparticles, were ordered through Biocom Biotech, and delivered to Synexa Life Sciences, where the antibody pair tests were scheduled. The list of ordered antibodies, as well as other biocomponents, is shown in table 4.1, and the data sheets of the antibodies and proteins used for final testing can be found in appendix A. Four different types of antibodies were ordered for CRP - one polyclonal and three monoclonal. Unfortunately, due to budget restrictions, polycloncal antibodies were not ordered for PCT. Therefore, three different types of monoclonal antibodies, targeting different epitopes, were ordered. Additionally, due to similar factors, insufficient PCT antibodies were ordered to justify testing each possible configuration during the pair testing. Thus, the PCT antibodies that

Table 4.1: Table of all biocomponents ordered through Biocom Africa

Name	Company	Type	Price (excl. VAT)
CRP Capture	Abcam	Polyclonal	R7 460.55
CRP Detection 1	BioVision	Monoclonal	R8 915.63
CRP Detection 2	Abcam	Monoclonal	R6 740.99
CRP Detection 3	Abnova	Monoclonal	R11 042.06
PCT Capture 1	GeneTex	Monoclonal	R10 105.69
PCT Capture 2	Cloud-Clone	Monoclonal	R6 196.28
PCT Detection	Abbexa	Monoclonal	R13 522.20
Recombinant Human CRP Protein	Abcam	N/A	R6 334.72
Recombinant Human PCT Protein	RayBiotech	N/A	R8 386.38
AuNP	Abcam	N/A	R6 408.83
LL Biotin Kit	Expedeon	N/A	R5 370.67
Purified Streptavidin	BioLegend	N/A	R2 472.81
Total			**R92 956.81**

were ordered with the largest quantity were chosen as detection antibodies, whilst the remaining two were assigned as capture antibodies.

The antibody pairing tests, where the optimal capture-detection antibody pairings were determined by experimentation with immunoassay, are documented in the validation chapter, section 5.1.

4.2 Sensor Design and Fabrication

The following section begins by describing the choice of sensor technology, thereafter detailing the design, fabrication and iterative optimisation process for the sensor.

4.2.1 Chosen Sensor Technology

As described in section 2.3, a biosensor uses specific biological interactions to detect biological compounds by the use of electrical, thermal or optical signals. Organic thin-film transistors (OTFTs), as a class of biosensors, have shown great promise as biosensors due to their easy manufacturability, low cost, high sensitivities and good biocompatibility. The two main architectures of OTFTs used for biosensing

applications are organic field-effect transistors (OFETs) and organic electrochemical transistors (OECTs), described in detail in sections 2.4.2 and 2.4.3 respectively.

Although both OECTs and OFETs have shown promise as biosensors, OECTs in particular have shown great performance as immunosensors, with the additional advantages of inherent signal amplification, inherent operation in aqueous electrolytes, simple device architecture, minimal material requirements and straightforward miniaturisation. These advantages, along with excellent published reviews on OECT sensor performance, led to the selection of the OECT architecture for the sensor design. Furthermore, according to reported literature, the requirements of the sensor, stated in section 3.2.3, can all be satisfied by an OECT sensor.

4.2.2 Chosen Sensor Patterning Method

In order to satisfy the requirements for a cheap, disposable and easily manufacturable sensor, an appropriate fabrication method was sought in literature. From the literature, briefly described in section 2.4.4, inkjet printing was identified as the preferred patterning method for the fabrication of many OECT-based biosensors, even on commercial scale. The only requirement for this method is that the choice of electrode material and organic semiconductor be solution processable. The advantages of inkjet printing are that it is an easily accessible technology, there are many commercially available conductive and semiconductor inks, the substrate (any type of gloss or photo paper) is cheap and readily available, paper is easily disposable, patterning to a relatively high resolution is possible, it is a high throughput process and it is straightforward. Furthermore, Retief et al. [64] of the SAND group in Stellenbosch University, modified a desktop inkjet printer as a low-cost material deposition device, for applications specifically related to organic electronics. For the advantages listed above and the convenience of having it readily available, inkjet printing was the chosen patterning technique.

4.2.3 Chosen Sensor Materials

As shown in the OECT architecture, the most basic components of an OECT are: the drain, source and gate electrodes, the semiconductor material, the substrate, and the electrolyte. The main requirement of these materials, apart from the electrolyte, are that they are stable in aqueous conditions and that they are suitable for inkjet printing.

Electrode Material

A solution processable conductive ink was required for the electrode material. Silver nanoparticle ink, especially developed for inkjet printing of thin-film organic electronic circuitry, already showed good performance when printed on the modified desktop inkjet printer. This ink, similar to many different conductive inks, requires an additional baking step, in an oven at 100 degrees Celsius for one hour, to ensure correct sintering of the nanoparticles. Despite this additional step, due to its availability, this ink was chosen for the electrode material of the OECT.

Semiconductor Material

The list of semiconductor materials that were suitable to application in the sensor were narrowed down into those that were commercially available for solution processing techniques. PEDOT:PSS was the favoured semiconductor for OECT applications in literature, and has is also available in aqueous form specifically for solution processing purposes. Furthermore, as noted in section 2.4.3, PEDOT:PSS based OECTs are highly biocompatible since they are normally-on devices, allowing low voltage operation. For the reasons mentioned above, PEDOT:PSS was the selected as the choice semiconductor.

Substrate Material

Materials that were considered for the substrate on which to print the sensor included different types of paper, polymers, plastic films and glass. The requirement for the sensor to be low cost and easily manufacturable narrowed the search down to paper only, since paper is the cheapest and most widely available of the aforementioned options. The additional requirement that the sensor be stable in aqueous conditions further narrowed the list of applicable paper types to those that showed improved water resistance. This would also ensure that the electrodes remain in a thin film on the surface of the substrate, instead of seeping into the paper and potentially causing a short-circuit.

The three paper types that were considered for the sensor substrate were: 1. Mitsubishi paper - especially designed for printed electronics, 2. Ultra gloss paper - designed for photo printing, 3. Waterproof paper - also designed for photo printing. Two tests were done to assess the performance of the different paper types. The first test entailed printing silver nanoparticle ink onto each of the three paper types, and subsequent baking at 100 degree Celsius, to assess their general print quality, resolution and series resistance. The second test entailed dropping a single water droplet on the surface of the paper and observing the water resistance of the paper. The results of the first test showed that the ultragloss paper

had the highest print resolution and lowest series resistance, but the silver ink was easily removed from the surface. The Mitsubishi paper had a slightly lower print resolution and a slightly higher series resistance, but the silver ink remained on the surface of the paper more easily. The waterproof paper showed bad print resolution and high series resistance due to the face that the silver nanoparticles could not sinter correctly on its surface. In the second test, the water resistance of the three paper types were about the same.

Due to its consistent performance in the tests mentioned above, the Mitsubishi paper was chosen as the sensor substrate.

Choice of Electrolyte

In the case of this sensor, and any OECT sensor, the analyte containing the CRP and PCT proteins can be used as the electrolyte necessary for the operation of the OECT. It is envisioned that in the future the sensor will operate in serum; however, for research purposes the use of serum is unnecessary. Phosphate buffered saline (PBS) is a highly biocompatibe electrolyte that is commonly used as a buffer for biological substances. All OECTs, including OECT-based immunosensors found in literature, made use of PBS as the electrolyte. Furthermore, immunoassays such as ELISA and MSD make use of PBS as the analyte buffer. Therefore, PBS was the chosen electrolyte (and analyte) for both OECT characterisation (no added proteins) and for sensing purposes (CRP and PCT added to PBS).

4.2.4 Iterative Sensor Design and Optimisation

The sensor design process began with the sensor requirements (stated in section 3.2.3) as well as the basic OECT architecture (shown in figures 2.3a and 2.3b) in mind, and was concerned with developing and characterising a working OECT. This process, being iterative, was extremely lengthy, with over 300 different prototypes being tested before arriving at a working OECT prototype. For the sake of brevity, the four most important iterations of the design process will be described. Additionally, it should be noted that the measurement system, described in section 4.3, was used to characterise the different OECT design iterations.

Iteration 1: All Printed OECT Layout

The first iteration describes the initial OECT design, comprised of electrodes and a semiconductor printed directly onto the substrate, based on the architecture shown in figure 2.3b. Here, the electrodes were first printed onto the paper, followed by the printing of three PEDOT:PSS layers and baking at 100 degrees Celsius for one

hour. In order to test the effect of different parameters on transistor performance, different electrode patterns were designed in GIMP (GNU Image Manipulation Program) [65], an open-source raster graphics editor, and subsequently tested.

Testing the output characteristics of the different configurations yielded similar results for each configuration: the addition of the PBS caused the device to lose functionality within the first minute of the sweep. These results are demonstrated by figure C.2 and figure C.3, where the device clearly ceases to function during the second gate voltage sweep.

From this point, a single transistor configuration was selected for subsequent optimisation, in order to limit variables in the iterative design procedure. Therefore the sensor configuration anticipated to hold the most promise as a sensor, shown in figure 4.2, was chosen. This configuration was chosen due to its anticipated sen-

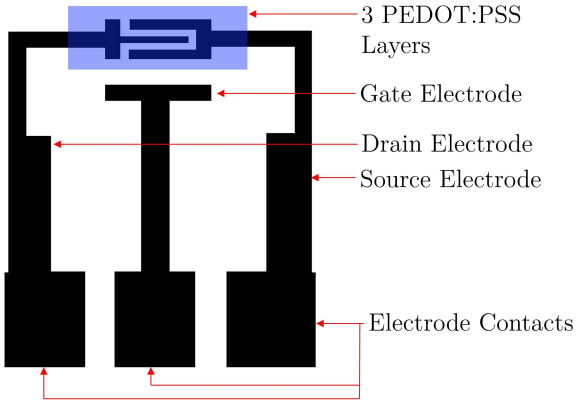

Figure 4.2: Initial OECT design showing the electrode pattern along with the PEDOT:PSS semiconductor layer. This configuration has a height of 7.5 mm, width of 7 mm and a channel width of 100 μm.

sitivity to the addition of the antibodies and proteins, due to its compact shape and relatively long channel.

Iteration 2: Addition of Photoresist Coating

In the second iteration, an additional step was added to the fabrication process to improve the stability of the OECT in aqueous conditions and ensure zero PBS seepage. A method developed by J.D. Retief [64] of the SAND group at Stellenbosch University (further described in section 4.4.1), allows the selective coating

of paper with S1818 photoresist, whilst leaving the printed circuitry and semiconductor uncoated. This method was employed, after the printing of the electrodes and PEDOT:PSS, to coat the bare paper with photoresist, increasing the stability of the OECT when immersed in PBS electrolyte. The addition of the photoresist layer is shown in figure 4.3.

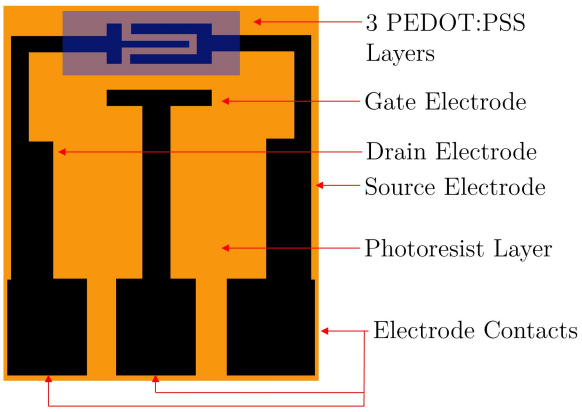

Figure 4.3: Second OECT design iteration showing the addition of the photoresist layer in orange.

The example output characteristics given by figures C.4 and C.5, show that the OECT had improved endurance, with the photoresist layer increasing the water resistance of the paper substrate. Despite this, however, the drain current was unresponsive to changes in supplied gate voltage, decreasing, instead of increasing, for a negative gate voltage sweep. This behaviour indicated that the OECT deteriorated over the sweep time period and that changes in the gate voltage were not causing a corresponding change in the doping level of the organic semiconductor, as required. Two further observations were made: the first being the oxidation of the gate electrode at the edge of the PBS droplet, causing the gate electrode to disconnect from the gate contact pad; the second observation was a noticeable change in colour of the source electrode as cations penetrated the semiconductor and flowed in the direction of majority carrier flow.

Iteration 3: Addition of Immersed Gate and Increased Amount of PEDOT:PSS Layers

The goal of the changes made in the third design iteration were to increase the effect of the gate voltage on the doping level of the semiconductor, and ensure the gate electrode did not lose functionality due to oxidation. It was hypothesised that the decrease in drain current over time was due to both the breakdown of

the PEDOT:PSS semiconductor, as well as the low anion density, with only three layers of PEDOT:PSS, causing early semiconductor saturation.

For this iteration, the amount of PEDOT:PSS layers were increased by 5 layers, to a total of 8 layers, to combat the breakdown of the PEDOT:PSS and to increase the amount of anions in the active semiconductor film. Additionally, the thin-film printed gate electrode was replaced by a sterling silver immersed electrode (as shown in the figure 2.3a schematic) to negate the effect of oxidation at the gate. Furthermore, a laser cut perspex well was attached to the sensor to constrain the PBS droplet on the surface of the sensor. The new print configuration (excluding the gate electrode and perspex well) is shown in figure 4.4.

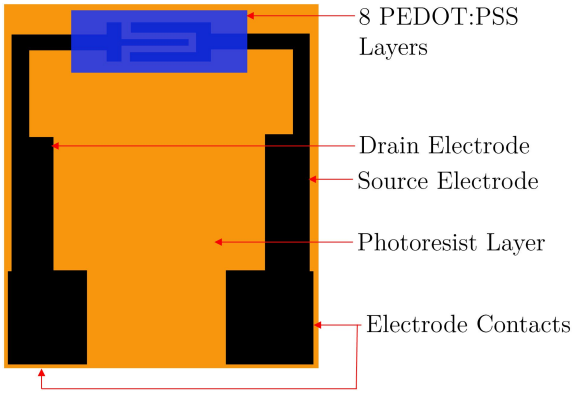

Figure 4.4: Third OECT design iteration showing the removal of the thin-film gate electrode.

The OECT output characteristics for the third iteration are shown in figures C.7 and C.8. Here, to ensure that the semiconductor was not broken down due to current spikes at the end of each sweep, the drain voltage sweep was changed to include a backward sweep following the peak value of the forward sweep, as shown in figure C.6. Additionally, the example output sweep shown here indicates a positive gate sweep, which should show decreasing values for the drain current in the output characteristics. In contrast, the output characteristics indicate an increasing drain current for increasing gate voltages. Although figure C.7 does not show conclusive information, figure C.8 shows the increasing trend in drain current linked to an increasing gate current. Here, the drain current clearly followed the gate current, with the gate current contributing towards the measured drain current.

Iteration 4: Addition of 5 μL Drop of PEDOT:PSS Semiconductor and Widening of Channel

In the third iteration, the domination of the gate current was attributed to the high transverse conductance and thin layer thickness of the PEDOT:PSS, allowing current to flow, with little resistance, between the immersed gate and the channel. Therefore, in the fourth and final design iteration, two changes were made to ensure the gate electrode affected the doping level of the PEDOT:PSS only, and did not contribute to the measured drain current. The first change was to dramatically increase the layer thickness of the PEDOT:PSS layer to ensure no current flow between the gate and the channel in a transverse direction, and to increase the capacity of the PEDOT:PSS layer for ion transfer between itself and the electrolyte. The second change was to increase the channel width, allowing the doping level of the semiconductor to have a larger effect on the channel current, by increasing the length of the current path through the PEDOT:PSS.

The PEDOT:PSS layer thickness was increased by replacing the 10 inkjet printed layers with a single 5 μL drop of PEDOT:PSS ink, dispersed by a pipette. The channel width was increased from 100 μm to 200 μm on the GIMP design. The final print configuration (excluding the gate electrode and PEDOT:PSS layer) is shown in figure 4.5. The fabrication process of this iteration is detailed in section 4.4.1.

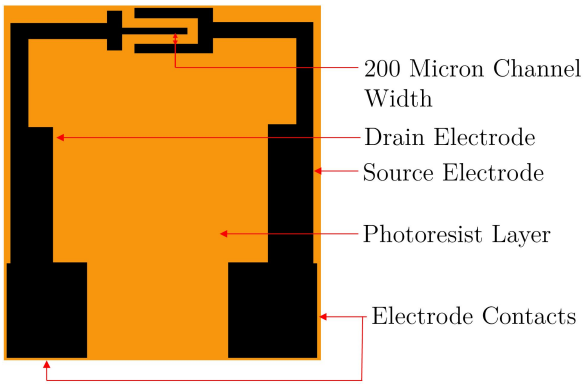

Figure 4.5: Fourth and final OECT design iteration showing the increased channel width and removal of the PEDOT:PSS layers.

The output characteristics of the fourth OECT design iteration are shown in figures C.10 and C.11. It can be seen by these figures that this iteration exhibited output characteristics indicative of an OECT. Here, an increasing gate voltage caused a corresponding increase in the amount of cations being injected into the

semiconductor, thus decreasing the doping level and the resulting channel current in the semiconductor. This resulted in an overall decrease in drain current corresponding to the increase in gate voltage.

A detailed characterisation of the working organic electrochemical transistors developed as described, showing the output and transfer characteristics, is given in section 5.3.

4.3 Measurement System Design

The measurement system has two main objectives, the first being to fully characterise the sensor, and the second being to perform the final sensor measurements. According to figure 3.2, the measurement system is made up of four components: supply signal to the sensor, output signal conditioning, output signal measurement and recording, and signal processing and display. The requirements of the measurement system are listed in section 3.2.3.

4.3.1 Measurement System Selection and Design

The sensor design, described in section 4.2, indicated that an organic electrochemical transistor with the p-doped organic semiconductor, PEDOT:PSS, was chosen and designed as the sensor. OECTs are three channel devices that consist of a source, drain and gate electrode, similar to the well-known MOSFET transistor. Since the majority carriers in p-doped semiconductors are holes, the OECT can be schematically represented by a PMOS transistor. The connection diagram for interfacing the measurement system with the OECT, represented by a PMOS transistor, is shown in figure 4.6.

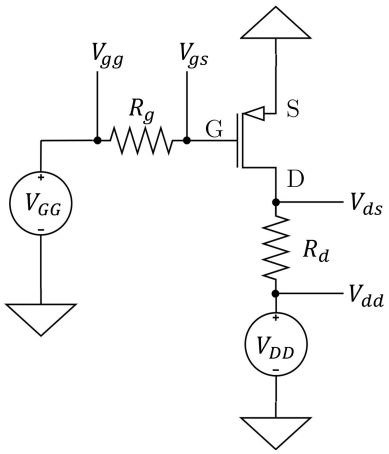

Figure 4.6: Diagram showing voltage supply and measurement points for the OECT, represented by an PMOS transistor.

Here, the source electrode is connected to ground, whilst the input signals are supplied at the gate (V_{GG}) and the drain (V_{DD}) electrodes respectively. Four voltage signals require measuring in order to fully characterise the transistor and determine current flow through the device. These are the two supply voltages: V_{gg} and V_{dd}, and the voltages at the gate and drain terminals: (V_{gs}) and (V_{ds}). By inserting resistors of known magnitude at the drain and gate terminals, the respective drain current (I_d) and gate leakage current (I_g) can be determined by Ohm's Law, since the voltages at each end of the resistor are known.

Instruments considered for the supply, measurement, recording and display of signals included microcontrollers, source meters, and data acquisition devices. The advantage of a microcontroller is its small and compact size, however, its use would require many peripheral components. Source-meters, such as the Keithley SourceMeter series, are often used for device characterisation and sensor measurements in literature [44]. These, however, are highly costly and were therefore not considered. Data acquisition devices (DAQs), especially National Instruments DAQs controlled by LabVIEW software, were used for device characterisation and sensor measurements in some literature, showing good performance [30].

The National Instruments Compact Data Acquisition (NI-cDAQ) system was found to be a convenient platform for the integration of many of the required hardware components, allowing a combination of hardware to be controlled by a single virtual user interface based on the LabVIEW software. This device, with a 16-channel differential input analogue-to-digital converter (ADC) module, as well as a 16-channel digital-to-analogue converter (DAC) module was chosen as the integrated

supply and measurement device. Furthermore, the device was coupled to the LabVIEW measurement software for control, signal conditioning, processing and display purposes, thus satisfying all requirements stated in section 3.2.3. The NI-cDAQ, showing the NI 9205 ADC module and the NI 9264 DAC module, as well as the DAQ connection diagram, are shown in figure 4.7. The DAQ was connected

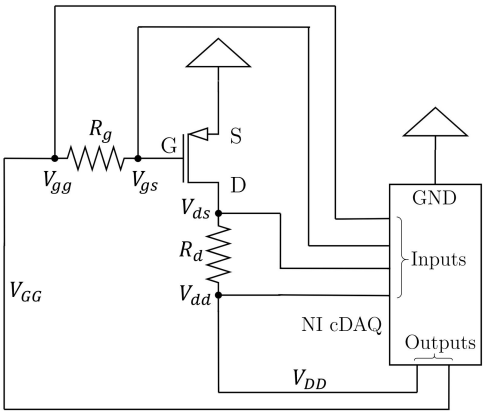

(a) Connection diagram of the NI cDAQ.

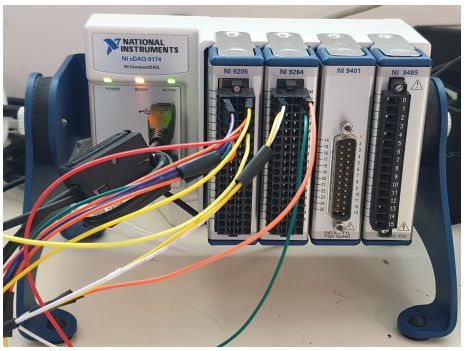

(b) Photo of the NI cDAQ showing the 9205 ADC module and the 9264 DAC module.

Figure 4.7: Connection diagram and photo of the NI cDAQ.

directly to the OECT via a PCB mounted in a 3D printed chassis. The PCB, containing the drain and gate resistors, was connected to the supply and measurement DAQ channels via shielded wires on the one end, and was connected to the OECT electrode contacts via spring-loaded contact pins on the other end. The immersed silver gate electrode was held into the PBS electrolyte via a suspended crocodile clip. This set-up is shown in figure 4.8.

4.3.2 LabView Control and Measurement Programs

The LabVIEW software was used to control the output signals of the DAQ and to record the input signals read at the outputs of the transistor. Three different programs were developed in LabVIEW. The first program was used to send constant DC voltages to both the drain and gate electrodes. The second program was designed to supply a constant value at one electrode, and sweep the voltage at the second electrode. This was used for the transfer sweep in order to develop the transfer curves. The final program was designed to sweep both the drain and the gate voltages sent to the OECT in order to determine the output characteristics of the transistor. The block diagrams corresponding to the three separate LabVIEW programs, as well as the designed virtual interface (VI), are shown in appendix E.

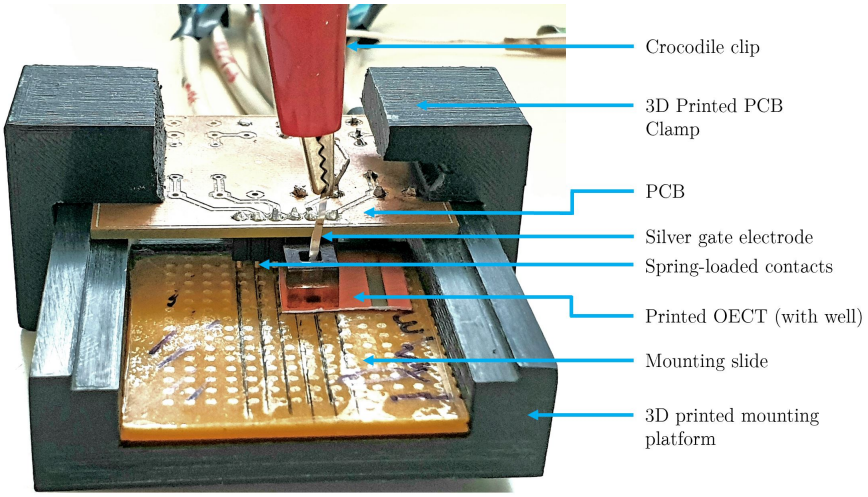

Figure 4.8: Sensor connection set-up.

4.4 Integrated Sensor Fabrication for Final Testing

The following section describes the process of fabricating a fully functional OECT, followed by the process of antibody immobilisation onto the OECT surface. This was the process followed for the fabrication and activation of the final sensors.

4.4.1 OECT Fabrication

The 6 step OECT fabrication process is listed below:

1. Print a batch of electrodes onto the Mitsubishi paper using the inkjet printer.
2. Spin coat the entire batch of transistors with S1818 photoresist. The spin coating process is described as:
   (a) spin the sample at 600 rpm whilst rapidly dripping 1 mL of photoresist at the center of the sample.
   (b) after 30 seconds, gently ramp the speed to 2000 rpm over 5 seconds.
   (c) leave the sample to spin for an additional 5 to 10 seconds before stopping.

   Figure 4.9 shows the electrodes before (i) and after (ii) spin coating, whilst the third image (iii) shows the result of incorrect spin coating, with the photoresist clearly covering the electrodes.

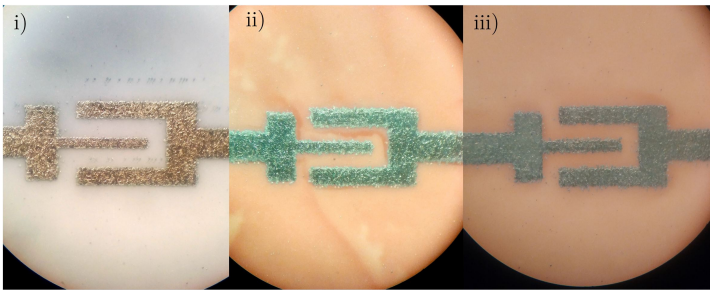

Figure 4.9: Optical microscope images of the OECT electrodes: i) before spincoating, ii) after spin coating, iii) incorrect spin coating.

3. Bake the spin coated electrodes at 100 degrees Celsius for one hour.
4. Add 5 μL drops of PEDOT:PSS onto the electrode area, ensuring the channel is properly covered, as shown in figure 4.10a.
5. After adding the PEDOT:PSS drops, bake the transistors (shown in figure 4.10a) at 100 degrees Celsius for 2 hours, resulting in a thin film of PEDOT:PSS covering the electrodes, as shown by figure 4.10b.
6. Add the clean laser cut perspex wells to each transistor, taking care not to contaminate the PEDOT:PSS layer.

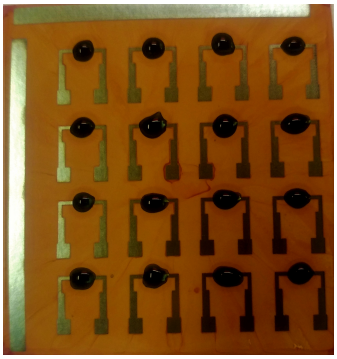

(a) Addition of the 5 μL drop of PEDOT:PSS to a printed and spin coated batch of OECTs.

(b) Optical microscope image of the PEDOT:PSS drop on the sensor, after baking.

Figure 4.10: 5 μL drop of PEDOT:PSS before and after baking.

After this fabrication process, the OECT is ready for capture antibody immobilisation.

4.4.2 Antibody Immobilisation onto OECT Sensor

The antibody immobilisation method consists of four main steps and is conducted over two days. A more detailed description of the immobilisation method, including the relevant reagent preparations, is given in appendix F.1. The four main steps are:

1. Immobilise streptavidin to the surface of the PEDOT:PSS layer.
2. Biotinylate the capture antibodies.
3. Immobilise the biotinylated capture antibodies to the sensor.
4. Add BSA to block all unbound binding sites.

After immobilisation, the OECT immunosensor is fully functional and ready to test.

Chapter 5

System Validation

5.1 Antibody Pairing Tests

The purpose of the antibody pairing tests were to determine the optimal capture-detection antibody pair, from the ordered antibodies. The performance of an antibody pair reflects the effectiveness of the antibody-antigen binding process, which has a major effect on the sensitivity of an immunosensor. Put simply, the more antigens (proteins) that bind to the capture antibodies, and the more detection antibodies that subsequently bind to those antigens (proteins), the stronger the signal and the higher the sensitivity of the biorecognition process.

5.1.1 Test Description

Two different immunoassays were used for the respective antibody pairings - a meso scale discovery (MSD) electrochemiluminescence (ECL) assay, and an enzyme-linked immunosorbent assay (ELISA). These immunoassays are the current laboratory standard for CRP and PCT detection and quantification and are briefly described in section 2.2.4. The CRP pairing was done on MSD and the PCT pairing was done on ELISA, due to the quantity of ordered PCT antibodies being too small to justify an MSD test.

The methodology followed for the antibody pairing tests is comprehensively documented in appendix B, while the results are given in the following section, section 5.1.2.

5.1.2 Antibody Pairing Results

The results of the pairing tests for CRP and PCT are shown in figure 5.1.

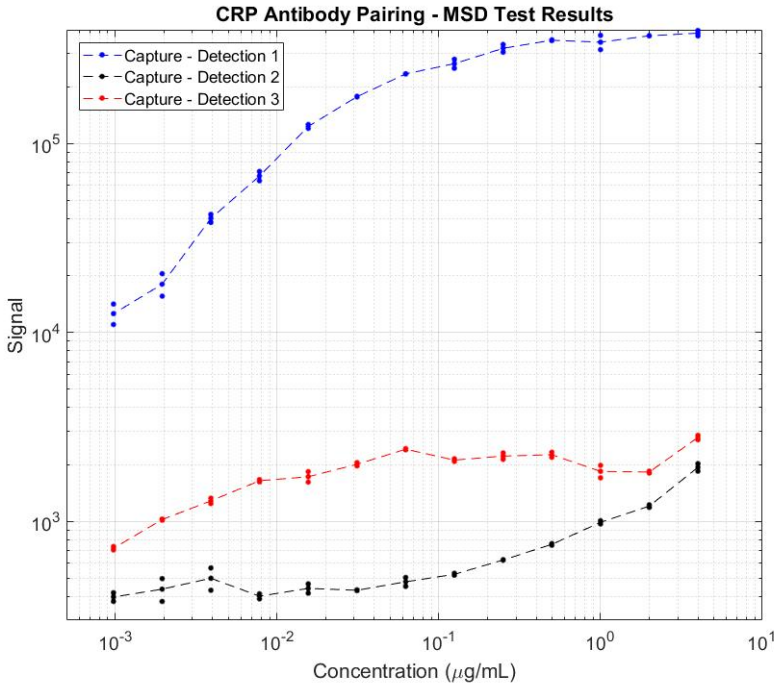

(a) Results from the MSD test for CRP antibody pairing

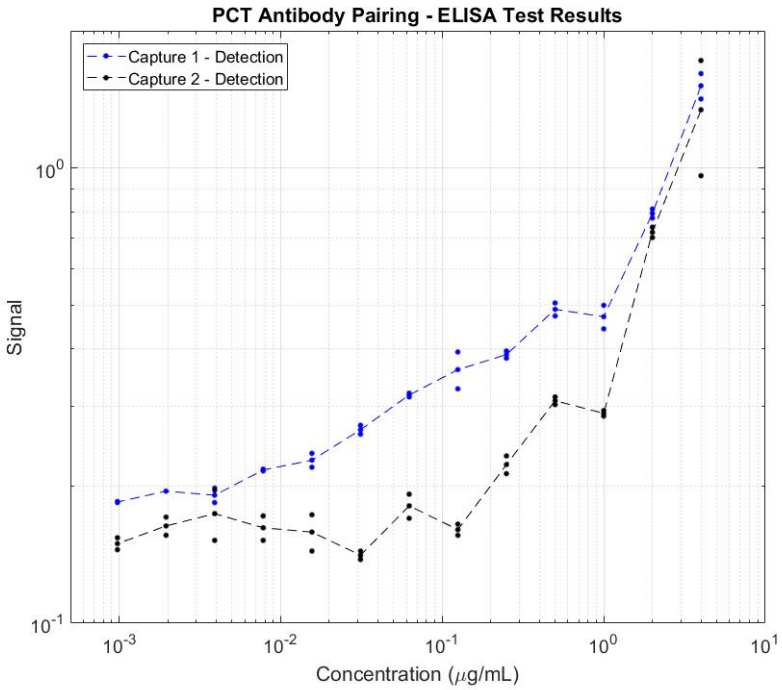

(b) Results from the ELISA test for PCT antibody pairing

Figure 5.1: Antibody pairing test results for CRP and PCT respectively

The plots shown in figure 5.1 were constructed from the raw data acquired from the MSD and ELISA tests respectively. Both the MSD and ELISA assays detect the the change in signal strength for different antigen concentrations (in an analyte) with respect to a blank control (containing no antigens). As stated in the methodology, sequential concentrations of the analyte, being CRP and PCT proteins in phosphate buffered saline (PBS), were added to every second well of the assay. Thus, two of the same analyte concentration were tested side-by-side for averaging purposes. The plots, therefore, show two slightly different signal strengths for the same concentration, with the dotted line joining the average signal strength for each sequential concentration.

Three different antibody pairs were tested for CRP according to the MSD methodology described in appendix B.2: Capture - Detection 1, Capture - Detection 2, and Capture - Detection 3. From the results shown in figure 5.1a, there are distinct differences in performance shown for the three respective pairings. The performance of a particular antibody pair is shown by the gradient of the averaged data points, that is, the degree to which the change in antigen concentration (independent variable) causes a corresponding change in signal strength (dependent variable). According to this, the best performing pair of CRP antibodies was the "Capture-Detection 1" pair, showing an overall higher signal strength as well as the steepest gradient over the given concentration range.

Similarly, two different antibody pairs for PCT were tested according to the ELISA methodology described in appendix B.1: Capture 1 - Detection and Capture 2 - Detection. The results of this test are plotted in figure 5.1b. Here, the "Capture 1 - Detection" pair showed the highest sensitivity, with a higher overall signal strength and a steeper gradient over the concentration range.

From these results, the antibody pairs selected for the final system design and testing were: "Capture - Detection 1" for CRP, and "Capture 1 - Detection" for PCT.

5.2 Measurement System Validation

The measurement system was validated in three different ways. First, the outputs of the DAC module were verified with an oscilloscope to determine the accuracy of the controlled output voltages. The DAC module performed satisfactorily in these tests. Secondly, the inputs of the ADC module were tested by inputting known voltages, and comparing the measured signal to the simultaneously measured oscilloscope reading. Again, the ADC module performed satisfactorily. The third test

conducted to validate the measurement system was to test the ability of the system to characterise an off-the-shelf NMOS transistor. Here, the NMOS transistor was connected to the measurement set-up and the three different LabVIEW programs were used to fully characterise the transistor. The results from testing the output sweep program are shown in figure 5.2. The output curves correspond with those shown in the datasheet of this particular NMOS, therefore validating the output sweep measurement program. In the same way, the transfer sweep program as well as the constant DC output program, were validated. The measurement system, therefore, showed good performance and was considered ready to perform OECT characterisation and final sensor tests.

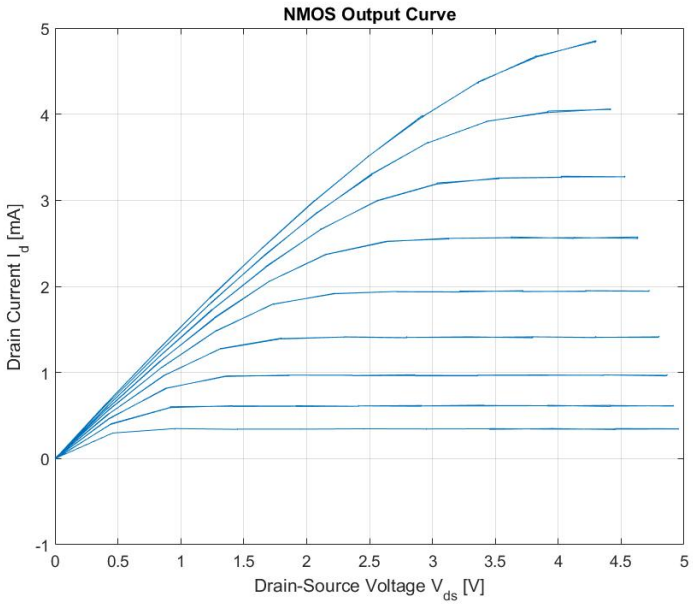

Figure 5.2: Output curves for the NMOS transistor for validation of the output sweep program developed in LabVIEW.

5.3 OECT Characterisation and Validation

The fourth iteration described in the OECT design process (section 4.2), led to the first working OECT. That is, the first OECT exhibiting output characteristics required for classification as an organic electrochemical transistor. Furthermore, in order to use the OECTs as sensors, it is first required that their output and transfer characteristics be known, for the OECT operating point (or biasing point) to be determined.

The OECTs were characterised using the NI cDAQ and corresponding measurement set-up, controlled by the relevant the LabVIEW programs, described in section 4.3. There were slight deviations in the performance and characteristics of different OECTs due to inconsistencies inherent to the manual fabrication process. The output and transfer characteristics of a selected transistor are described in this section. The characteristics of three other OECTs are given in appendix D.

5.3.1 Output Characteristics

The output characteristics of the OECT were determined by conducting an output voltage sweep and measuring the response of the transistor to each incremental gate voltage, using the measurement system described in section 4.3. The output characteristics are shown in figure 5.3.

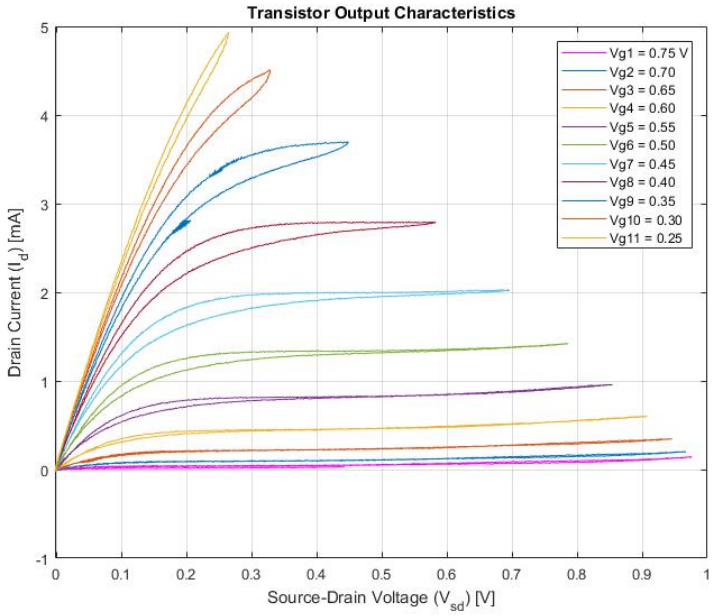

Figure 5.3: OECT output characteristics for a gate voltage varying from 0.75 to 0.25 V.

The output characteristics of the OECT resemble those found in literature [44; 51], such as those shown in figure 2.5 [46]. These results show an increasing gate voltage causing a corresponding decrease in drain current, as a result of a reduction in the ion penetration (de-doping) of the PEDOT:PSS. They also indicate two

specific regions - a non-saturation and a saturation region. In the non-saturation region, the drain current is dependent on both the source-drain voltage and the gate voltage. In the saturation region, the drain current in dependent on the gate voltage alone, and is independent of the source-drain voltage. This is particularly useful in amplification and sensing applications, where the OECT is typically biased in the saturation region. Furthermore, figure 5.3 shows a difference in the measured value between the forward and backward sweeps, known as hysteresis error. Hysteresis error indicates that the output of the system at a specific point is dependent on the previous state, which affects the repeatability of a device. This dependency is brought about by the capacitive effects of residual charge trapped in the semiconductor, as well as the low ion mobility limiting the response time of the OECT.

5.3.2 Transfer Characteristics

The transfer characteristics of the OECTs were determined by biasing the OECT at a specific drain voltage, and sweeping the gate voltage. The transfer curve along with the corresponding gate leakage current are plotted in figure 5.4.

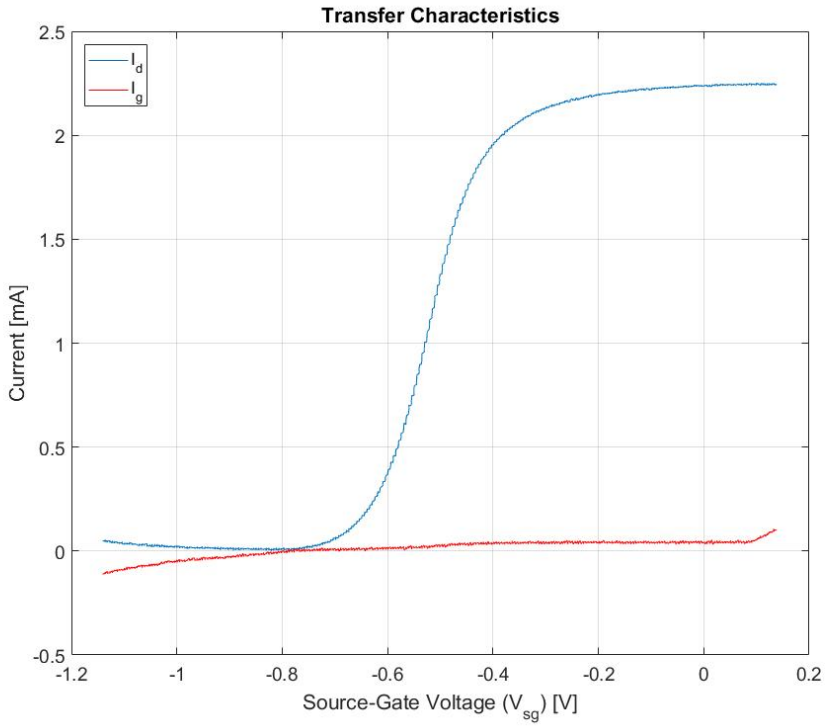

Figure 5.4: OECT transfer characteristics for a drain voltage of 0.34 V.

The transfer characteristics are in agreement with those found in literature, such as the transfer curve shown in figure 2.6. The transfer curve is useful in determining both the turn-on voltage of the OECT and the point at which the peak transconductance occurs. Transconductance describes the extent to which a change in gate voltage causes a corresponding change in drain current. It is, therefore, the main transistor parameter that governs signal amplification, and thus affects the sensitivity of OECT-based sensor. The transconductance is described by the gradient of the transfer curve, with the peak transconductance occurring at the inflection point (or point of steepest gradient) of the transfer curve. Figure 5.5 shows the transconductance plotted for the transfer curve shown in figure 5.4. From this, the peak transconductance occurs at $V_{sg} = -0.5$ V.

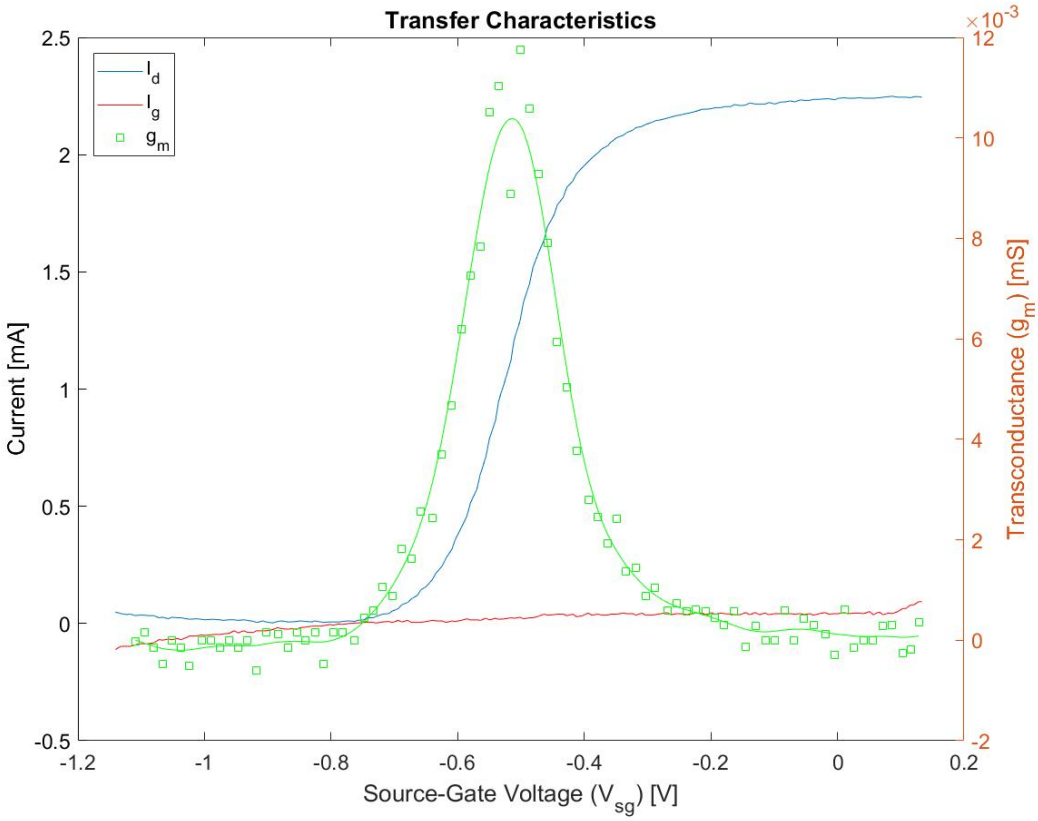

Figure 5.5: Transfer characteristics plotted with corresponding DC transconductance ($\delta I_d/\delta V_g$).

Chapter 6

Results and Discussion

The following chapter first describes the tests that were conducted to evaluate the performance of the immunosensor. It then presents the results of each test, both for CRP and PCT, and finally discusses the results from the tests in order to draw a conclusion on the sensor performance.

6.1 Test Description and Methodology

In order to test the performance of the OECT-based immunosensors, for both CRP and PCT, three different tests were conducted, using the measurement system and LabVIEW programs described in section 4.3. Each test was designed with the literature and the objectives in mind. Literature showed that the sensing mechanism relied on the change in effective gate voltage due to the binding of the biomarkers to cause a change in the drain current, whilst the objectives imposed a time limit on the tests.

The sensors for these tests were fabricated according to the method described in section 4.4, while the AuNP-labelled detection antibody solution and the PBS-buffered recombinant protein dilutions required for each test were prepared according to the methodology described in appendix F.2.

6.1.1 Test 1

The goal of the first test on the OECT immunosensors was to qualitatively determine the effect of the serial addition of recombinant protein dilutions, buffered in PBS, on the transfer characteristics of a transistor. Analogous to cyclic voltammetry, this was done by biasing the OECT at a drain voltage of $V_{DD} = -0.4$ V, whilst sweeping the gate voltage back and forth between $V_{GG} = 1.2$ V and $V_{GG} = -0.2$ V,

and adding sequential protein dilutions at the start of each sweep (i.e. where $V_{GG} = 1.2$ V). In order to determine the effect of the addition of ions to the system when adding PBS (in which the proteins were buffered), this test was first done by adding PBS only, to establish a baseline. The test was then repeated three more times with the sequential protein dilutions. The pair of each forward and backward sweep took about 100 seconds, and the elapsed time for each test was about 15 minutes. Furthermore, it should be noted that this test was done with the recombinant proteins only, and the AuNP-labelled detection antibodies were not added, due to the nature of the test requiring sequential addition of differing protein dilutions. The results of this test, for PBS only, CRP and PCT, are shown in section 6.2.1, where the drain current is plotted against the source-gate voltage for each test.

6.1.2 Test 2

The second test was designed with the goal of establishing a calibration curve for the immunosensors (like that shown in figure 2.9), in which a certain concentration corresponds to a specific change in drain current. In this test, the OECT was initially biased at $V_{GG} = 0.4$ V and $V_{DD} = -0.4$ V, and the OECT's response to a gate voltage step was measured by stepping the gate voltage from 0.4 V to 0.8 V. The gate voltage was stepped one minute after adding: PBS, a single dilution of recombinant proteins, and the AuNP-labelled detection antibodies. This was done for six different recombinant protein dilutions in an attempt to quantify the effect of protein binding, and subsequent AuNP-labelled detection antibody binding, on the response of the sensor. Figure 6.4 shows the results of stepping the gate voltage after adding PBS, a CRP recombinant protein dilution at a concentration of 20 μg/mL, and the labelled detection antibodies. The calibration curves were subsequently determined by plotting the normalised change in drain current in response to the corresponding gate voltage step, for each different protein dilution. The calibration curves are shown for CRP in figures 6.5 and 6.6, and PCT in figures 6.7 and 6.8.

6.1.3 Test 3

The third test, in a similar way to the first test, was concerned with determining the effect of protein binding on the transfer characteristics of the sensor. However, in this case, the transfer characteristics were determined before the addition of a protein dilution and after the addition of both a protein dilution and AuNP-labelled detection antibodies. This was done by first performing a transfer sweep with PBS, thereafter adding a dilution of recombinant proteins, waiting five minutes before adding the AuNP-labelled detection antibody reagent, waiting another five

minutes, and finally conducting another transfer sweep. In this case, the sweeps were conducted by biasing the sensor at $V_{DD} = -0.4$ V and sweeping the gate voltage from $V_{GG} = 1$ V to $V_{GG} = -0.2$ V, in the forward direction only. These tests were done with six different recombinant protein concentrations, and the results before and after the addition of a recombinant CRP dilution, at a particular concentration, are plotted in figure 6.9. To establish a calibration curve from each set of results, the normalised change in drain current (at a specific source-gate voltage) before and after having added the particular recombinant protein dilution and AuNP-labelled detection antibodies, were plotted. These are shown for CRP and PCT in figures 6.10 and 6.11 respectively.

6.2 Test Results

6.2.1 Test 1

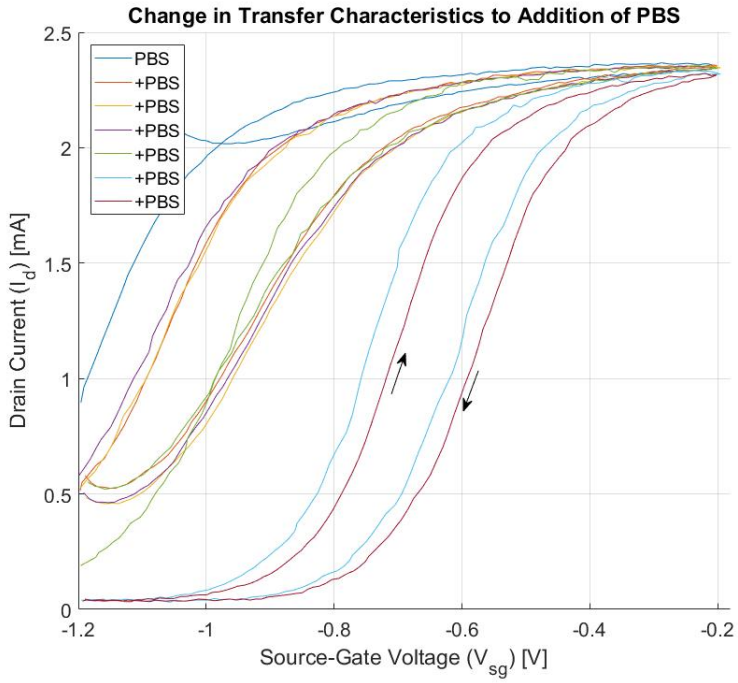

Figure 6.1: Effect of cumulative addition of PBS on the sensor transfer characteristics.

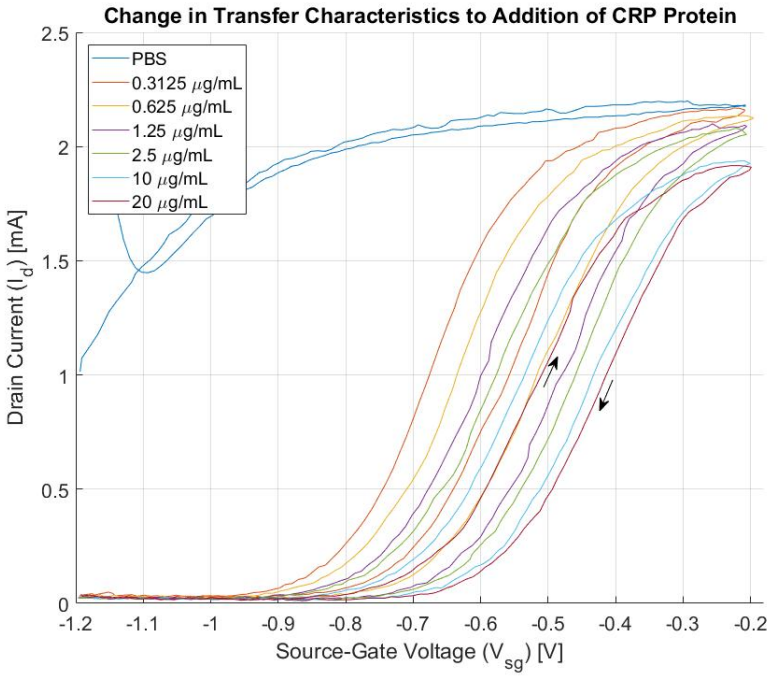

Figure 6.2: Effect of sequential addition of CRP on sensor transfer characteristics.

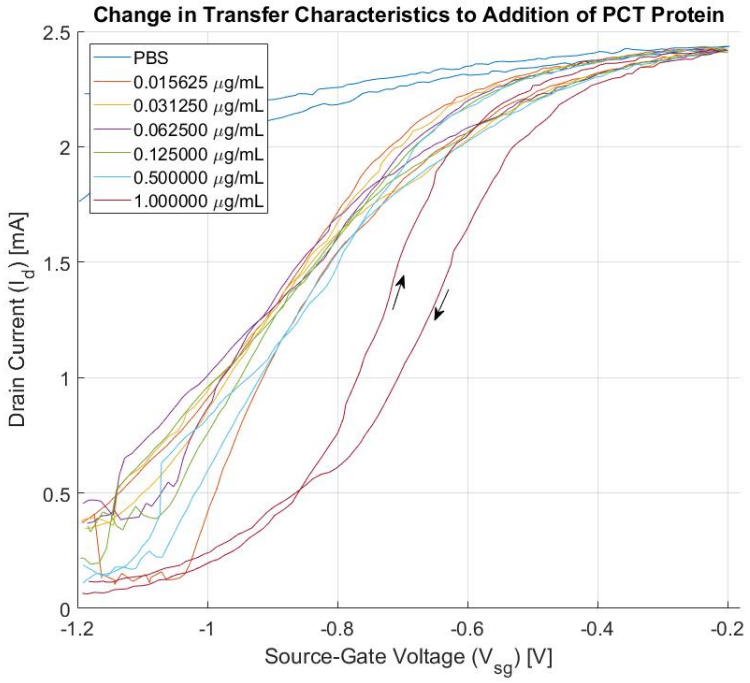

Figure 6.3: Effect of sequential addition of PCT on sensor transfer characteristics.

6.2.2 Test 2

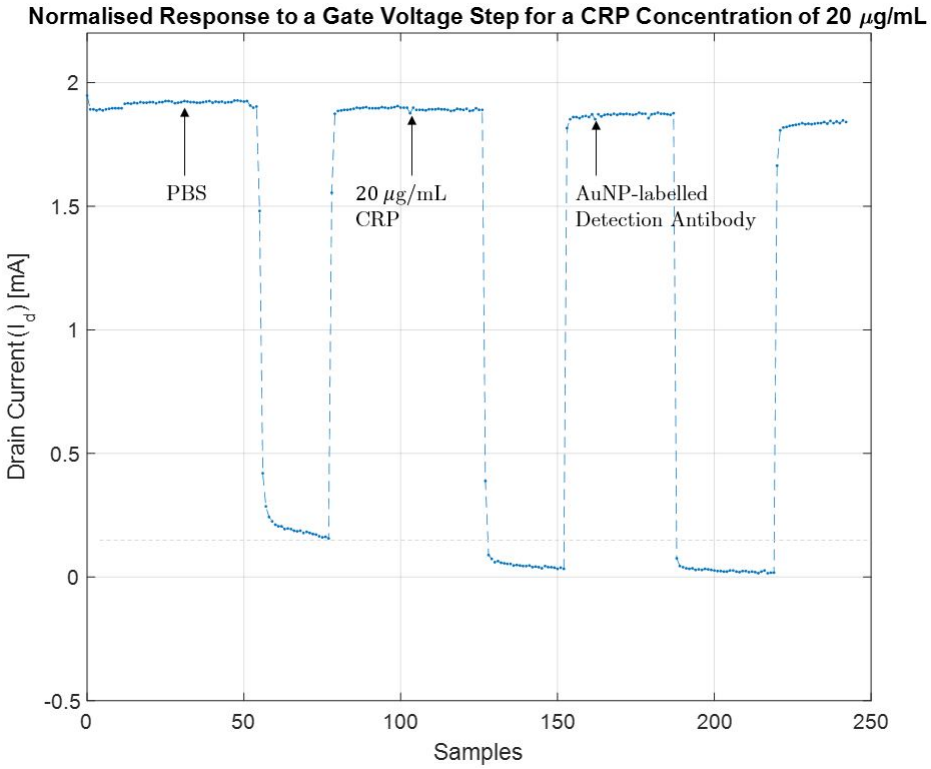

Figure 6.4: Example of the response of the sensor after adding PBS, CRP protein at a concentration of 20 μg/mL, and the the AuNP-labelled detection antibody reagent.

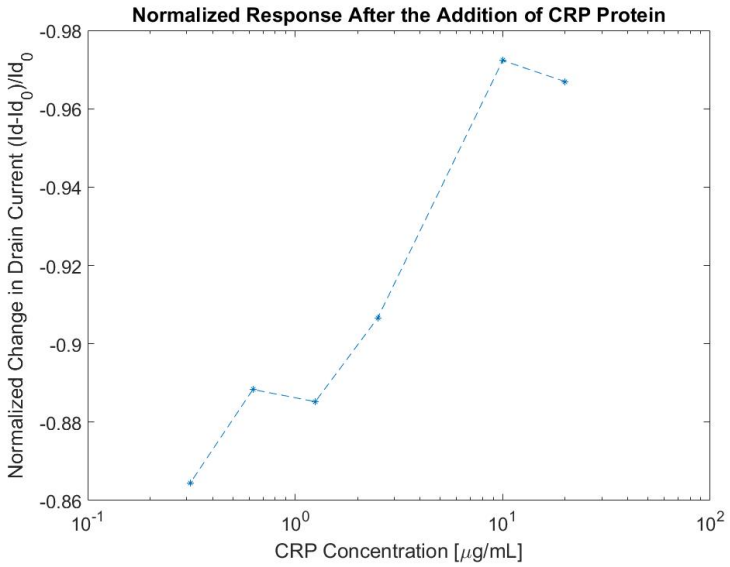

Figure 6.5: Calibration curve for the addition of varying CRP protein concentrations: 0.3125 μg/mL; 0.625 μg/mL; 1.25 μg/mL; 2.5 μg/mL; 10 μg/mL and 20 μg/mL.

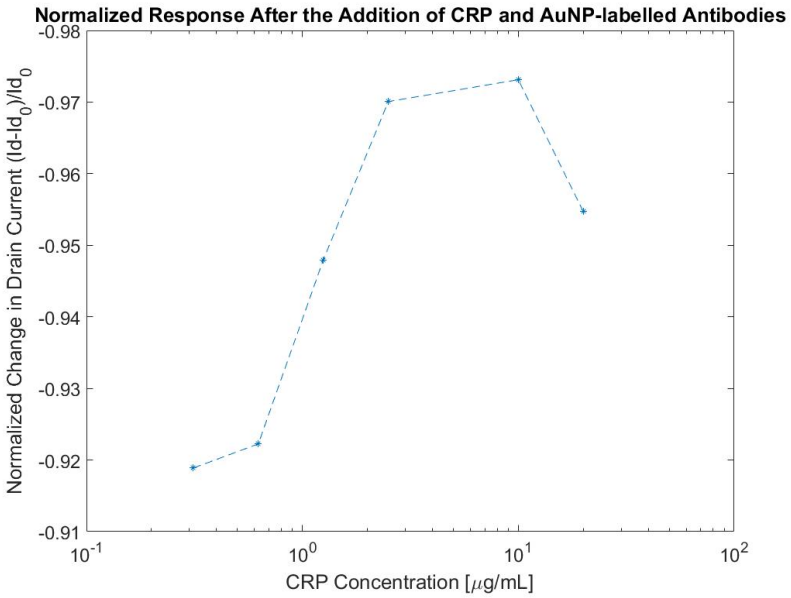

Figure 6.6: Calibration curve after the addition of AuNP-labelled detection antibodies for the same varying CRP protein concentrations shown in figure 6.5.

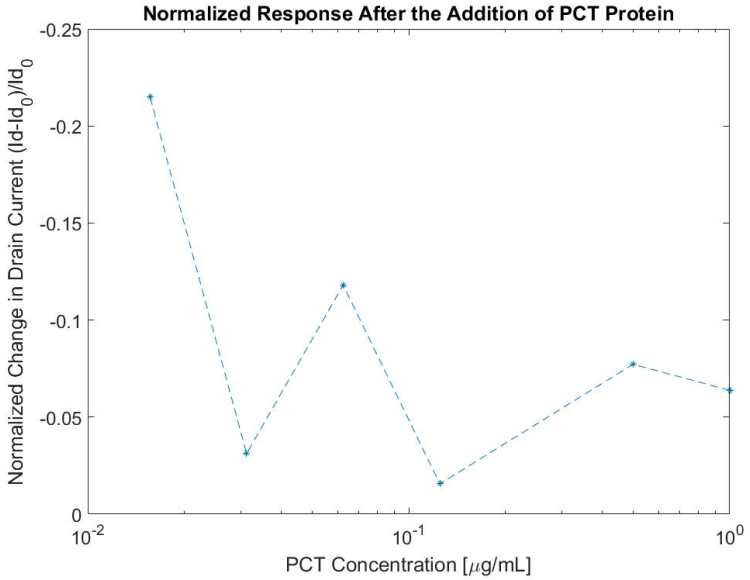

Figure 6.7: Calibration curve for the addition of varying PCT protein concentrations: 0.015625 μg/mL; 0.03125 μg/mL; 0.0625 μg/mL; 0.0125 μg/mL; 0.5 μg/mL; 1 μg/mL.

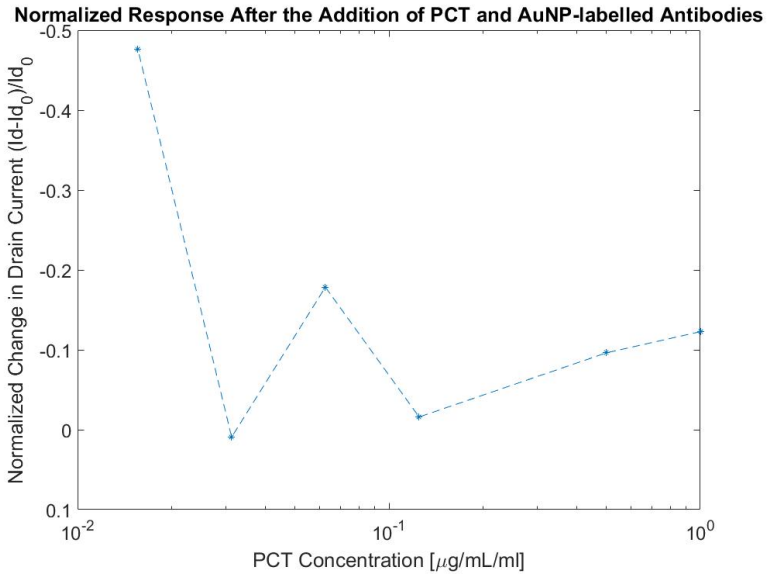

Figure 6.8: Calibration curve after the addition of AuNP-labelled detection antibodies for the same varying PCT protein concentrations shown in figure 6.7.

6.2.3 Test 3

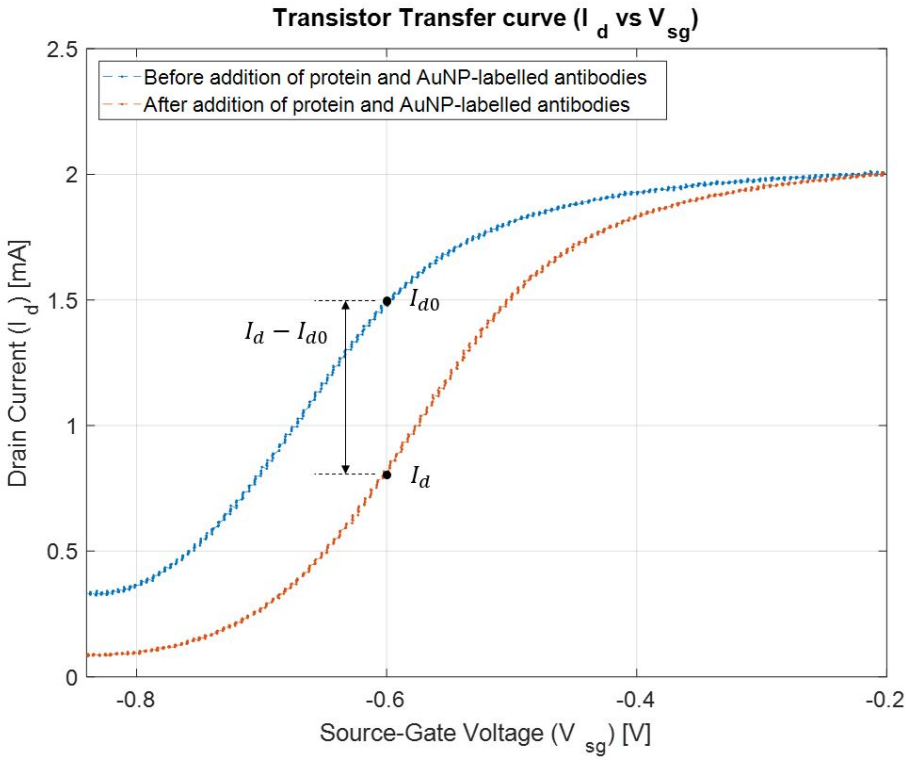

Figure 6.9: Example of the sensor transfer curve before and after addition of CRP protein at a concentration of 0.3125 μg/mL and the the AuNP-labelled detection antibody reagent.

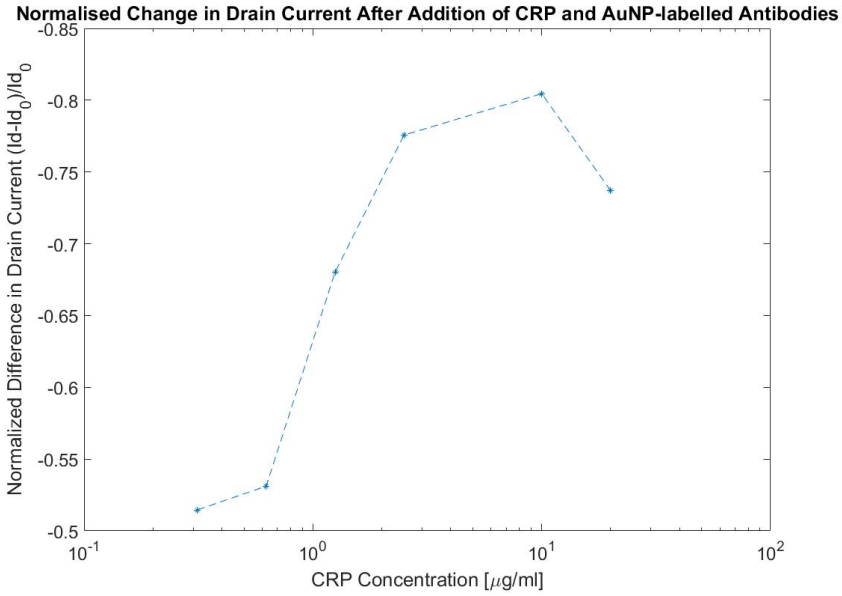

Figure 6.10: Sensor calibration curve for the six CRP concentrations: 0.3125 μg/mL; 0.625 μg/mL; 1.25 μg/mL; 2.5 μg/mL; 10 μg/mL and 20 μg/mL

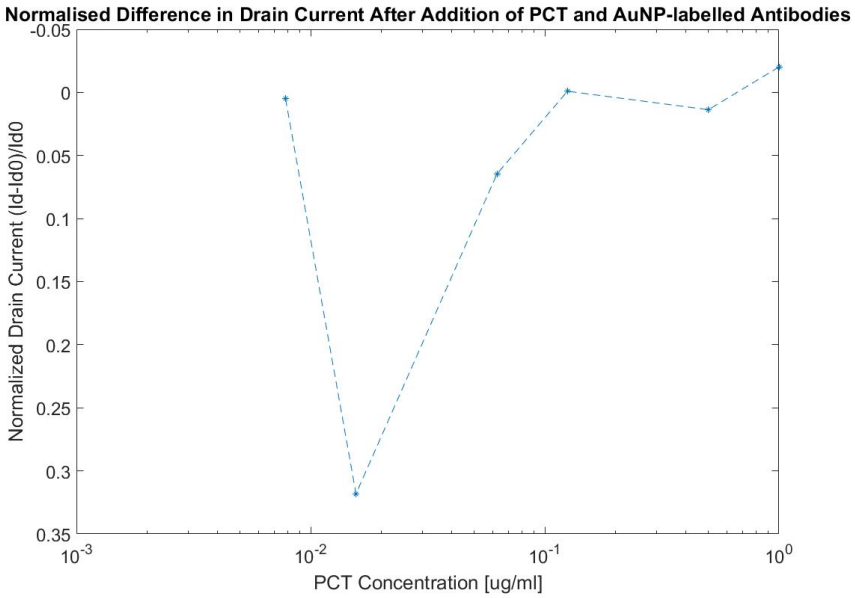

Figure 6.11: Sensor calibration curve for the six PCT concentrations: 0.015625 μg/mL; 0.03125 μg/mL; 0.0625 μg/mL; 0.0125 μg/mL; 0.5 μg/mL; 1 μg/mL.

6.3 Discussion of Results

6.3.1 Test 1

The first plot shown for test 1, in figure 6.1, demonstrates the change in transfer characteristics of the OECT sensor, immersed in PBS, to the addition of more PBS buffer at the start of each gate voltage sweep. According to literature, the addition of ions to the operational electrolytic solution by increasing the volume of electrolyte should result in a change in the "turn on" voltage of the transistor [26]. Here, it was indeed observed that the addition of ions to the system shifted the "turn on" voltage of the transistor in the positive V_{sg} direction, without affecting the peak value of the sweep.

Figure 6.2 shows the effect of the sequential addition of varying CRP protein concentrations on the transfer characteristics of the sensor. Here, the "turn on" voltage of the sensor clearly shifted with increasing ion levels, due to the addition of PBS buffer containing the protein concentrations. In contrast to figure 6.1, however, the drain current decreased (shifted down) with increasing protein concentrations, indicating a response to the addition of the CRP proteins.

In this test, the sequential addition of varying PCT concentrations had no effect on the transfer characteristics of the sensor, as shown in figure 6.3. Here, there is an evident shift in the "turn on" voltage of the sensor due to increasing ion levels with the addition of PBS buffer; however, unlike the CRP sensors, there is no evident downward shift in the drain current. Additionally, the transfer curves are less well defined and show more fluctuation than the curves shown in the CRP tests.

6.3.2 Test 2

The plot shown in figure 6.4 demonstrates the drain current response to a gate voltage step: 1. after adding PBS, 2. after adding CRP protein buffered in PBS at a concentration of 20 μg/mL, and 3. after adding AuNP-labelled detection antibody reagent buffered in PBS. This plot shows an observable change in drain current response for each respective step, indicating increased sensitivity of the drain current to changes in the gate voltage after the addition of CRP protein and the subsequent addition of AuNP-labelled detection antibodies. With the goal of drawing sensor calibration curves, the same test was conducted on different CRP sensors for six different concentrations of CRP protein, between 20 and 0.3125 μg/mL. These tests showed similar responses to the example shown in figure 6.4. From these, the normalised drain current response for each concentration was

determined by dividing the size of the drain current step (I_d-I_{d0}) by the starting current (I_{d0}). The two corresponding calibration curves are shown in figures 6.5 and 6.6.

The calibration curve, for the addition of CRP proteins only, shows a clear increasing trend for increasing CRP concentrations. This indicates that the sensor was sensitive to varying CRP protein concentrations, detecting CRP protein at a minimum concentration of 0.3125 μg/mL. The calibration curve showing the effect of the addition of AuNP-labelled detection antibodies, also indicates an increasing trend for increasing CRP concentrations. The AuNP-conjugated detection antibodies increased the size of the overall change in drain current slightly, in effect amplifying the detected signal, which is in line with the literature [29; 50].

The PCT sensors were tested by the same methodology described above and shown in figure 6.4. Here, neither of the two calibration curves, shown in figures 6.7 and 6.8, show any discernible trend. In the same way as described in test 1, the PCT sensors displayed high variability and no response to the PCT protein.

6.3.3 Test 3

The third and final test demonstrated the change in the transfer characteristics of the sensors, after a five minute incubation period, immersed in the recombinant protein reagent, and a subsequent five minute incubation period immersed in the AuNP-labelled detection antibody reagent. Here, the downward shift in the transfer curve at a specific source-gate voltage, before and after the addition of biomolecules, was determined, as shown in figure 6.9. This, again, was carried out for six varying concentrations of recombinant CRP protein. The normalised downward shift (or difference) in drain current, corresponding to each different concentration, is plotted on the calibration curve shown in figure 6.10.

The first observation from the calibration curve shown for CRP, is the increasing trend in the normalised difference in drain current for increasing CRP concentrations, indicating that the sensor was indeed able to detect the different concentrations of CRP protein. A second, and important, observation from the calibration curve, is the resemblance of this calibration curve to the second calibration curve from test 2, shown in figure 6.6. In both instances, CRP protein as well as AuNP-labelled detection antibody reagent were added to the sensor, with the sensor responding in an identical manner.

The calibration curve shown for the PCT sensors was developed in the same way as for the CRP tests described above, and is shown in figure 6.11. By discounting

the second lowest PCT concentration, there is clearly no increasing trend shown in the difference in drain current.

6.3.4 General Discussion

The three tests detailed above demonstrate the performance of the initial prototype sensors in the detection of CRP and PCT proteins. The CRP sensors successfully detected sequential concentrations of CRP protein in PBS buffer down to a limit of 0.3125 μg/mL. The addition of the AuNP-labelled detection antibodies in tests 2 and 3 increased the sensitivity of the sensors slightly, and the calibration curves are shown to be identical. This observation, therefore, validates the sensitivity of the CRP sensor to the addition of varying CRP concentrations between 0.3125 and 20 μg/mL. It should be noted that due to the pioneering nature of this work, the value of the results was to obtain semi-quantitative responses to different concentrations of CRP, and in this phase of their development, the CRP sensors were not statistically validated.

The PCT sensors on the other hand did not show any response to varying concentrations of PCT protein in PBS buffer. The main observation in this regard was that the actual OECTs showed hindered performance after the PCT capture antibody immobilisation. Possible causes for this hindered functionality may be the longer storage time of the PCT sensors in the capture reagent prior to testing, causing the PEDOT:PSS semiconductor layer to lose functionality by dissolving into solution. Additional causes for the lack of sensor performance may have been the denaturing of the capture antibodies prior to testing, or human pipetting error in the capture antibody immobilisation procedure. The PCT sensors could not be re-tested due to an insufficient amount of capture antibodies. Although only very minute quantities of antibody are required per sensor, the antibody reagents are prepared in a single batch, and denature over time, thus limiting the amount of tests that can be carried out.

Furthermore, it is important to note that all tests were carried out using PBS buffer for the dual purpose of analyte and functional electrolyte. The reason for this being that the initial testing and optimisation of immunosensors is simpler and more practical in PBS since both the initial ion and biomarker concentrations are known at all times and can be easily adjusted. As the end goal of the sensor is to measure serum or saliva concentrations of CRP and PCT, *in vitro*, to assist in the screening for infectious diseases, the working electrolyte and analyte will have to be replaced by one of these biological fluids in the next phase of work. The use of biological fluids will have a negative effect on the sensor performance. Although the ion concentrations of PBS match those of the human body, biologi-

cal fluids (such as serum) contain many other biological substances (not only the target biomarker) that can increase the noise of a reading, thus interfering with the correct detection of the target biomarker.

Chapter 7

Closing Summary, Conclusions and Recommendations

For ease of reference, the following chapter is divided into three sections. The first section offers a closing summary of the work flow; the second section concludes on the reported project and the third section offers recommendations for future work in order to further develop the device.

7.1 Closing Summary

One of the main factors contributing to the imminent threat of antimicrobial resistance is the misappropriation of antibiotics, due to the lack of clinically differentiable features distinguishing bacterial infection from viral infection. Some clinicians have access to the testing of a broad array of quantifiable markers, known as biomarkers, that can aid in screening for infectious diseases; however, most existing biomarker tests require well-equipped laboratory set-ups, are highly costly and are time-consuming. Furthermore, in resource-poor settings, lacking well-equipped laboratories, clinicians do not have access to these tests. The costliness, time required and infrastructure needed to perform these biomarker tests often leads to clinicians making decisions based on clinical symptoms alone.

With the above in mind, the aim of the reported project was to develop a rapid biomarker test to aid in the screening of infectious diseases. The main objectives of the project were listed in section 1.3.

In the literature, C-reactive protein (CRP) and procalcitonin (PCT) have been shown to hold much promise as biomarkers for infectious diseases. Their combination has been recommended for the differentiation between bacterial and viral

infections, since CRP is sensitive to both viral and bacterial infections and PCT is sensitive to bacterial infections. These advantages, amongst others described in section 2.1, led to these biomarkers being chosen as the targets for the rapid test.

In addition to the selection of appropriate target biomarkers, it was also required that a suitable sensing method be selected. To that end, an organic electrochemical transistor (OECT) based immunosensor, as a subclass of organic thin-film transistors (OTFTs), was chosen as the sensing platform, due to their low cost, simple fabrication, high sensitivity and good biocompatibility.

Three main subsystems were identified for the development of the rapid biomarker test. These are: (1) the biorecognition elements; (2) the sensor; and (3) the measurement system.

For the biorecognition element subsystem, a sandwich-type immunosensor configuration was chosen, consisting of a capture antibody and a nanoparticle-labelled detection antibody. Different antibodies were ordered for both CRP and PCT, and gold nanoparticles (AuNPs) were chosen as the detection antibody label due to their reported signal amplification ability. The performance of the different capture-detection antibody pairs were tested on ELISA and MSD respectively, with the results indicating that the "capture - detection 1" antibody pair for CRP, and the "capture 1 - detection" antibody pair for PCT, yielded the highest signal strength and thus sensitivity to the binding of the target biomarkers.

For the sensor platform, the OECTs were designed to be fabricated with the low cost inkjet printing method, using a combination of silver nanoparticle ink for the electrodes and PEDOT:PSS organic semiconductor ink for the semiconductor layer. After many design iterations (the four most significant iterations reported on in section 2.4.3), and over 300 different tests, a working organic electrochemical transistor prototype was developed according to the methodology described in section 4.4.1, and characterised as shown in section 5.3.

The measurement system was comprised of the National Instruments cDAQ data acquisition system coupled to LabVIEW control software. This system was used to perform all required OECT characterisation tests as well as final sensor tests. The measurement system was verified by successfully characterising an off-the-shelf NMOS transistor.

For the final tests, the OECTs were fabricated and coupled to the capture antibodies according to the biotin-streptavidin immobilisation method, described in

section 4.4, to produce the immunosensors. Three primary tests were conducted on the immunosensors to assess their performance, as described in section 6.1. The results of these tests, shown in section 6.2, indicated that the CRP sensors detected sequential concentrations of recombinant CRP protein, between 0.3125 and 20 μg/mL. Furthermore, the addition of AuNP-labelled detection antibodies indicated an amplification in measured signal strength, which is in accordance with literature. In contrast, the PCT sensors exhibited no measurable change in signal in response to the addition of the PCT protein dilutions.

7.2 Conclusions

One of the main findings was that the project successfully demonstrated functional paper-based, inkjet-printed, organic electrochemical transistors (OECTs). It was found that the main success factors for a working OECT were: increased layer thickness of the organic semiconductor, resistance of the gate electrode to oxidation and the paper substrate's resistance to liquid seepage. This is an important finding since it enables the simple and low-cost production of disposable organic electrochemical transistors that can be used not only for sensing, but a variety of organic printed electronics, provided an electrolytic solution (like PBS) is used.

Furthermore, from the literature the clinically relevant CRP cut-off value for viral infection is between 10 and 20 μg/mL, while for bacterial infection it is greater than 20 μg/mL. For PCT, the clinically relevant cut-off value for bacterial infection is 0.25 ng/mL. Although, at this phase of the development, the CRP sensors were not statistically validated, the results indicate that the sensors did indeed respond to changes in concentration within the clinically relevant range. The PCT sensors, on the other hand, failed to respond to changes in PCT concentration due to the deterioration of the sensors post immobilisation.

The CRP sensors, therefore, demonstrated an easily manufacturable and low cost first prototype, whilst the PCT sensors require further work. Apart from the faulty PCT sensors, other limitations of the device include that the tests were solely conducted in PBS buffer and not in biological fluids, the fabrication of the sensors was tedious and not fully automated (i.e. the addition of the PEDOT:PSS layer and the antibodies was manual), and the sensors' performance deteriorated when exposed to aqueous conditions for longer time periods (as described in section 6.3.4).

In conclusion, the following objectives of the project (as stated in section 1.3) were achieved: (1) the CRP and PCT proteins were chosen as ideal biomarkers for the screening of infectious diseases; (2) an OECT-based immunosensor was

identified as the ideal biosensing technique for the low-cost and rapid detection of CRP; (3) a prototype sensor, based on OECT immunosensor technology, was designed and fabricated; (4) a measurement system for the sensor was designed and validated; (5) the main components of the prototype sensor were successfully validated; the performance of the prototype sensors were tested, with the CRP sensors showing good sensitivity to CRP protein concentrations between 0.3125 and 20 μg/mL. The PCT sensors, on the other hand, showed no response to the addition of PCT protein.

However, the CRP sensors, as is, require further refinement before they can be used as a first screening method for infection, as do the PCT sensors. Recommendations for future work are described in the following section.

7.3 Recommendations for Future Work

It is recommended that future work should first focus on further development of the PCT sensors to ensure they respond to varying concentrations of PCT. This could be done by ensuring that the sensors are tested directly after antibody immobilisation and are not stored for extended time periods in aqueous environments, by experimenting with other low cost substrates with better performance in aqueous conditions (such as various polymers), or by making the PEDOT:PSS semiconductor less soluble once deposited onto the substrate. Additionally, further testing of the CRP sensors is required in order to develop repeatable calibration curves for the sensors, in which specific CRP concentrations correlate to specific changes in signal strength. The same should be done once working PCT sensors are developed. Once both the CRP and PCT sensors function correctly, calibration curves should be generated in biological fluid, such as serum or saliva, in order to determine the performance of the sensors *in vitro*. These sensors should then be statistically validated in biological media.

From a manufacture standpoint, the manufacture method requires increased automation, in which both the PEDOT:PSS semiconductor as well as the capture antibodies are deposited in an automated process, such as inkjet printing. This in turn will dramatically increase their repeatability and overall performance, their manufacture time and their cost.

Finally, the current measurement system is unsuitable for many point-of-care (POC) applications due to its high cost, large size and requirement for the LabVIEW software on up-to-date PC hardware. Future work should, therefore, focus on developing a portable device, able to run the respective tests in any setting.

Appendix A

Antibody and Recombinant Protein Datasheets

A.1 CRP Capture 1

abcam

Product datasheet

Anti-C Reactive Protein antibody ab31156

★★★★★ 2 Abreviews 2 References 1 Image

Overview

Product name	Anti-C Reactive Protein antibody
Description	Rabbit polyclonal to C Reactive Protein
Host species	Rabbit
Tested applications	**Suitable for:** ELISA, WB, Immunoelectrophoresis, Immunodiffusion, IHC-P
Species reactivity	**Reacts with:** Human
Immunogen	Full length native protein (purified) (Human).
Positive control	This antibody gave a positive result in IHC in the following FFPE tissue: Human normal liver.

Properties

Form	Liquid
Storage instructions	Shipped at 4°C. Store at +4°C short term (1-2 weeks). Upon delivery aliquot. Store at -20°C long term.
Storage buffer	Preservative: 0.02% Sodium Azide Constituents: 0.14M Sodium chloride, 10mM PBS, pH 7.2
Purity	Protein A purified
Purification notes	Purity wad determined by SDS PAGE (blue stain), showing that the IgG constitute was greater than 90% of total protein.
Clonality	Polyclonal
Isotype	IgG

Applications

Our Abpromise guarantee covers the use of **ab31156** in the following tested applications.

The application notes include recommended starting dilutions; optimal dilutions/concentrations should be determined by the end user.

Application	Abreviews	Notes
ELISA	★★★★★	Use at an assay dependent concentration.

A.2 CRP Detection

BioVision

12/16

For research use only

C-reactive/CRP Monoclonal Antibody

CATALOG NO:	A1208-100
ALTERNATIVE NAMES:	CRP, PTX1, C-reactive protein
AMOUNT:	100 µg
IMMUNOGEN:	Human CRP Protein
HOST/ISOTYPE:	Mouse IgG
SPECIES REACTIVITY:	Human
PURIFICATION:	>95%, Protein G purified
FORM:	Liquid
FORMULATION:	In NaCl with 15 mM NaN_3 (pH 7.4)
STORAGE CONDITIONS:	For long term storage store at -20°C in small aliquots to prevent freeze-thaw cycles.
DESCRIPTION:	C-reactive protein (CRP) is an annular (ring-shaped), pentameric protein found in blood plasma, the levels of which rise in response to inflammation (i.e., C-reactive protein is an acute-phase protein of hepatic origin that increases following interleukin-6 secretion from macrophages and T cells). Its physiological role is to bind to lysophosphatidylcholine expressed on the surface of dead or dying cells (and some types of bacteria) in order to activate the complement system via the C1Q complex. CRP is synthesized by the liver in response to factors released by macrophages and fat cells (adipocytes).It is a member of the pentraxin family of proteins. It is not related to C-peptide (insulin) or protein C (blood coagulation). C-reactive protein was the first pattern recognition receptor (PRR) to be identified.
APPLICATION:	ELISA, LEITA, LFIA **Note: This information is only intended as a guide. The optimal dilutions must be determined by the user.**

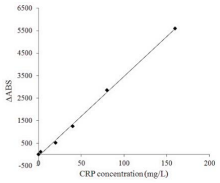

Fig1. Calibration curve for CRP in latex-enhanced turbidimetric immmmunoassay (LETIA): CRP proteins react with anti-CRP antibody precoated onto latex beads to form insoluble complex, resulting in turbidity increasing with was then detected by automatic biochemical analyzer.

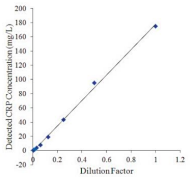

Fig2. Determination of the CRP concentration by serial dilution of clinical serum: The high value CRP serum was 2-fold serially diluted with physiological saline and measured on LETIA platform showed decline in CRP concentrations along with serial dilution of blood samples

RELATED PRODUCTS:

- Human CellExp™ C-reactive/CRP, human recombinant **(Cat. No. 7242-100)**
- CRP, human recombinant **(Cat. No. 4864-250, -1000)**

FOR RESEARCH USE ONLY! Not to be used on humans.

BioVision Incorporated
155 S. Milpitas Boulevard, Milpitas, CA 95035 USA

Tel: 408-493-1800 | Fax: 408-493-1801
www.biovision.com | tech@biovision.com

A.3 PCT Capture

GeneTex
Quality Antibodies · Quality Results

Datasheet

GeneTex, Inc : Toll Free 1-877-GeneTex (1-877-436-3839) Fax:1-949-309-2888 info@genetex.com
GeneTex International Corporation : Tel:886-3-6208988 Fax:886-3-6208989 infoasia@genetex.com

Date : 2017/10/27

Catalog Number	GTX14813 Package:100 µg
Product Name	Procalcitonin antibody [27A3]
Full Name	calcitonin-related polypeptide alpha
Synonyms	CALC1, CGRP, CGRP-I, CGRP1, CT, KC, MGC126648, CGRP I, CGRPI
Specificity	Specific for N-terminal fragment
Background	Procalcitonin (PCT) is a 116 amino acid residue peptide with molecular weight of about 13 kDa. The amino acid sequence of PCT was firstly described by Moullec et al. in 1984. It belongs to a group of related proteins including calcitonin gene-related peptides I and II, amylin, adrenomodulin and calcitonin (CAPA peptide family). PCT, like other peptides of CAPA family, appears from the common precursor pre-procalcitonin consisting of 141 amino acids by removal of 25 a.a.r. from N-terminus. PCT is produced normally in C-cells of the thyroid glands. It undergoes successive cleavages to form three molecules: N-terminal fragment (55 a.a.r.), calcitonin (32 a.a.r.) and katacalcin (21 a.a.r.). It has been shown that the level of PCT in serum increases significantly during an infection of bacterial origin (Assicot M, et al). Today PCT is considered to be one of the earliest and most specific markers of sepsis. However, several studies revealed that elevated PCT level in human blood could be detected not only in case of sepsis and infection, but also in cases of surgery, polytrauma, heat shock and cardiogenic shock (Meisner M. & Reinhart K). The importance of PCT measurements in combination with cTnT or cTnI during heart transplantation to predict an early graft failure has been proved(Potapov EV., et al).
Host	Mouse
Clonality	Monoclonal
Clone Name	27A3
Isotype	IgG2a
Immunogen	Full length native protein, internal calcitonin fragment (purified) (Human)
Antigen Species	Human
Species Reactivity	Human
Applications	ELISA, WB
Application Note	This clone 27A3 can be used as the capture antibody and paired with clone 14A2 (GTX39509 Calcitonin antibody) for detection.
Cellular Localization	Secreted
Conjugation	Unconjugated
Form Supplied	Liquid
Purification	Protein A purified
Concentration	Batch dependent (Please refer to the vial label for the specific concentration)
Storage Buffer	Phosphate-buffered saline, pH 7.4, containing 0.1% sodium azide
Storage Instruction	Keep as concentrated solution, aliquot and store at 4°C. Do not freeze.
Notes	For *In vitro* laboratory use only. Not for any clinical, therapeutic, or diagnostic use in humans or animals. Not for animal or human consumption.
ResearchArea	Cancer > Tumor biomarkers Cancer > Type of cancer > Ovarian Cell Biology > Cell adhesion > Cell-cell adhesion > Leukocyte

A.4 PCT Detection 1

Abbexa Ltd, Innovation Centre, Cambridge Science Park, Cambridge, CB4 0EY, UK
Telephone: +44 (0) 1223 755950 - Fax: +44 (0) 1223 755951 - E-Mail: info@abbexa.com

DATASHEET

PCT (Capture) Antibody

Catalogue No.:abx019247

PCT (Capture) Antibody against Human PCT. PCT is a peptide precursor of the hormone calcitonin, the latter being involved with calcium homeostasis. It is composed of 116 amino acids and is produced by parafollicular cells (C cells) of the thyroid and by the neuroendocrine cells of the lung and the intestine. Measurement of procalcitonin can be used as a marker of severe sepsis caused by bacteria and generally grades well with the degree of sepsis, although levels of procalcitonin in the blood are very low. PCT has the greatest sensitivity (85%) and specificity (91%) for differentiating patients with systemic inflammatory response syndrome (SIRS) from those with sepsis, when compared with IL-2, IL-6, IL-8, CRP and TNF-alpha. It is a biomarker of bacterial infection which may help gauge the severity and prognosis of patients with CAP. In addition to clinical predictors, PCT may assist in decisions pertaining to timing of discharge from hospital and the discontinuation of antibiotics.

It is recommended to use abx019247 (this product) as the capture antibody and abx019248 as the detection antibody.

Target:	PCT
Reactivity:	Human
Host:	Mouse
Clonality:	Monoclonal
Tested Applications:	ELISA, WB, CLIA, TIA
Recommended dilutions:	Optimal dilutions/concentrations should be determined by the end user.
Immunogen:	Recombinant PCT protein.
Purity:	> 95% by HPLC & SDS-PAGE.
Purification:	Protein A or G purified.
Form:	Liquid
Isotype:	IgG_{2b}
Conjugation:	Unconjugated
Specificity:	Specifically recognises human PCT.
Storage:	Aliquot and store at -20°C for long-term storage. Avoid repeated freeze and thaw cycles.
Buffer:	0.01 M PBS (pH7.4) and 0.15 M NaCl. Does not contain preservatives.

A.5 Recombinant CRP Protein

abcam

Product datasheet

Recombinant Human C Reactive Protein ab167710

1 Image

Overview

Product name	Recombinant Human C Reactive Protein
Protein length	Full length protein

Description

Nature	Recombinant
Source	HEK 293 cells

Amino Acid Sequence

Accession	P02741
Species	Human
Sequence	FGQTDMSRKA FVFPKESDTS YVSLKAPLTK PLKAFTVCLH FYTELSSTRG YSIFSYATKR QDNEILIFWS KDIGYSFTVG GSEILFEVPE VTVAPVHICT SWESASGIVE FWVDGKPRVR KSLKKGYTVG AEASIILGQE QDSFGGNFEG SQSLVGDIGN VNMWDFVLSP DEINTIYLGG PFSPNVLNWR ALKYEVQGEV FTKPQLWP
Molecular weight	23 kDa including tags
Amino acids	17 to 224
Tags	His tag C-Terminus

Specifications

Our Abpromise guarantee covers the use of **ab167710** in the following tested applications.

The application notes include recommended starting dilutions; optimal dilutions/concentrations should be determined by the end user.

Applications	SDS-PAGE
Endotoxin level	< 1.000 Eu/µg
Purity	>95% by SDS-PAGE .
Form	Lyophilised

A.6 Recombinant PCT Protein

RayBiotech | Empowering your proteomics

3607 Parkway Lane Suite 200
Norcross, GA 30092
Tel: 1-888-494-8555
Email: info@raybiotech.com

Recombinant Human procalcitonin (PCT)

Recombinant human procalcitonin
CODE: 230-00041

Synonyms

Calcitonin; Calcitonin carboxyl-terminal peptide

Species

Human

Source

Expression System	Escherichia coli (E.coli)
Gene Symbol	PCT
Uniprot Accession #	P01258
NCBI Gene ID	796
Expressed Region	Ala26-Asn141
Conjugation/Tag	N-terminal 6x histidine tag
Molecular Mass (kDa)	15.1

Preparation

Purification
His-tag affinity purification by immobilized metal ion affinity chromatography (IMAC)

Purity > 95%

Purity determined by
SDS-PAGE under reducing conditions and visualized by Coomassie blue staining

SDS-PAGE Image

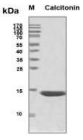

Specifications

Appendix B

Antibody Pairing Test Methodology

The following appendix details the antibody pairing test methodology followed to determine optimal capture-detection antibody pair. The antibody pairing tests were conducted at Synexa Life Sciences, Cape Town, over two days. Two different tests were conducted to test the respective antibody pairs - an MSD test was conducted for the CRP pairing, and an ELISA test was conducted for the PCT pairing. The following section describes the methodology followed, first for the ELISA tests conducted for the PCT antibody pairings; then for the MSD tests, conducted for the CRP antibody pairings.

B.1 PCT - Enzyme-linked Immunosorbent Assay (ELISA) Methodology

B.1.1 ELISA Reagent Preparation

In order to ensure efficiency of the test procedure, all reagents were prepared before commencement of the ELISA testing procedure. The reagent preparation procedure is listed as follows:

1. Preparation of capture antibodies:
   (a) Capture Antibody 1 Dilution (Coating Solution 1): Prepare 1 mL of a dilution of 1μg/mL anti-PCT Capture Antibody 1 in PBS buffer.
   (b) Capture Antibody 2 Dilution (Coating Solution 2): Prepare 1 mL of a dilution of 1μg/mL anti-PCT Capture Antibody 2 in PBS buffer.
2. Wash Buffer: Prepare 1 L of 0.05 % Tween-20 in PBS buffer. e.g. add 0.5 mL of Tween-20 to 999.5 mL PBS.

3. Assay Buffer: Prepare 50 mL of 1 wt% BSA (bovine serum albumin) in PBS buffer. e.g. add 0.5 g BSA to 50 mL PBS.

4. Blocking Buffer: Prepare 50 mL of 3 wt% BSA (bovine serum albumin) in PBS buffer. e.g. add 1.5 g BSA to 50 mL PBS.

5. Recombinant PCT Protein Dilutions: add here.

6. Biotinylated Antibody Solution: Prepare the biotinylated anti-PCT detection antibody 1 solution in assay buffer according to the Lightning-Link® Rapid Biotin Conjugation Kit protocol. In order to ensure sufficient antibodies remaining for final sensor tests, adjust the solution quantities in the protocol as advised by Synexa scientist. The adjusted biotinylation procedure is listed as follows (values in brackets show the originally specified quantities):

   (a) (Additional step) Allot 40 μL of anti-PCT detection antibody 1 solution.

   (b) Add 1 μL of LL modifier reagent per 10 μL of antibody to be labelled and mix gently. In this case, add 4 μL of LL modifier reagent to the 40 μL of antibody.

   (c) (Additional step) Dilute the antibody-modifier sample with 50 μL of PBS.

   (d) Remove the cap from the Lightening-Link® Rapid mix and pipette the diluted antibody-modifier sample directly onto the lyophilized material. Resuspend and re-dispense the liquid gently to mix.

   (e) Replace the cap on the vial and leave standing for 30 (15) minutes at room temperature for incubation. Since the amount of antibody being conjugated in this step is less than the amount specifiedin the original protocol, double the incubation time (i.e. from 15 to 30 minutes) to ensure Alternatively, incubate overnight at room temperature. Longer incubation times do not have a negative effect on the conjugation.

   (f) After the incubation, add 1 μL of LL Rapid Quencher reagent for every 10 μL of antibody used. In this case, add 4 μL of LL Rapid Quencher.

   (g) The conjugate can be used after 5 minutes and does not require purification.

7. Streptavidin-HRP Solution: Prepare a 1/1000 dilution of Streptavidin-HRP stock in Assay Buffer. e.g. add 13μL stock to 12987 μL assay buffer.

8. TMB Substrate Solution: Prepare a 1:1 solution of TMB Reagent A and TMB Reagent B. Note that solutions are light sensitive - therefore keep

away from light until use. e.g. add 6 mL of TMB Reagent A to 6 mL of TMB Reagent B.

9. Stop Solution: Prepare 2N HCL Solution

B.1.2 ELISA Test Procedure

Following the preparations of the respective reagents, the ELISA test protocol was followed. The protocol is listed as follows:

1. Day 1 procedure:
   (a) Ensure that both anti-PCT coating solutions (capture antibodies) have been prepared.
   (b) Fill each of the relevant wells with 100 μL of the required anti-PCT coating solution. Fill the first 48 wells with anti-PCT coating solution 1 and the second 48 wells with anti-PCT coating solution 2.
   (c) Seal the plate with the plate sealer. Incubate the sealed ELISA plate overnight, in the dark at 4 °C.
2. Day 2 procedure:
   (a) Remove ELISA plate from storage place and wash plate three times with 300 μL/well of wash buffer.
   (b) Add 300 μL of blocking buffer to each well and incubate for at least 90 minutes at room temperature whilst shaking at 350 rpm. Record the start and end times of the incubation process.
   (c) Remove the ELISA plate from the shaker and wash it three times with 300 μL/well of wash buffer.
   (d) Since two different antibody pairs are being evaluated, the 96-well ELISA plate must be split into two 48-well sections. Two lots of each different recombinant PCT protein dilution must be added to each side of the ELISA plate. Exactly 100 μL of each dilution must be added per well. Finally, at the end of the sequence, two wells must be filled with 100 μL of PBS blank . The layout of the ELISA plate as described is shown in figure B.1.
   (e) Seal the plate with the plate sealer. Incubate the plate for one hour at room temperature with gentle shaking at 350 rpm. Record the start and end times of the incubation process.
   (f) Remove the ELISA plate from the shaker and wash it three times with 300 μL/well of wash buffer.

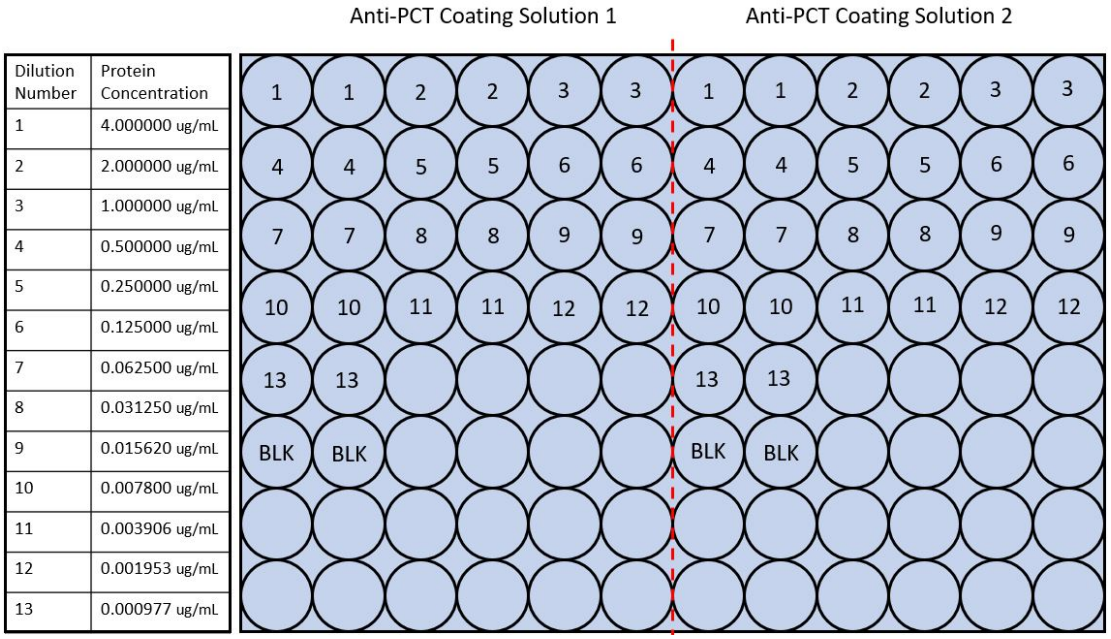

Dilution Number	Protein Concentration
1	4.000000 ug/mL
2	2.000000 ug/mL
3	1.000000 ug/mL
4	0.500000 ug/mL
5	0.250000 ug/mL
6	0.125000 ug/mL
7	0.062500 ug/mL
8	0.031250 ug/mL
9	0.015620 ug/mL
10	0.007800 ug/mL
11	0.003906 ug/mL
12	0.001953 ug/mL
13	0.000977 ug/mL

Figure B.1: Schematic showing the 13 different dilutions of recombinant PCT protein and the corresponding layout of the 96-well ELISA plate.

(g) Add 100 μL of biotinylated detection antibody solution to each well.

(h) Seal the plate with the plate sealer. Incubate the plate for one hour at room temperature with gentle shaking at 350 rpm. Record the start and end times of the incubation process.

(i) Remove the plate from the shaker and wash three times with 300 μL/well of wash buffer.

(j) Add 100 μL streptavidin-HRP solution to each well.

(k) Seal the plate with the plate sealer. Incubate the plate for one hour at room temperature with gentle shaking at 300 rpm. Record the start and end times of the incubation process.

(l) Remove the plate from the shaker and wash three times with 300 μL/well of wash buffer.

(m) Add 100 μL of TMB substrate to each well.

(n) Incubate the plate without the plate sealer at room temperature whilst shaking at 350 rpm for up to 30 minutes. Check plate regularly to ensure that colour does not over-develop.

(o) Add 50 μL/well of stop solution.

(p) Read the plate absorbance at a wavelength of 450 nm.

B.2 CRP - Meso Scale Discovery (MSD) Methodology

B.2.1 Reagent Preparation

Meso Scale Discovery (MSD) was used to determine the most suitable capture-detection pair for the anti-CRP antibodies. Again, all reagents necessary for the MSD testing process were prepared beforehand. The reagent preparation procedure is listed as follows:

1. Capture Antibody Dilution (Coating Solution): Prepare 1 mL (quantity?) of a dilution of 1μg/mL anti-CRP Capture Antibody in PBS buffer.
2. Wash Buffer: Prepare 1 L of 0.05 % Tween-20 in PBS buffer. e.g. add 0.5 mL of Tween-20 to 999.5 mL PBS.
3. Assay Buffer: Prepare 50 mL of 1 wt% BSA (bovine serum albumin) in PBS buffer. e.g. add 0.5 g BSA to 50 mL PBS.
4. Blocking Buffer: Prepare 50 mL of 3 wt% BSA (bovine serum albumin) in PBS buffer. e.g. add 1.5 g BSA to 50 mL PBS.
5. Recombinant CRP Protein Dilutions: add here.
6. Preparation of detection antibodies:
   (a) Prepare 2 μg/mL Anti-CRP Detection Antibody 1 solution in assay buffer. e.g. Add 5μL anti-CRP Detection Antibody 1 stock to 2495 μL assay buffer.
   (b) Prepare 2 μg/mL Anti-CRP Detection Antibody 2 solution in assay buffer. e.g. Add 5μL anti-CRP Detection Antibody 2 stock to 2495 μL assay buffer.
   (c) Prepare 2 μg/mL Anti-CRP Detection Antibody 3 solution in assay buffer. e.g. Add 5μL anti-CRP Detection Antibody 3 stock to 2495 μL assay buffer.
7. Anti-mouse SULFO-TAG Solution: Prepare goat anti-mouse SULFO-TAG antibody solution in assay buffer. e.g. Add 8 μL goat anti-mouse SULFO-TAG labelled antibody stock solution to 3992 μL assay buffer.
8. Read Buffer: Prepare MSD Read Buffer T in distilled water. e.g. Add 10 mL MSD Read Buffer T to 10 mL of dH2O.

B.2.2 MSD Test Procedure

Following the preparations of the respective reagents, the MSD test protocol was followed. The protocol is listed as follows:

1. Day 1 procedure:
   (a) Ensure that the anti-CRP coating solution (capture antibody) has been prepared.
   (b) Fill each of the 96 wells with 25 μL of the required anti-CRP coating solution.
   (c) Seal the plate with the plate sealer. Incubate the sealed MSD plate overnight, in the dark at 4 °C.
2. Day 2 procedure:
   (a) Remove MSD plate from storage place and wash plate three times with 300 μL/well of wash buffer.
   (b) Add 200 μL of blocking buffer to each well and incubate for at least two (2) hours at room temperature whilst shaking at 350 rpm. Record the start and end times of the incubation process.
   (c) Remove the MSD plate from the shaker and wash it three times with 300 μL/well of wash buffer.
   (d) Add 25 μL of blanks (PBS) and the prepared sample solutions to each of the relevant wells. Since there are three different antibody pairings, add the sequential dilutions to each third of the plate. The layout of the MSD plate as described is shown in figure B.2.
   (e) Seal the plate with the plate sealer. Incubate the plate for one hour at room temperature with gentle shaking at 350 rpm. Record the start and end times of the incubation process.
   (f) Remove the MSD plate from the shaker and wash it three times with 300 μL/well of wash buffer.
   (g) Add 25 μL of detection antibody solution to each relevant well. There are three different detection antibody solutions, therefore
   (h) Seal the plate with the plate sealer. Incubate the plate for one hour at room temperature with gentle shaking at 350 rpm. Record the start and end times of the incubation process.
   (i) Remove the plate from the shaker and wash three times with 300 μL/well of wash buffer.

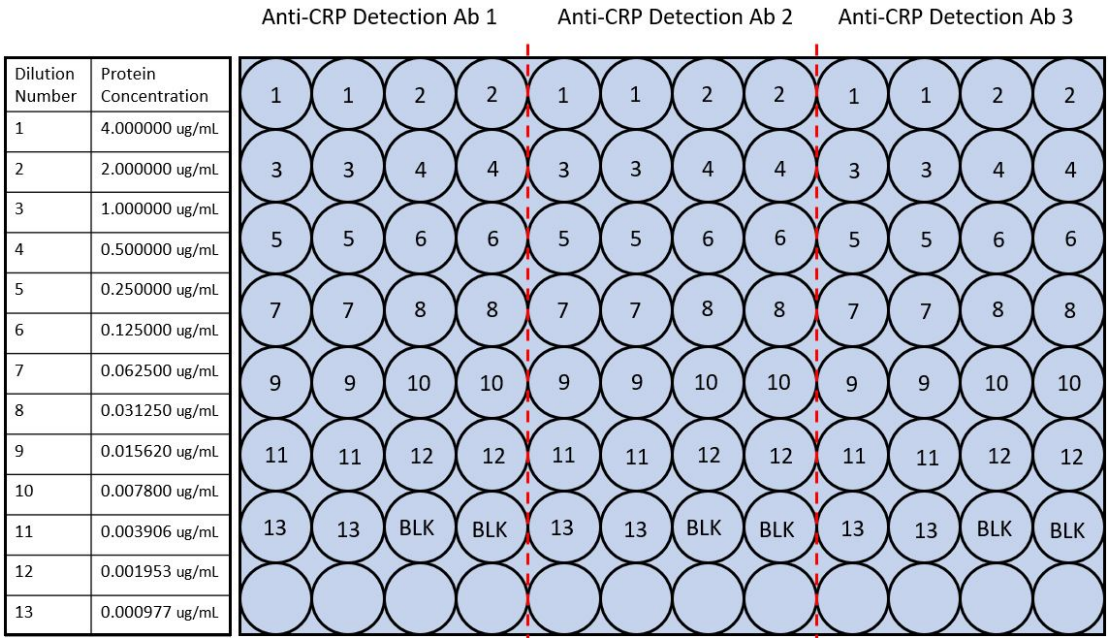

Dilution Number	Protein Concentration
1	4.000000 ug/mL
2	2.000000 ug/mL
3	1.000000 ug/mL
4	0.500000 ug/mL
5	0.250000 ug/mL
6	0.125000 ug/mL
7	0.062500 ug/mL
8	0.031250 ug/mL
9	0.015620 ug/mL
10	0.007800 ug/mL
11	0.003906 ug/mL
12	0.001953 ug/mL
13	0.000977 ug/mL

Figure B.2: Schematic showing the 13 different dilutions of recombinant CRP protein and the corresponding layout of the 96-well MSD plate

(j) Add 100 μL streptavidin-HRP solution to each well.

(k) Seal the plate with the plate sealer. Incubate the plate for one hour at room temperature with gentle shaking at 300 rpm. Record the start and end times of the incubation process.

(l) Remove the plate from the shaker and wash three times with 300 μL/well of wash buffer.

(m) Add 100 μL of TMB substrate to each well.

(n) Incubate the plate without the plate sealer at room temperature whilst shaking at 350 rpm for up to 30 minutes. Check plate regularly to ensure that colour does not over-develop.

(o) Add 50 μL/well of stop solution.

(p) Read the plate absorbance at a wavelength of 450 nm.

Appendix C

Output Curves of the Four OECT Iterations

The following appendix shows the output characteristics of selected transistors from the first three OECT iterations. Output characteristics are obtained by sweeping the drain voltage for different sequential gate voltages, as shown in the example figure C.1.

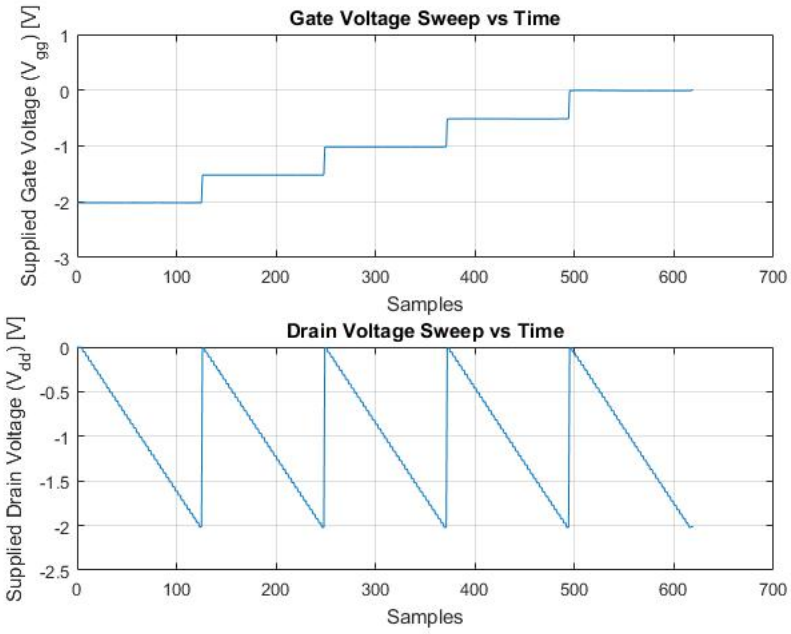

Figure C.1: Example plot of an output sweep

C.1 Iteration 1: All Printed OECT Layout

An example output curve from the first iteration of OECTs is shown in figure **??**. To demonstrate their deterioration over time, the drain current is plotted against samples (time) in figure E.6

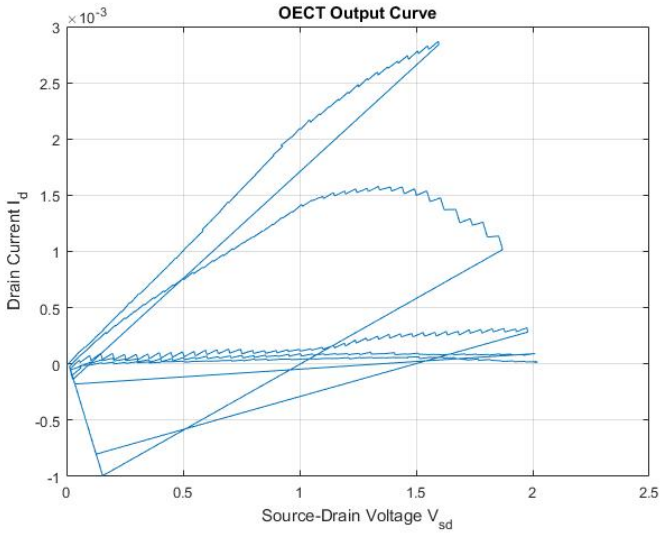

Figure C.2: Example output characteristics from the first iteration

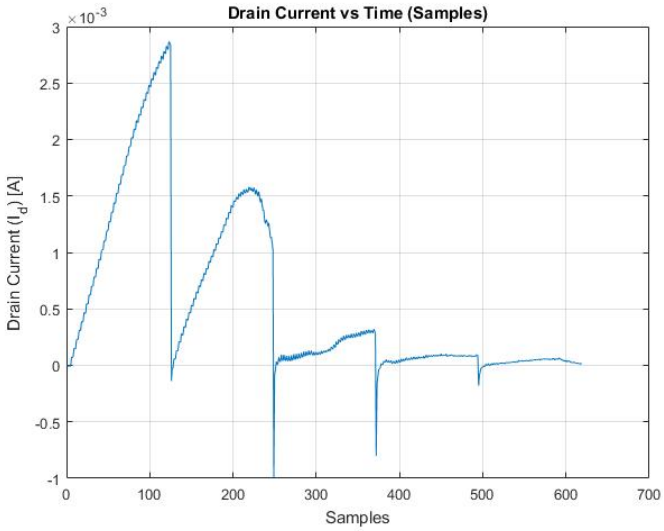

Figure C.3: Loss of functionality due to PBS seepage into paper

C.2 Iteration 2: Addition of Photoresist Coating

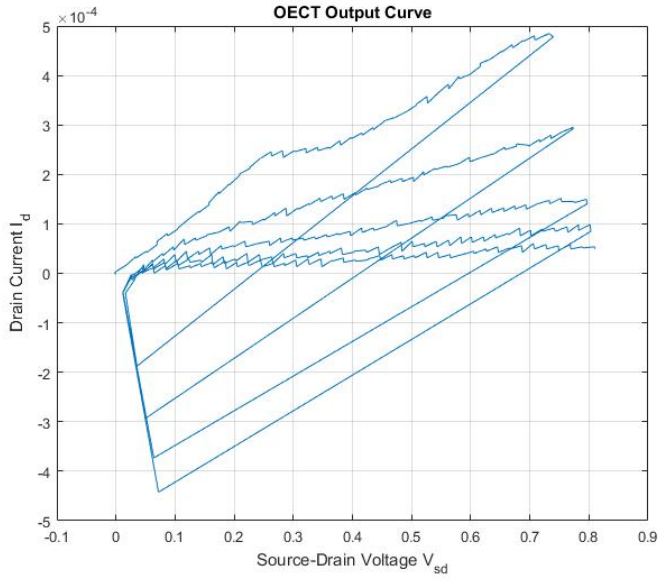

Figure C.4: Example output characteristics from the second iteration

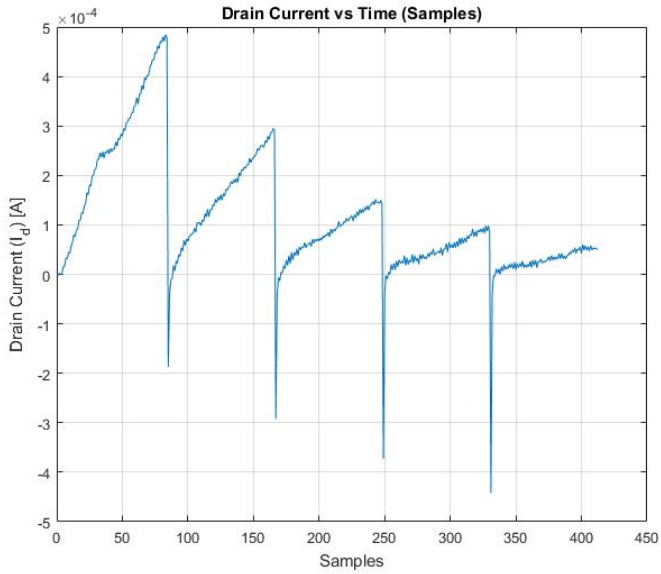

Figure C.5: Deterioration of the OECT over time due to PEDOT:PSS breakdown

C.3 Iteration 3: Addition of Immersed Gate and Increased Amount of PEDOT:PSS Layers

For the third iteration, the sweep conditions were changed to include a forward and backward sweep on the drain voltage. Furthermore, in the example sweep shown here, the gate voltage was stepped in a positive direction, which should cause a corresponding decrease in drain current.

Figure C.7 shows the output characteristics corresponding to the sweep conditions shown in figure C.6. Figure C.8 shows the drain and gate current over the sweep time period.

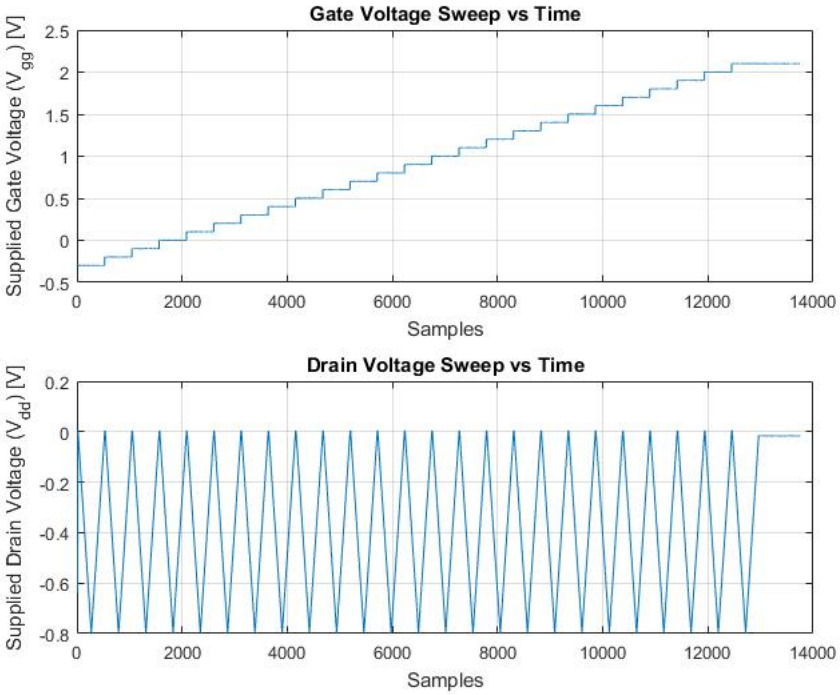

Figure C.6: Sweep conditions for the output curves given below, showing the forward and reverse drain voltage sweeps for increasing gate voltage steps.

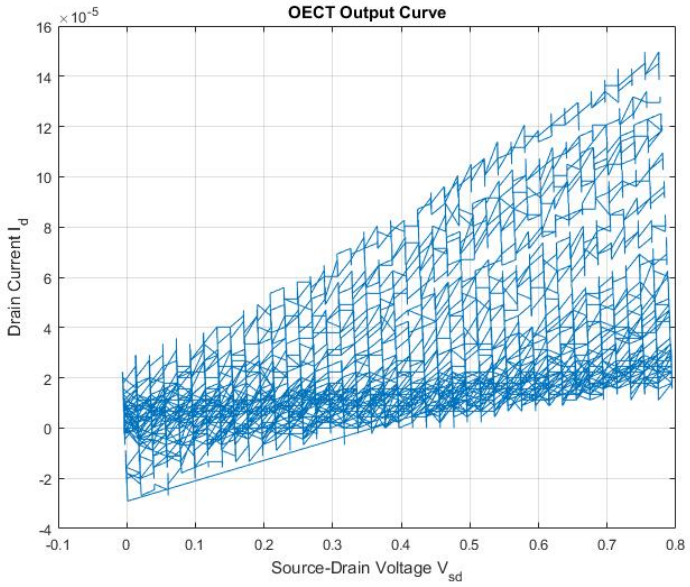

Figure C.7: Example output characteristics from the third iteration

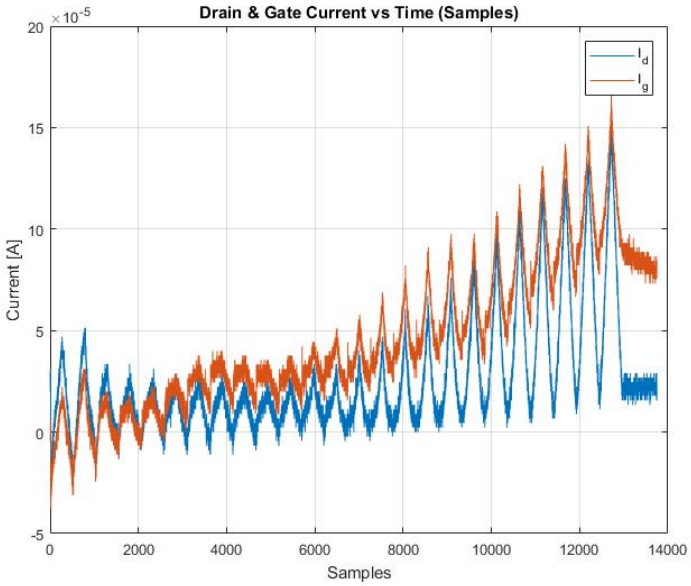

Figure C.8: Drain (blue) and gate (red) current over the sweep time period. The gate current clearly dominates, contributing to the measured drain current.

C.4 Iteration 4: Addition of 5 μL Drop of PEDOT:PSS Semiconductor and Widening of the Channel

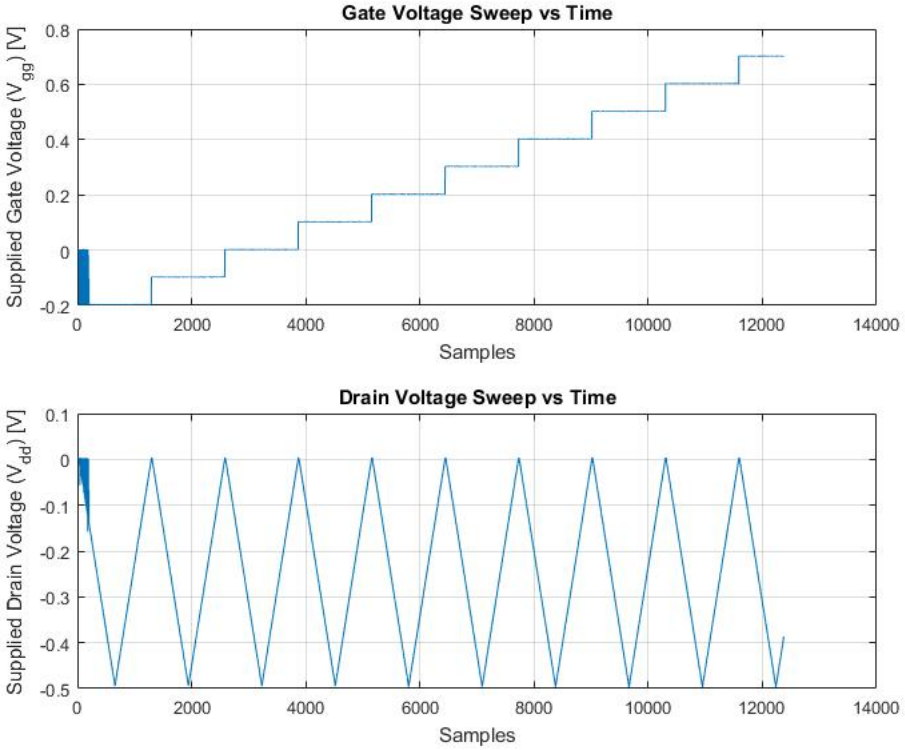

Figure C.9: Sweep conditions for the output curves given below, showing the forward and reverse drain voltage sweeps for increasing gate voltage steps.

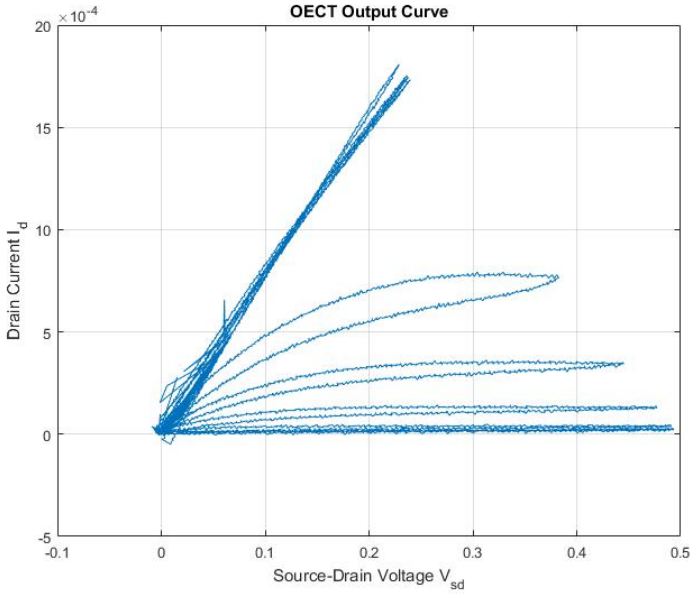

Figure C.10: Output characteristics from the first OECT of the fourth design iteration.

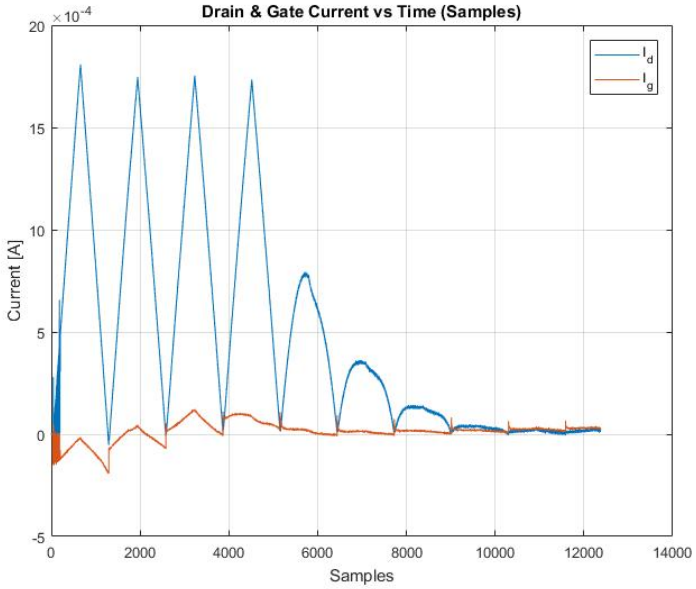

Figure C.11: Drain (blue) and gate (red) current over the sweep time period. The gate current was clearly suppressed in comparison to the third iteration.

Appendix D

Characteristics of Differerent OECTs

D.1 OECT 1

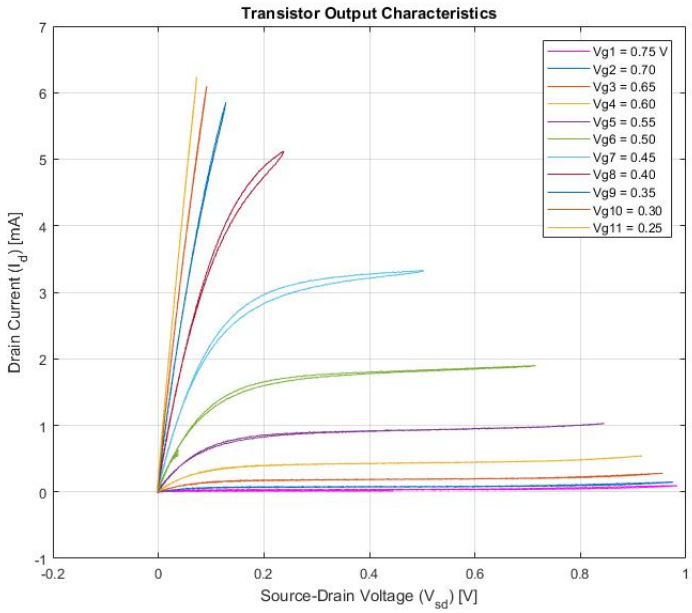

Figure D.1: OECT 1 output characteristics.

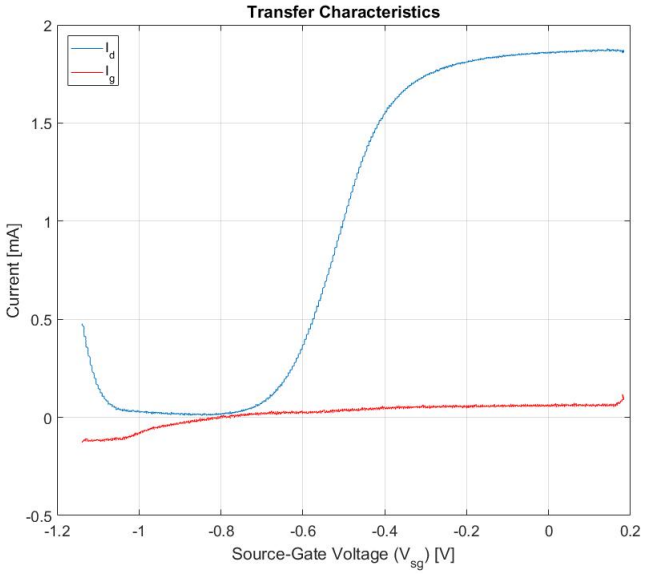

Figure D.2: OECT 1 transfer characteristics.

D.2 OECT 2

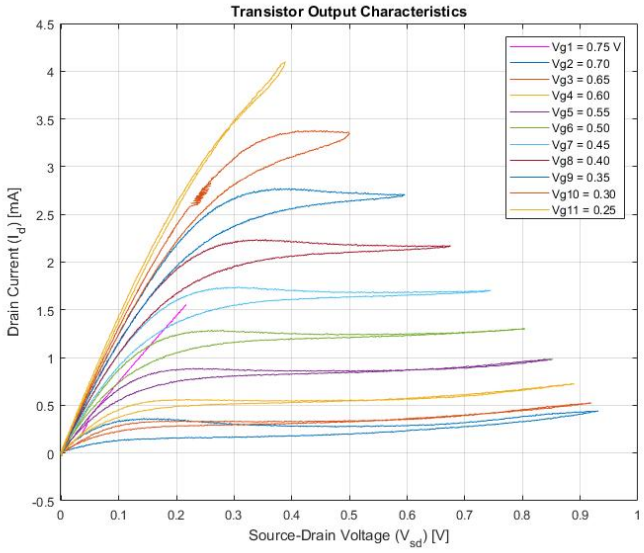

Figure D.3: OECT 2 output characteristics.

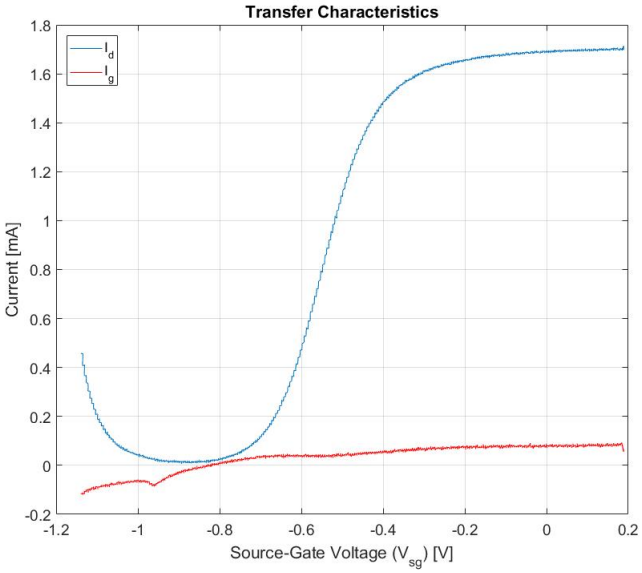

Figure D.4: OECT 2 transfer characteristics.

D.3 OECT 3

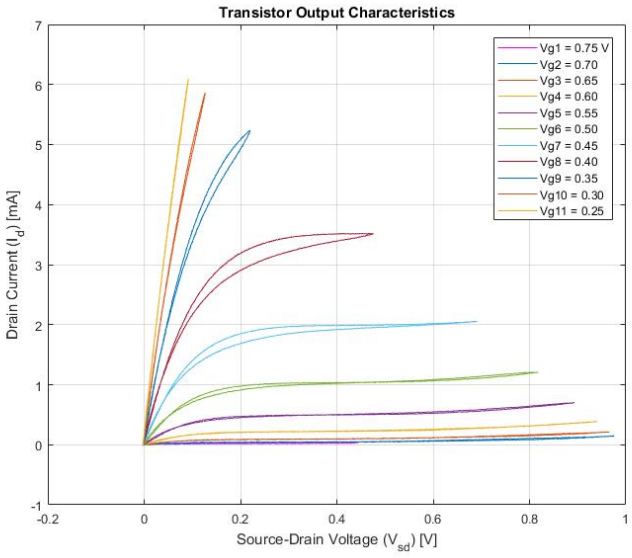

Figure D.5: OECT 3 output characteristics.

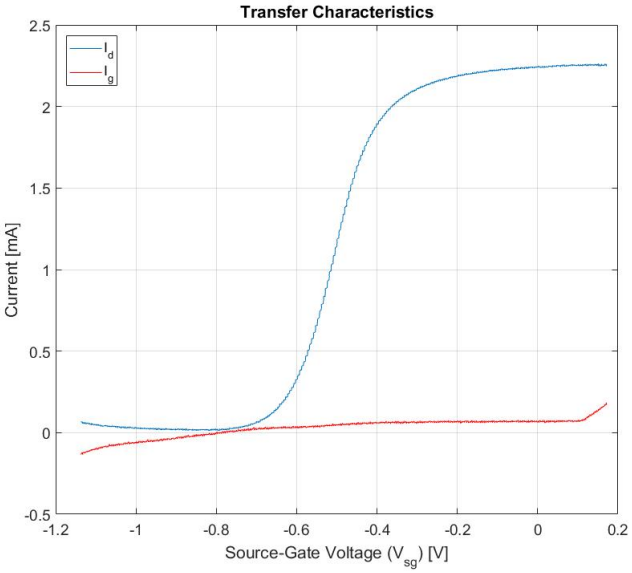

Figure D.6: OECT 3 transfer characteristics.

Appendix E

LabVIEW Programs

E.1 Constant DC Output Program

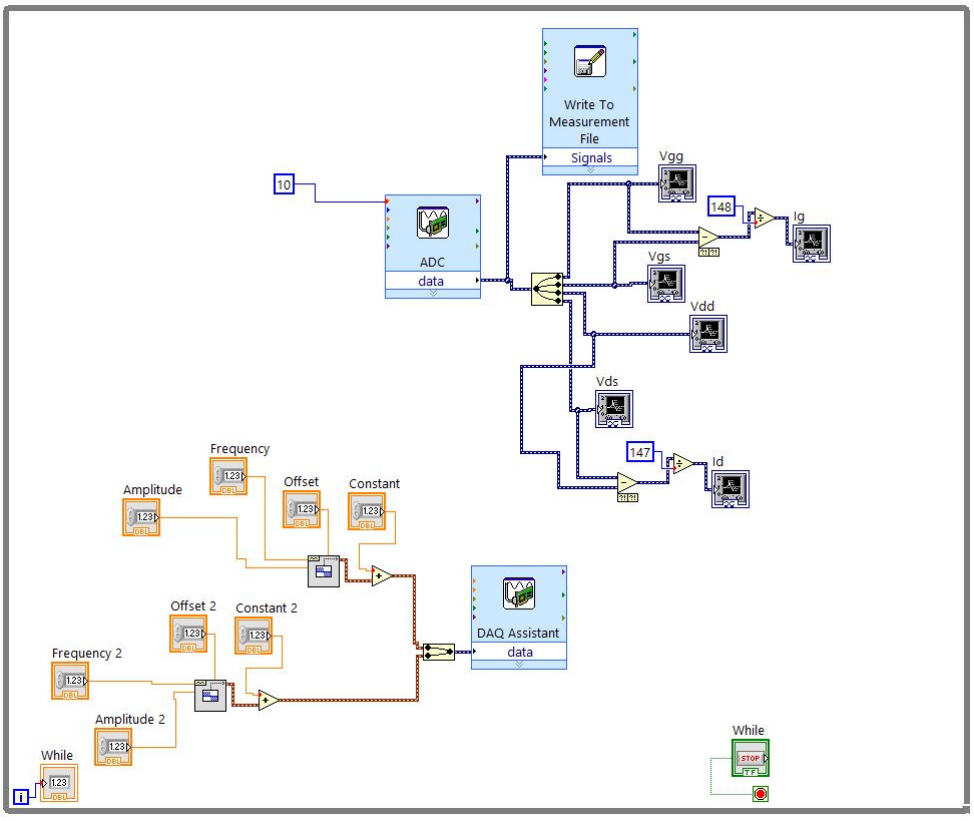

Figure E.1: Block diagram of the constant DC output program.

E.2 Transfer Curve Sweep Program

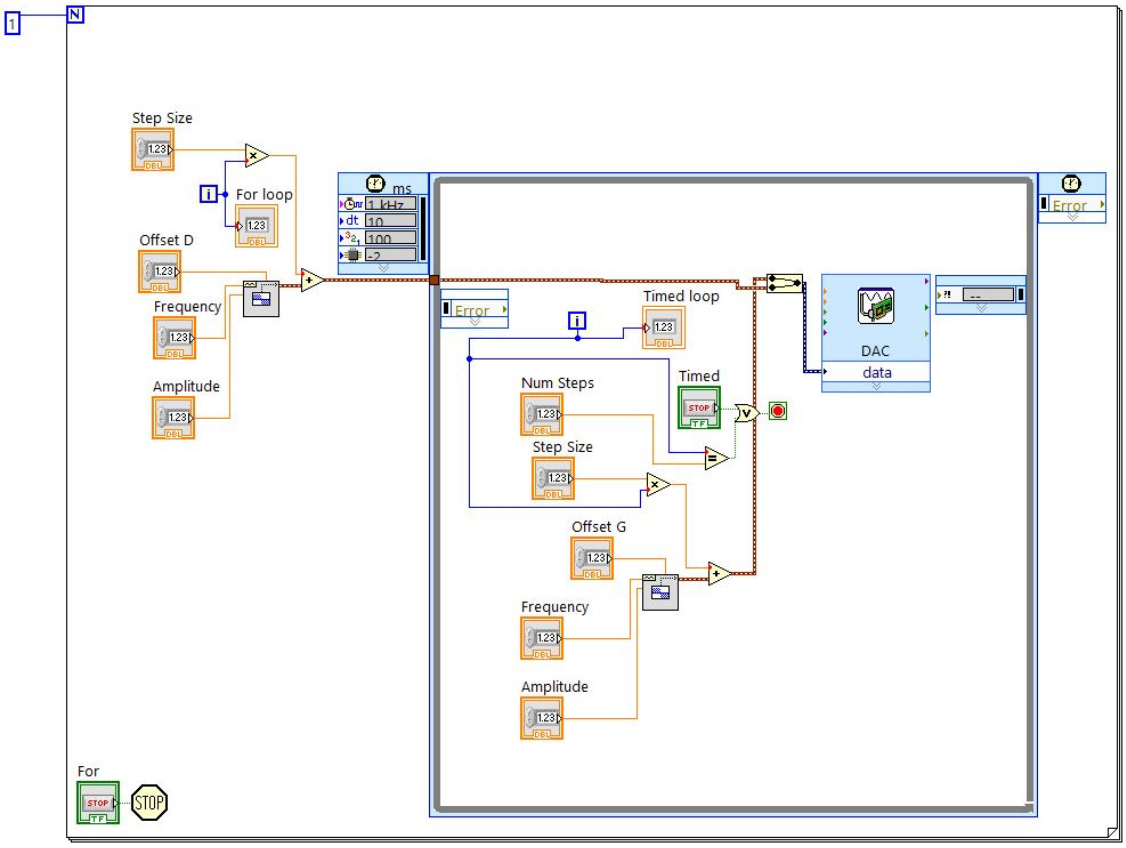

Figure E.2: Block diagram of the transfer sweep program.

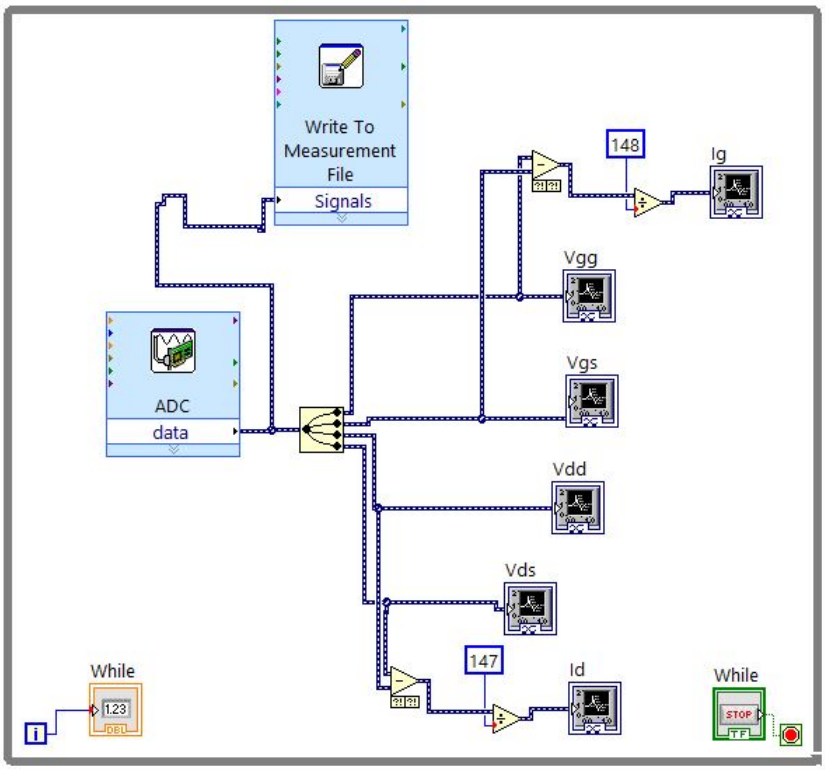

Figure E.3: Block diagram of the transfer sweep program continued.

E.3 Output Curve Sweep Program

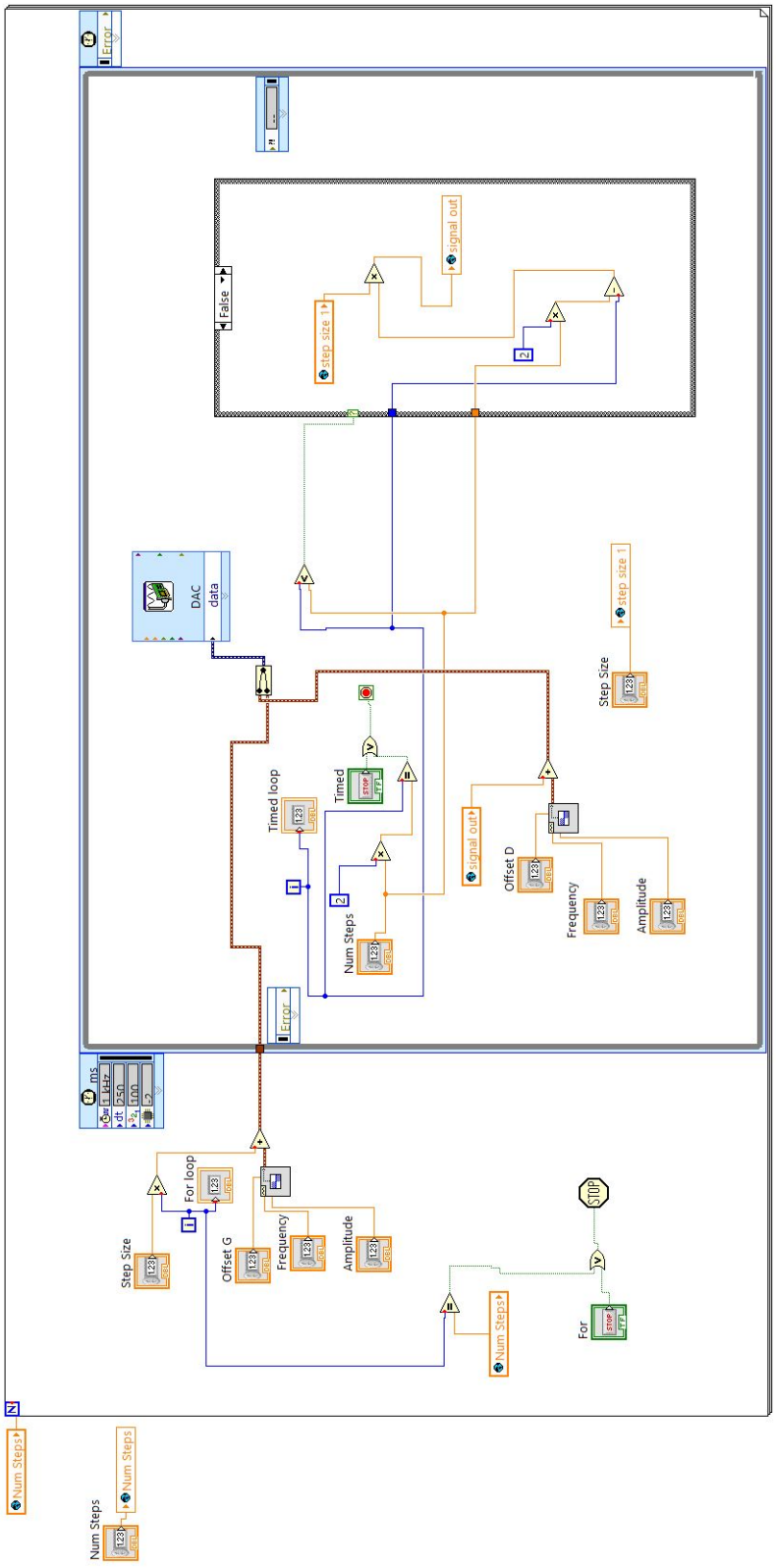

Figure E.4: Block diagram of the output curve sweep program.

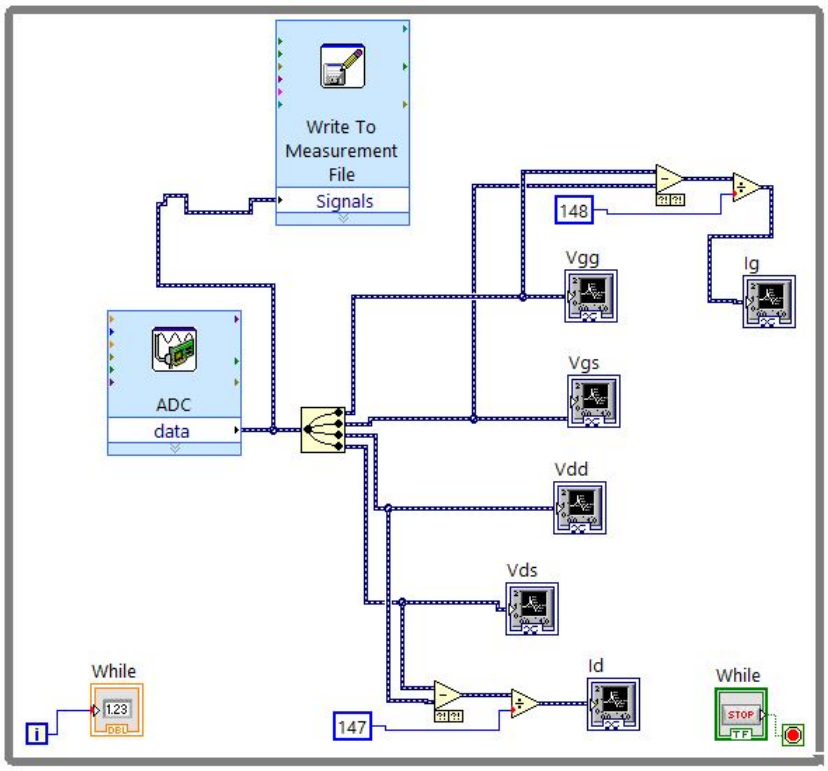

Figure E.5: Block diagram of the output curve sweep program continued.

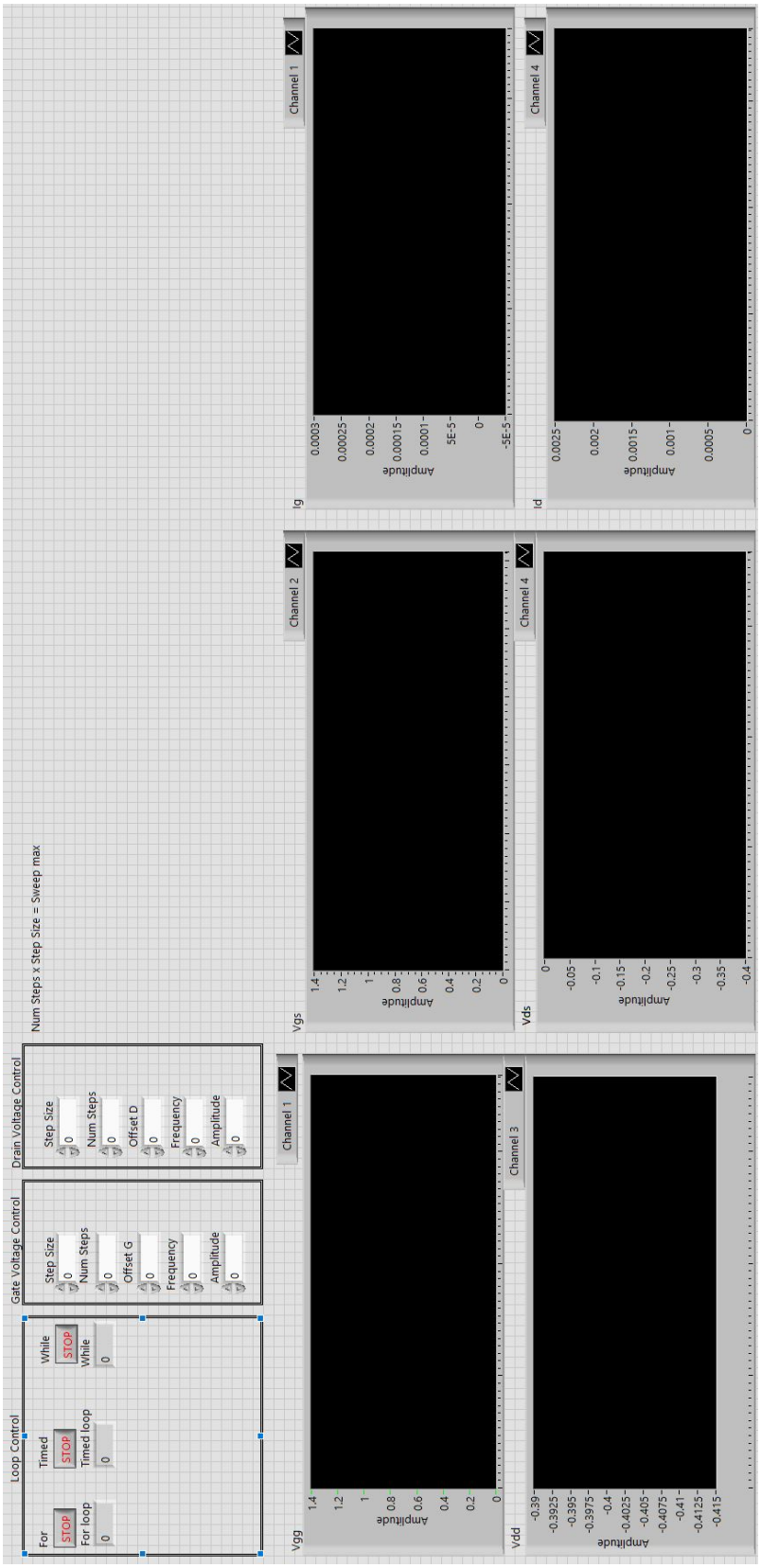

Figure E.6: Virtual interface (VI) of the LabVIEW programs.

Appendix F

Antibody Immobilisation and Reagent Preparation

The following appendix briefly describes the methodology followed for the immobilisation of the capture antibodies as well as the reagent preparation for final testing.

F.1 Antibody Immobilisation Methodology

The capture antibody immobilisation method is identical for both CRP and PCT, and is listed as follows:

1. Prepare the streptavidin reagent at a concentration of 20 μg/mL in PBS.
2. Add 20 μL of streptavidin reagent to the well of each sensor. Pipette up and down to mix gently.
3. Cover wells and incubate for 24 hours at four degrees Celsius.
4. Take the sensors out and wash each well three times with 20 μL of PBS.
5. Biotinylate the capture antibodies according to the Lightening-Link Biotinylation Kit protocol.
6. Prepare the biotinylated capture antibody reagent in assay buffer at a concentration of 10 μg/mL.
7. Fill each well with 20 μL biotinylated capture antibody reagent. Pipette up and down to mix gently.
8. Cover wells and incubate at four degrees Celsius for two hours.

9. Wash each well three times with 20 μL of PBS.

The capture antibodies were then successfully immobilised to the sensor substrate and the sensors were ready to test.

F.2 Reagent Preparation for Final Testing

The detection antibody reagent as well as the recombinant protein dilutions were prepared in the same way for both CRP and PCT. Each respective procedure is detailed below.

F.2.1 Detection Antibody Reagent

The following simple process was followed for the preparation of detection antibody reagents:

1. Dilute the stock antibody to a concentration of 100μg/mL in the gold nanoparticle conjugate modifier.
2. Follow the gold nanoparticle conjugation kit protocol.
3. Dilute the resulting conjugate reagent in PBS to a concentration of 10 μg/mL.

The AuNP-labelled detection antibody was then ready for testing.

F.2.2 Recombinant Protein Dilutions

The following protocol was followed to prepare the necessary recombinant protein dilutions:

1. Dilute the stock proteins in PBS to a concentration of 1 mg/mL.
2. Dilute further to the required starting concentration using PBS.
3. Take half of the first dilution and add it to a matching volume of PBS. This will half the concentration of the recombinant protein reagent.
4. Repeat step four until required concentration is reached.

The respective protein dilutions were then ready for testing.

Appendix G

Biomarker Categories

Table G.1: Different Biomarker Categories and Descriptions (adapted from the BEST Resource [7])

Biomarker Category	Description
Diagnostic Biomarker	A biomarker used to detect or confirm presence of a disease or condition of interest or to identify individuals with a subtype of the disease.
Monitoring Biomarker	A biomarker measured serially for assessing status of a disease or medical condition or for evidence of exposure to (or effect of) a medical product or an environmental agent.
Pharmacodynamic Biomarker	A biomarker used to show that a biological response has occurred in an individual who has been exposed to a medical product or an environmental agent.
Predictive Biomarker	A biomarker used to identify individuals who are more likely than similar individuals without the biomarker to experience a favourable or unfavourable effect from exposure to a medical product or an environmental agent.
Prognostic Biomarker	A biomarker used to identify likelihood of a clinical event, disease recurrence or progression in patients who have the disease or medical condition of interest.
Safety Biomarker	A biomarker measured before or after an exposure to a medical product or an environmental agent to indicate the likelihood, presence, or extent of toxicity as an adverse effect.
Susceptibility/ Risk Biomarker	A biomarker that indicates the potential for developing a disease or medical condition in an individual who does not currently have clinically apparent disease or the medical condition.

Bibliography

[1] Sambursky, R. and Shapiro, N.: Evaluation of a combined MxA and CRP point-of-care immunoassay to identify viral and/or bacterial immune response in patients with acute febrile respiratory infection. *European Clinical Respiratory Journal*, vol. 2, no. 1, p. 28245, 2015.

[2] Schuetz, P., Albrich, W., Christ-Crain, M., Chastre, J. and Mueller, B.: Procalcitonin for guidance of antibiotic therapy. *Expert Review of Anti-infective Therapy*, vol. 8, no. 5, pp. 575–587, 2010.

[3] Evans, A.T., Husain, S., Durairaj, L., Sadowski, L.S., Charles-Damte, M. and Wang, Y.: Azithromycin for acute bronchitis: A randomised, double-blind, controlled trial. *Lancet*, vol. 359, no. 9318, pp. 1648–1654, 2002.

[4] Costelloe, C., Metcalfe, C., Lovering, A., Mant, D. and Hay, A.D.: Effect of antibiotic prescribing in primary care on antimicrobial resistance in individual patients: systematic review and meta-analysis. *Bmj*, vol. 340, p. c2096, 2010.

[5] Huovinen, P. and Cars, O.: Control of antimicrobial resistance: time for action. The essentials of control are already well known. *BMJ (Clinical research ed.)*, vol. 317, no. 7159, pp. 613–614, 1998.

[6] Strimbu, K. and Tavel, J.a.: What are Biomarkers? *Curr Opin HIV AIDS*, vol. 5, no. 6, pp. 463–466, 2011.

[7] FDA-NIH: Best (biomarkers, endpoints, and other tools) resource. 2016.

[8] Atkinson, A.J., Colburn, W.A., DeGruttola, V.G., DeMets, D.L., Downing, G.J., Hoth, D.F., Oates, J.A., Peck, C.C., Schooley, R.T., Spilker, B.A., Woodcock, J. and Zeger, S.L.: Biomarkers and surrogate endpoints: Preferred definitions and conceptual framework. *Clinical Pharmacology and Therapeutics*, vol. 69, no. 3, pp. 89–95, 2001.

[9] Mohan, A. and Harikrishna, J.: Biomarkers for the diagnosis of bacterial infections: in pursuit of the 'Holy Grail'. *The Indian journal of medical research*, vol. 141, no. 3, pp. 271–3, mar 2015.

[10] Lee, H.: Procalcitonin as a biomarker of infectious diseases. *The Korean journal of internal medicine*, vol. 28, no. 3, p. 285, 2013.

[11] Qu, J., Lü, X., Liu, Y. and Wang, X.: Evaluation of procalcitonin, c-reactive protein, interleukin-6 & serum amyloid a as diagnostic biomarkers of bacterial infection in febrile patients. *The Indian journal of medical research*, vol. 141, no. 3, p. 315, 2015.

[12] Meem, M., Modak, J.K., Mortuza, R., Morshed, M., Islam, M.S. and Saha, S.K.: Biomarkers for diagnosis of neonatal infections: A systematic analysis of their potential as a point-of-care diagnostics. *Journal of global health*, vol. 1, no. 2, pp. 201–209, 2011.

[13] Hedegaard, S.S., Wisborg, K. and Hvas, A.M.: Diagnostic utility of biomarkers for neonatal sepsis - a systematic review. *Infectious Diseases*, vol. 47, no. 3, pp. 117–124, 2015.

[14] Meem, M., Modak, J.K., Mortuza, R., Morshed, M., Islam, M.S. and Saha, S.K.: Biomarkers for diagnosis of neonatal infections: A systematic analysis of their potential as a point-of-care diagnostics. *Journal of global health*, vol. 1, no. 2, p. 201, 2011.

[15] Magliulo, M., De Tullio, D., Vikholm-Lundin, I., Albers, W.M., Munter, T., Manoli, K., Palazzo, G. and Torsi, L.: Label-free c-reactive protein electronic detection with an electrolyte-gated organic field-effect transistor-based immunosensor. *Analytical and bioanalytical chemistry*, vol. 408, no. 15, pp. 3943–3952, 2016.

[16] Pepys, M.B.: Acute phase proteins. *Encyclopedia of Immunology*, vol. 2, pp. 18–20, 1998.

[17] Salonen, E.-M. and Vaheri, A.: C-reactive protein in acute viral infections. *Journal of medical virology*, vol. 8, no. 3, pp. 161–167, 1981.

[18] Hatzistilianou, M.: Diagnostic and prognostic role of procalcitonin in infections. *The Scientific World Journal*, vol. 10, pp. 1941–1946, 2010.

[19] Uusitalo-Seppälä, R., Koskinen, P., Leino, A., Peuravuori, H., Vahlberg, T. and Rintala, E.M.: Early detection of severe sepsis in the emergency room: diagnostic value of plasma C-reactive protein, procalcitonin, and interleukin-6. *Scandinavian journal of infectious diseases*, vol. 43, no. 11-12, pp. 883–90, 2011.

[20] Leli, C., Cardaccia, A., Ferranti, M., Cesarini, A., DAlò, F., Ferri, C., Cenci, E. and Mencacci, A.: Procalcitonin better than c-reactive protein, erythrocyte sedimentation rate, and white blood cell count in predicting dnaemia in patients with sepsis. *Scandinavian journal of infectious diseases*, vol. 46, no. 11, pp. 745–752, 2014.

[21] Fee lookups. 2018.
Available at: `https://www.pathcare.co.za/feelookups/`

[22] McNaught, A.D. and McNaught, A.D.: *Compendium of chemical terminology*, vol. 1669. Blackwell Science Oxford, 1997.

[23] Sin, M.L., Mach, K.E., Wong, P.K. and Liao, J.C.: Advances and challenges in biosensor-based diagnosis of infectious diseases. *Expert review of molecular diagnostics*, vol. 14, no. 2, pp. 225–244, 2014.

[24] Wang, D., Noël, V. and Piro, B.: Electrolytic Gated Organic Field-Effect Transistors for Application in Biosensors - A Review. *Electronics*, vol. 5, no. 1, p. 9, 2016.

[25] Mehrotra, P.: Biosensors and their applications–a review. *Journal of oral biology and craniofacial research*, vol. 6, no. 2, pp. 153–159, 2016.

[26] Liao, C. and Yan, F.: Organic semiconductors in organic thin-film transistor-based chemical and biological sensors. *Polymer Reviews*, vol. 53, no. 3, pp. 352–406, 2013.

[27] Tang, H., Lin, P., Chan, H.L.W. and Yan, F.: Highly sensitive dopamine biosensors based on organic electrochemical transistors. *Biosensors and Bioelectronics*, vol. 26, no. 11, pp. 4559–4563, 2011.

[28] Kergoat, L., Piro, B., Berggren, M., Horowitz, G. and Pham, M.-C.: Advances in organic transistor-based biosensors: from organic electrochemical transistors to electrolyte-gated organic field-effect transistors. *Analytical and bioanalytical chemistry*, vol. 402, no. 5, pp. 1813–1826, 2012.

[29] Kim, D.-J., Lee, N.-E., Park, J.-S., Park, I.-J., Kim, J.-G. and Cho, H.J.: Organic electrochemical transistor based immunosensor for prostate specific antigen (PSA) detection using gold nanoparticles for signal amplification. *Biosensors & bioelectronics*, vol. 25, no. 11, pp. 2477–2482, jul 2010.

[30] Tybrandt, K., Kollipara, S.B. and Berggren, M.: Organic electrochemical transistors for signal amplification in fast scan cyclic voltammetry. *Sensors and Actuators, B: Chemical*, vol. 195, pp. 651–656, 2014.

[31] Baude, P., Ender, D., Haase, M., Kelley, T., Muyres, D. and Theiss, S.: Pentacene-based radio-frequency identification circuitry. *Applied Physics Letters*, vol. 82, no. 22, pp. 3964–3966, 2003.

[32] Sirringhaus, H., Tessler, N. and Friend, R.H.: Integrated optoelectronic devices based on conjugated polymers. *Science*, vol. 280, no. 5370, pp. 1741–1744, 1998.

[33] Shirakawa, H., Louis, E.J., MacDiarmid, A.G., Chiang, C.K. and Heeger, A.J.: Synthesis of electrically conducting organic polymers: halogen derivatives of polyacetylene,(ch) x. *Journal of the Chemical Society, Chemical Communications*, , no. 16, pp. 578–580, 1977.

[34] Köhler, A. and Bässler, H.: *Electronic processes in organic semiconductors: An introduction*. John Wiley & Sons, 2015.

[35] Cotrone, S., Cafagna, D., Cometa, S. and Giglio, E.D.: Microcantilevers and organic transistors : two promising classes of label-free biosensing devices which can be integrated in electronic circuits. pp. 1799–1811, 2012.

[36] Nambiar, S. and Yeow, J.T.: Conductive polymer-based sensors for biomedical applications. *Biosensors and Bioelectronics*, vol. 26, no. 5, pp. 1825–1832, 2011.

[37] Naveen, M.H., Gurudatt, N.G. and Shim, Y.-b.: Applications of conducting polymer composites to electrochemical sensors: A review. *Applied Materials Today*, vol. 9, pp. 419–433, 2017.

[38] Pretl, S., Hamáček, A., Reboun, J., Čengery, J., Džugan, T. and Kroupa, M.: Electrical characterization of PEDOT:PSS. In: *Electronics System Integration Technology Conference, ESTC 2010 Proceedings*, April 2015. 2010. ISBN 9781424485536.

[39] Inal, S., Malliaras, G.G. and Rivnay, J.: Benchmarking organic mixed conductors for transistors. *Nature Communications*, vol. 8, no. 1, pp. 1–6, 2017.

[40] Satyanarayana, D.M.: Polymers: Conducting polymer. 2014.

[41] Stoliar, P., Bystrenova, E., Quiroga, S., Annibale, P., Facchini, M., Spijkman, M., Setayesh, S., De Leeuw, D. and Biscarini, F.: Dna adsorption measured with ultrathin film organic field effect transistors. *Biosensors and Bioelectronics*, vol. 24, no. 9, pp. 2935–2938, 2009.

[42] Bai, H. and Shi, G.: Gas sensors based on conducting polymers. *Sensors*, vol. 7, no. 3, pp. 267–307, 2007.

[43] White, H.S., Kittlesen, G.P. and Wrighton, M.S.: Chemical derivatization of an array of three gold microelectrodes with polypyrrole: fabrication of a molecule-based transistor. *Journal of the American Chemical Society*, vol. 106, no. 18, pp. 5375–5377, 1984.

[44] Wang, N., Liu, Y., Fu, Y. and Yan, F.: AC Measurements Using Organic Electrochemical Transistors for Accurate Sensing. *ACS Applied Materials & Interfaces*, p. acsami.7b07668, 2017.

[45] Cicoira, F., Sessolo, M., Yaghmazadeh, O., Defranco, J.A., Yang, S.Y. and Malliaras, G.C.: Influence of device geometry on sensor characteristics of planar Organic electrochemical transistors. *Advanced Materials*, vol. 22, no. 9, pp. 1012–1016, 2010.

[46] Macchia, E., Ghittorelli, M., Torricelli, F. and Torsi, L.: Organic electrochemical transistor immuno-sensor operating at the femto-molar limit of detection. In: *Advances in Sensors and Interfaces (IWASI), 2017 7th IEEE International Workshop on*, pp. 68–72. IEEE, 2017.

[47] Faddoul, R., Coppard, R. and Berthelot, T.: Inkjet printing of organic electrochemical immunosensors. *Proceedings of IEEE Sensors*, vol. 2014-Decem, no. December, pp. 1088–1091, 2014.

[48] Nilsson, D., Chen, M., Kugler, T., Remonen, T., Armgarth, M. and Berggren, M.: Bi-stable and dynamic current modulation in electrochemical organic transistors. *Advanced Materials*, vol. 14, no. 1, pp. 51–54, 2002.

[49] Bernards, D.A. and Malliaras, G.G.: Steady-state and transient behavior of organic electrochemical transistors. *Advanced Functional Materials*, vol. 17, no. 17, pp. 3538–3544, 2007.

[50] Fu, Y., Wang, N., Yang, A., Law, H.K.-w., Li, L. and Yan, F.: Highly Sensitive Detection of Protein Biomarkers with Organic Electrochemical Transistors. *Advanced Materials*, vol. 1703787, p. 1703787, 2017. ISSN 09359648.

[51] Khodagholy, D., Rivnay, J., Sessolo, M., Gurfinkel, M., Leleux, P., Jimison, L.H., Stavrinidou, E., Herve, T., Sanaur, S., Owens, R.M. and Malliaras, G.G.: High transconductance organic electrochemical transistors. *Nature Communications*, vol. 4, 2013. `NIHMS150003`.

[52] Alberga, D., Mangiatordi, G.F., Torsi, L. and Lattanzi, G.: Effects of annealing and residual solvents on amorphous p3ht and pbttt films. *The Journal of Physical Chemistry C*, vol. 118, no. 16, pp. 8641–8655, 2014.

[53] Sirringhaus, H., Brown, P., Friend, R., Nielsen, M.M., Bechgaard, K., Langeveld-Voss, B., Spiering, A., Janssen, R.A., Meijer, E., Herwig, P. *et al.*: Two-dimensional charge transport in self-organized, high-mobility conjugated polymers. *Nature*, vol. 401, no. 6754, p. 685, 1999.

[54] Derby, B.: Inkjet printing of functional and structural materials: fluid property requirements, feature stability, and resolution. *Annual Review of Materials Research*, vol. 40, pp. 395–414, 2010.

[55] What is an antibody. 2018.
Available at: `https://www.pacificimmunology.com/resources/antibody-introduction/what-is-an-antibody/`

[56] Mandal, A.: What is an antibody? Aug 2018.
Available at: `https://www.news-medical.net/health/What-is-an-Antibody.aspx`

[57] Jung, Y., Jeong, J.Y. and Chung, B.H.: Recent advances in immobilization methods of antibodies on solid supports. *The Analyst*, vol. 133, no. 6, p. 697, 2008.

[58] Moina, C. and Ybarra, G.: Fundamentals and applications of immunosensors. In: *Advances in immunoassay technology*. InTech, 2012.

[59] de Moraes, A.C.M. and Kubota, L.T.: Recent trends in field-effect transistors-based immunosensors. *Chemosensors*, vol. 4, no. 4, p. 20, 2016.

[60] Cho, I.-H., Paek, E.-H., Lee, H., Kang, J.Y., Kim, T.S. and Paek, S.-H.: Site-directed biotinylation of antibodies for controlled immobilization on solid surfaces. *Analytical biochemistry*, vol. 365, no. 1, pp. 14–23, 2007.

[61] Ates, H.C., Ozgur, E. and Kulah, H.: Comparative study on antibody immobilization strategies for efficient circulating tumor cell capture. *Biointerphases*, vol. 13, no. 2, p. 021001, 2018.

[62] Salvo, P., Dini, V., Kirchhain, A., Janowska, A., Oranges, T., Chiricozzi, A., Lomonaco, T., Di Francesco, F. and Romanelli, M.: Sensors and biosensors for c-reactive protein, temperature and ph, and their applications for monitoring wound healing: a review. *Sensors*, vol. 17, no. 12, p. 2952, 2017.

[63] Figliola, R.S. and Beasley, D.: *Theory and design for mechanical measurements*. John Wiley & Sons, 2015.

[64] Retief, J., Fourie, P. and Perold, W.: Modified desktop inkjet printer as low-cost material deposition device. In: *Biomedical Engineering Conference (SAIBMEC), 2018 3rd Biennial South African*, pp. 1–4. IEEE, 2018.

[65] Gimp.
Available at: `https://www.gimp.org/`